



University of Kentucky
UKnowledge

University of Kentucky Doctoral Dissertations

Graduate School

2010

ADVANCEMENTS IN TRANSMISSION LINE FAULT LOCATION

Ning Kang

University of Kentucky, gluckenkama@hotmail.com

[Right click to open a feedback form in a new tab to let us know how this document benefits you.](#)

Recommended Citation

Kang, Ning, "ADVANCEMENTS IN TRANSMISSION LINE FAULT LOCATION" (2010). *University of Kentucky Doctoral Dissertations*. 69.

https://uknowledge.uky.edu/gradschool_diss/69

This Dissertation is brought to you for free and open access by the Graduate School at UKnowledge. It has been accepted for inclusion in University of Kentucky Doctoral Dissertations by an authorized administrator of UKnowledge. For more information, please contact UKnowledge@lsv.uky.edu.

ABSTRACT OF DISSERTATION

Ning Kang

The Graduate School
University of Kentucky

2010

ADVANCEMENTS IN TRANSMISSION LINE FAULT LOCATION

ABSTRACT OF DISSERTATION

A dissertation submitted in partial fulfillment of the
requirements for the degree of Doctor of Philosophy in the
College of Engineering
at the University of Kentucky

By

Ning Kang

Lexington, Kentucky

Director: Dr. Yuan Liao, Professor of Electrical and Computer Engineering

Lexington, Kentucky

2010

Copyright © Ning Kang 2010

ABSTRACT OF DISSERTATION

ADVANCEMENTS IN TRANSMISSION LINE FAULT LOCATION

In modern power transmission systems, the double-circuit line structure is increasingly adopted. However, due to the mutual coupling between the parallel lines it is quite challenging to design accurate fault location algorithms. Moreover, the widely used series compensator and its protective device introduce harmonics and non-linearities to the transmission lines, which make fault location more difficult. To tackle these problems, this dissertation is committed to developing advanced fault location methods for double-circuit and series-compensated transmission lines.

Algorithms utilizing sparse measurements for pinpointing the location of short-circuit faults on double-circuit lines are proposed. By decomposing the original network into three sequence networks, the bus impedance matrix for each network with the addition of the fictitious fault bus can be formulated. It is a function of the unknown fault location. With the augmented bus impedance matrices the sequence voltage change during the fault at any bus can be expressed in terms of the corresponding sequence fault current and the transfer impedance between the fault bus and the measured bus. Resorting to VCR the superimposed sequence current at any branch can be expressed with respect to the pertaining sequence fault current and transfer impedance terms. Obeying boundary conditions of different fault types, four different classes of fault location algorithms utilizing either voltage phasors, or phase voltage magnitudes, or current phasors, or phase current magnitudes are derived. The distinguishing characteristic of the proposed method is that the data measurements need not stem from the faulted section itself. Quite satisfactory results have been obtained using EMTP simulation studies.

A fault location algorithm for series-compensated transmission lines that employs two-terminal unsynchronized voltage and current measurements has been implemented. For the distinct cases that the fault occurs either on the left or on the right side of the series compensator, two subroutines are developed. In addition, the procedure to identify the correct fault location estimate is described in this work. Simulation studies carried out with Matlab SimPowerSystems show that the fault location results are very accurate.

KEYWORDS: bus impedance matrix, double-circuit transmission lines, fault location, series-compensated transmission lines, sparse measurements

Ning Kang

29 September, 2010

ADVANCEMENTS IN TRANSMISSION LINE FAULT LOCATION

By

Ning Kang

Dr. Yuan Liao
(Director of Dissertation)

Dr. Stephen Gedney
(Director of Graduate Studies)

29 September, 2010
(Date)

DISSERTATION

Ning Kang

The Graduate School
University of Kentucky

2010

ADVANCEMENTS IN TRANSMISSION LINE FAULT LOCATION

DISSERTATION

A dissertation submitted in partial fulfillment of the
requirements for the degree of Doctor of Philosophy in the
College of Engineering
at the University of Kentucky

By

Ning Kang

Lexington, Kentucky

Director: Dr. Yuan Liao, Professor of Electrical and Computer Engineering

Lexington, Kentucky

2010

Copyright © Ning Kang 2010

ACKNOWLEDGEMENTS

I would like to express the most sincere gratitude to my advisor, Dr. Yuan Liao, who has guided me through one and another obstacles with his outstanding expertise and patience throughout my entire research. I also wish to extend my appreciation to Dr. Yuming Zhang, Dr. Jimmie Cathey, Dr. Joseph Sottile, and Dr. Caicheng Lu for their insightful advice and willingness to serve on the Dissertation Advisory Committee.

I want to thank my parents and my great friends Robert Nikutta, Xiaoxia Qu, Xingxing Zhang, Yucheng Liu and Sandra Holly, for their endless support.

Financial support from the National Science Foundation under Grant No. ECCS-0801367 is greatly acknowledged.

Contents

Acknowledgements	iii
List of Tables	viii
List of Figures	x
1 Introduction	1
1.1 Analysis of Fault Location Algorithms	1
1.1.1 Review of Existing Double-Circuit Line Fault Location Algorithms	2
1.1.2 Review of Existing Fault Location Algorithms for Series-Compensated Lines	5
1.2 Objectives	6
1.3 Proposed New Methods	7
1.4 Summary	8
2 Fault Location Using Sparse Voltage Measurements Based on Lumped Parameter Line Model	10
2.1 Introduction	10
2.2 Fault Location Basis	11
2.2.1 Construction of Bus Impedance Matrix with Addition of the Fault Bus	12
2.2.2 Alternative Way of Construction of Bus Impedance Matrix with Addition of the Fault Bus	17

2.2.3	Relation Between Voltage Change and Augmented Bus Impedance Matrix	24
2.3	Proposed Fault Location Method	24
2.3.1	Fault Location Algorithms Utilizing Voltage Phasors	24
2.3.1.1	Fault Scenarios with Measurements from Two Buses	25
2.3.1.2	Fault Scenarios with Measurements from a Single Bus	26
2.3.2	Fault Location Algorithms Utilizing Phase Voltage Magnitudes	29
2.3.2.1	Algorithms with Voltage Magnitudes from One Bus .	30
2.3.2.2	Algorithms with Voltage Magnitudes from Multiple Buses	32
2.3.2.3	Newton-Raphson Method and Least Squares Method	33
2.4	Simulation Studies	34
2.4.1	Case Studies for Fault Location Using Voltage phasors	35
2.4.2	Case Studies for Fault Location Using Phase Voltage Magnitudes	37
2.5	Summary	38
3	Fault Location Using Sparse Current Measurements Based on Lumped Parameter Line Model	40
3.1	Introduction	40
3.2	Fault Location Basis	41
3.3	Proposed Fault Location Method	49
3.3.1	Fault Location Algorithms Using Current Phasors	49
3.3.1.1	Fault Scenarios with Measurements from Two Branches	50
3.3.1.2	Fault Scenarios with Measurements from One Branch	50
3.3.2	Fault Location Algorithms Using Phase Current Magnitudes .	52
3.3.2.1	Algorithms with Current Magnitudes from One Branch	53
3.3.2.2	Algorithms with Current Magnitudes from Multiple Branches	55
3.4	Simulation Studies	56
3.4.1	Case Studies for Fault Location Using Current Phasors	57

3.4.2	Case Studies for Fault Location Using Phase Current Magnitudes	60
3.5	Summary	60
4	Fault Location Utilizing Sparse Voltage Measurements Based on Distributed Parameter Line Model	62
4.1	Introduction	62
4.2	Zero-Sequence Equivalent PI Model of Double-Circuit Line	62
4.3	Fault Location Basis	73
4.3.1	Construction of Zero-Sequence Augmented Bus Impedance Matrix	74
4.3.2	Construction of Positive-Sequence Augmented Bus Impedance Matrix	80
4.4	Proposed Fault Location Method	84
4.4.1	Two-Bus Fault Location Algorithms	84
4.4.2	One-Bus Fault Location Algorithms	86
4.5	Optimal Fault Location Estimation Considering Measurement Errors	88
4.5.1	Proposed Optimal Estimator	88
4.5.2	Detection and Identification of Bad Measurements	90
4.6	Simulation Studies	90
4.7	Summary	93
5	Fault Location for Series-Compensated Lines	100
5.1	Introduction	100
5.2	Nomenclature	101
5.3	Proposed Fault Location Algorithms	102
5.3.1	Subroutine 1: Location for Fault on the Left Side of Series Compensator	102
5.3.2	Subroutine 2: Location for Fault on the Right Side of Series Compensator	106
5.3.3	Fault Location Identification Method	108
5.4	Evaluation Study	109

5.4.1	System Configuration	109
5.4.2	Fault Location Results	111
5.5	Summary	113
6	Conclusions	114
	Bibliography	117
	Vita	124

List of Tables

2.1	Transmission line data	34
2.2	Generator data	34
2.3	Fault location results using voltage phasors at two buses	36
2.4	Fault location results using voltage phasors at a single bus for AG and BCG faults	37
2.5	Fault location results using voltage phasors at a single bus for BC and ABC faults	38
2.6	Fault location results using voltage sag data	39
3.1	Fault location results using current phasors from two branches	58
3.2	Fault location results using current phasors from one branch for AG fault	58
3.3	Fault location results using current phasors from one branch for BCG fault	59
3.4	Fault location results using current phasors from one branch for BC and ABC faults	59
3.5	Fault location results using phase current magnitudes	60
4.1	Two-bus fault location results	95
4.2	One-bus fault location results for AG and BCG faults	96
4.3	One-bus fault location results for BC and ABC faults	97
4.4	Optimal estimates with bad magnitude measurement	98
4.5	Optimal estimates with bad magnitude measurement removed	98
4.6	Optimal estimates with bad angle measurement	98

4.7	Optimal estimates with bad angle measurement removed	99
5.1	Voltage source data	110
5.2	Transmission line data	110
5.3	Fault location results	112

List of Figures

1.1	Voltage and current waveforms during a-g fault.	6
1.2	Voltage and current waveforms during a-b-c fault.	7
1.3	A sample wide area monitoring system.	8
2.1	Pre-fault zero-sequence network.	12
2.2	Zero-sequence network with an additional fault bus.	13
2.3	Zero-sequence network with a branch removed.	13
2.4	Zero-sequence network with addition of branch pr	14
2.5	Pre-fault positive-sequence network.	16
2.6	Positive-sequence network with an additional fault bus.	17
2.7	Zero-sequence network with 1 A injected to bus k	18
2.8	Zero-sequence network with 1 A injected into bus r	19
2.9	Positive-sequence network with 1 A injected to a single bus k	21
2.10	Positive-sequence network with 1 A injected to a single bus r	22
2.11	The studied 4-bus power system.	35
3.1	The i^{th} -sequence network of a single-circuit unfaulted line.	42
3.2	The positive/negative-sequence network of a double-circuit faulted line.	42
3.3	The zero-sequence network of a double-circuit faulted line.	43
3.4	The positive/negative-sequence network of an unfaulted double-circuit line.	46
3.5	The zero-sequence network of an unfaulted double-circuit line.	46
3.6	The diagram of studied 4-bus power system with current indicated.	57
4.1	Mutually coupled zero-sequence networks of a parallel line.	64

4.2	Equivalent π model of the zero-sequence double-circuit line.	64
4.3	Pre-fault zero-sequence network.	75
4.4	Zero-sequence network with two additional fictitious buses.	76
4.5	Zero-sequence network with 1 A injected to a single bus k	77
4.6	Zero-sequence network with 1 A injected to bus r	79
4.7	Pre-fault positive-sequence network.	80
4.8	Positive-sequence network with additional fictitious buses.	81
4.9	Positive-sequence network with 1 A injected to bus r	83
4.10	Schematic diagram of the studied 27-bus system.	92
5.1	A schematic diagram of a series-compensated transmission line. . . .	102
5.2	The i^{th} -sequence transmission line with fault on the left side of series compensator.	103
5.3	Pre-fault positive-sequence series-compensated transmission line. . . .	105
5.4	The i^{th} -sequence transmission line with fault on the right side of series compensator.	106
5.5	V-I characteristic of MOV.	111

Chapter 1

Introduction

Power transmission lines play an important role in delivering power safely and continuously. Modern power systems cover a large geographic area and are exposed to external events and circumstances such as lightning, falling trees, dirt, animals, ice, etc. These events sometimes would cause faults rendering the lines out of service. Upon occurrence of the fault it is of vital importance for the utility company to send out the maintenance crew to repair the faulted component and to restore the service as soon as possible. The company's ability to do so relies on fast and accurate fault location.

There are eleven types of short-circuit faults that can occur on transmission lines: single line-to-ground faults (a-g, b-g, c-g), line-to-line faults (a-b, b-c, c-a), line-to-line-to-ground faults (a-b-g, b-c-g, c-a-g), and three-phase faults (a-b-c, a-b-c-g). Single line-to-ground faults are the most common type of fault usually caused by lightning stroke. Three-phase faults are the least common type of fault.

Most transmission lines possess a single-circuit line structure. On the other hand, in modern power systems double-circuit transmission lines have been increasingly adopted, mainly because they can improve the reliability and capacity of energy transmission. Due to the mutual coupling between the parallel lines it is still challenging to design an accurate fault location algorithm [1–3], despite the wider application of double-circuit lines.

The Series Compensator (SC) is a device that is sometimes installed for long transmission lines to improve power transfer capability, enhance power system stability, damp power system oscillations, etc. The SC device can be either a capacitor bank or a thyristor-based power-flow controller, which is usually protected by a Metal Oxide Varistor (MOV). For such series-compensated lines the harmonics and non-linearities introduced by the SC and its MOV make transmission line protection and fault location more difficult [4–7].

1.1 Analysis of Fault Location Algorithms

Many research efforts have been undertaken on fast and accurate fault location algorithms for single-circuit, double-circuit and series-compensated transmission lines.

They can be classified into the following four categories: phasor based, time-domain based, traveling-wave based, and others.

Phasor based algorithms take terminal voltage and/or current phasors as input. The method comprises one-terminal, two-terminal and multi-terminal algorithms [1–3, 8–23].

In high-speed tripping applications it is desirable for the fault location to be completed before the current disappears due to relay operations [24]. For phasor-based algorithms the acquisition of high-accuracy phasor estimates needs to obtain at least one cycle of data. Therefore the algorithms in this category are not fit for high-speed applications. Instead, some time-domain algorithms have been developed for single-circuit networks [24–28]. For example, [26] only requires a data window of 1/4 of a cycle, satisfying the requirement of high-speed fault location.

Represented by references [29, 30] the traveling-wave based algorithms use the return time of the reflected waves traveling from the fault point to the line terminal as a measure of distance to the fault. Other algorithms using wavelet techniques [31, 32], artificial neural networks [33–36], and support vector machines [37] have been developed as well.

In general these are the major sources of error in any fault location algorithm:

1. Line asymmetry. Algorithms developed under the assumption of the transposed lines are applied to untransposed lines, and will introduce errors in consequence.
2. Shunt capacitance. Most algorithms utilize the lumped parameter model which neglects the charging effect of the lines. However, for long transmission lines an exact representation of the line needs to fully consider shunt capacitance.
3. Fault resistance.
4. Load current.
5. Source impedances. In practical power systems the equivalent source impedance of every terminal changes continuously.

1.1.1 Review of Existing Double-Circuit Line Fault Location Algorithms

Diverse fault location algorithms designed for double-circuit lines have been developed in the past few decades and will be henceforth reviewed.

In the phasor-based fault location category, some methods utilize only one-terminal [38–46] data to locate a fault. The authors of [38] assume that the angles of a fault current and the fault current distribution from the load end are equal. They propose an algorithm that utilizes one-terminal voltage and current data. Because of their approximation the accuracy of their fault location is affected by the fault resistance and the asymmetrical arrangement of the transmission lines.

Eriksson et al. [39] employ phase voltages and currents from the near end of the faulted line, and a zero-sequence current from the near end of the healthy line as

input signals. To fully compensate the error introduced by the fault resistance (or the impact of the remote infeed), source impedance values are required.

Kawady and Stenzel [40] use a modal transformation to decouple the initially coupled transmission lines. Their method utilizes as input voltage and current phasors from a locally installed relay. Compared with Eriksson et al. [39], this algorithm does not need source impedances. It modifies the apparent impedance seen from the relay location. This is, however, based on the assumption that the line is homogeneous. Simulations show that the accuracy is still sufficient when the algorithm is applied to an untransposed structure. Also, the effects of load current, shunt capacitance and fault resistance are negligible for the purpose of fault location.

The authors of [41] construct a voltage equation from the local end through a faulty line to the fault point. Then they construct another voltage equation from the local end, through a sound line and a faulty path, to the fault point. The remote infeed can then be eliminated by inserting one equation into another. Then, three such equations for positive-, negative- and zero-sequence circuits are obtained. Next, based on the boundary conditions for different fault types, these three equations can be combined differently in order to solve for the fault resistance and the fault distance. Their algorithm is independent of fault resistance, load currents and source impedance. However, their model neglects shunt capacitance for long lines.

Non-earth faults on one of the circuits of parallel transmission lines are dealt with in [42]. Similar to [41], the authors establish three voltage equations from the local end via a faulty line to the fault point, based on three phase networks. Then these three equations are added, forming an equation with fault resistance and fault current as unknowns. Next, by applying the Kirchhoff voltage law (KVL) the fault current can be expressed as a function of fault distance. Solving for the fault resistance and the fault distance is then trivial. This algorithm is not influenced by fault resistance, load currents and source impedance. It, however, does not consider shunt capacitance, which will introduce errors for the fault location on long transmission lines.

The fault distance equations in [41, 42] all include the current phasors of the adjacent sound line's local-end, which are assumed known. However, in some practical systems such current phasors are not available. Similar to [42], Ahn et al. [43] also construct the voltage equations that contain the sought-after fault resistance and fault location. By introducing the concept of current distribution factors the influence of the load current is eliminated. Since their formula for calculating the fault distance includes both local and remote source impedances, errors are introduced. The algorithm, however, is robust enough since it is largely insensitive to the variation in source impedances.

J. Izykowski et al. [44] utilize all the voltage and current phasors of the local end from both the sound and the faulted lines as input. The zero-sequence impedance of a line will adversely influence the fault location accuracy. In their expression for the fault path voltage drop the weight of the zero-sequence fault current is set to zero to exclude the zero-sequence component. Since the fault distance formula does not contain any source impedances, the algorithm is not influenced by the varying source impedances nor by the fault resistance.

Using a technique similar to [41–44], [45] have developed a fault location algorithm

applicable to untransposed lines. It utilizes the lumped line model that ignores shunt capacitance. Because of that the accuracy of the algorithm is not guaranteed for long transmission lines. In summary [41–45] are similar in eliminating remote infeed. They achieve this by formulating appropriate KVL equations around the parallel lines loop.

A. J. Mazon et al. [46] introduce a new concept of *distance factor*, which is the ratio of the positive-sequence pre-fault currents of both the sound and faulted lines at the local end. By comparing this value to the one calculated from system parameters when fault occurred, the fault location can be evaluated. Their algorithm is not affected by fault resistance or load current. Also, fault type classification is not necessary. However, the method is sensitive to variations in source impedances.

Next we will review two-terminal and multi-terminal algorithms [47–51]. They usually provide more accurate fault location results than one-terminal algorithms, but require the synchronization of every terminal.

A. T. Johns et al. [47] provide a distributed-parameter based algorithm which fully considers the effect of shunt capacitance. It requires voltage and current phasors from both terminals of the faulted line. The algorithm is independent of fault resistance and source impedances. It does not require fault classification or synchronization of the two terminals. Although their method was designed for transposed lines, it also works satisfactorily when used for untransposed lines. The authors in [48] have proposed an iterative approach to improve the accuracy of fault distance estimation in [47].

D. J. Lawrence et al. [49] relate the voltage and current phasors of the sending and receiving ends with *ABCD parameters*, where the fault distance and fault resistance are included. For different types of fault different equations are derived. The synchronized phasors of two terminals are needed to feed the algorithm. The method can also be used for untransposed lines, and is independent of fault resistance and source impedances.

T. Nagasawa et al. [50] present an algorithm based on the lumped parameter model, which may introduce errors for long lines. Their procedure needs only the magnitude of the differential current of each terminal. It is the difference of the currents in both circuits measured at the same terminal. Since their method was developed for three-terminal parallel transmission lines, any n -terminal network must be converted to an equivalent three-terminal network first. Because only the magnitudes of differential currents are required, synchronization of the terminals is not necessary. Their algorithm is independent of fault resistance and of any source impedances. Furthermore, it does not demand fault classification. However, their approach is designed for transposed transmission lines only.

T. Funabashi et al. [51] have presented multi-terminal algorithms based on the lumped parameter model. Their algorithm 1 is based on an *impedance calculation* that makes use of phase current data at each terminal, phase voltage data at the locator terminal, and all the phase components of the line impedance. Algorithm 2 introduces the *current diversion ratio* method. It utilizes phase current data at each terminal and all the phase components of the line impedance. Both algorithms are applicable to all types of single-circuit or inter-circuit faults. The fault location is independent of fault resistance and the method does not require knowledge of

source impedances. Since the phase component of the line impedance is utilized it is suitable both for balanced and unbalanced lines. Fault classification is irrelevant for this algorithm, but synchronization of the terminal voltages and currents is needed.

In the realm of time-domain fault location methods, [52] decomposes the transmission lines into a common component net and a differential component net, each of which is a single-circuit network. For the differential component net the voltages at both terminals are zero. Based on the distributed parameter time-domain equivalent model, two voltage distributions along the line can be calculated from the two terminal currents, respectively. The proposed approach exploits the fact that the difference between these two voltages is smallest at the point of fault. The algorithm has the following advantages:

- A data window less than one cycle long, satisfying high-speed tripping requirements.
- No requirement to synchronize the two terminal currents.
- No need for voltage data.
- No source impedance exists in the differential component net.
- Independence from fault resistance.
- Full account of the influence of shunt capacitance.
- Suitable both for the transposed and untransposed lines.

All the existent algorithms for double-circuit transmission lines have different advantages. Unfortunately, these methods share a common drawback, namely that the measurements have to be taken from one or two terminals of the faulted section, or even at all the terminals of the entire network. From a practical point of view the data may not be available at the terminals of the faulted line, let alone from all the buses.

1.1.2 Review of Existing Fault Location Algorithms for Series-Compensated Lines

Various one-end and two-end fault location algorithms for series-compensated lines have been developed using synchronous or asynchronous data [53–56].

A one-end fault location algorithm using phase coordinates has been proposed in [53]. Based on the distributed time-domain model, two voltages are calculated from synchronized voltages and synchronized currents at two terminals. The fault distance is the point where these two voltages are equal [54]. A two-end unsynchronized fault location technique based on the distributed parameter line model is presented in [55].

Reference [56] presents a time-domain two-end algorithm that uses the lumped parameter model, ignoring the shunt and mutual capacitances. It estimates the instantaneous voltage drop across the compensation device.

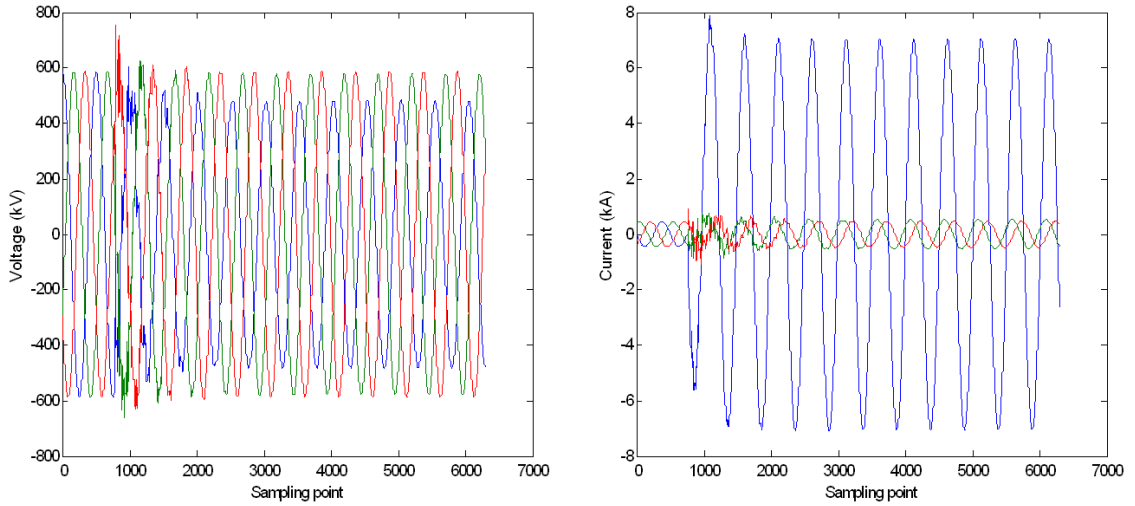


Figure 1.1: Voltage and current waveforms during a-g fault.

Summarizing, in these classical algorithms the calculation of the voltage drop across the compensation device relies on the equivalent model of the SCs & MOVs. This will inevitably introduce errors.

1.2 Objectives

In recent years intelligent instruments such as Digital Fault Recorder (DFR) and Phasor Measurement Unit (PMU) have been installed in power systems. These devices are able to provide highly accurate phasor measurements. The most prominent benefit brought by the PMU is the synchronization of phasors, which greatly simplifies the fault location problem and improves the fault location accuracy [13]. However, due to the expensive cost of these units they are only sparsely deployed in the networks. Having the field conditions in mind this dissertation focuses on a network analysis approach that is based on the bus impedance matrix technique. The approach leads to two kinds of accurate phasor-based fault location algorithms for double-circuit lines. They utilize sparse voltage phasors or current phasors, respectively.

A large number of monitoring devices such as power quality meters have been deployed in the systems. Some meters can only capture the voltage magnitude (also called voltage sag) or the current magnitude instead of phasors. The voltage and current waveforms at one terminal of a double-circuit line that has been affected by an a-g fault or an a-b-c fault are shown in Figs. 1.1 and 1.2, respectively.

The question how to exploit magnitude data in locating faults is of practical significance. Algorithms that use voltage or current magnitudes for fault location on double-circuit lines have been extensively explored in this dissertation.

In an effort to precisely locate the fault on series-compensated single-circuit transmission lines, a novel method employing two-terminal unsynchronized voltage and current phasors has been devised. In contrast to established methods this ansatz

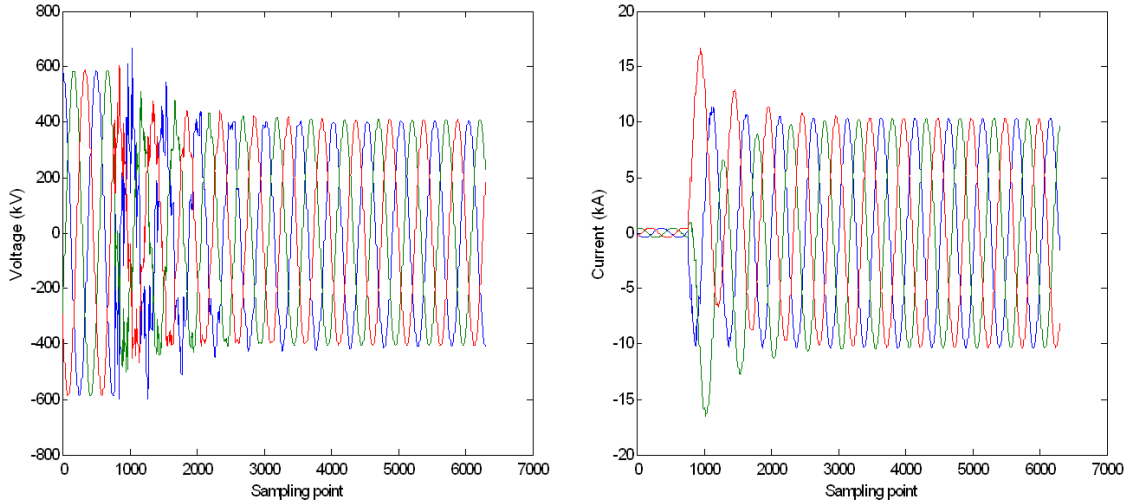


Figure 1.2: Voltage and current waveforms during a-b-c fault.

avoids the use of the equivalent voltage-current (V-I) model of SCs & MOVs.

1.3 Proposed New Methods

The fundamental principle of the proposed fault location method for double-circuit lines is to add to the original network a fictitious bus where the fault occurs. Hence, the bus impedance matrix is augmented by one order. Then, the driving point impedance of the fault bus and the transfer impedances between this bus and other buses are expressed as functions of the unknown fault distance. Based on the definition of the bus impedance matrix, the change of the sequence voltage at any bus during the fault is formulated in terms of the corresponding transfer impedance and sequence fault current. Depending on the boundary conditions for different fault types, we can obtain the fault location equation using voltage phasors as input.

Two chapters of this dissertation are dedicated to fault location algorithms that use voltage phasors. Those based on the lumped parameter line model are investigated in Chapter 2, whereas those adopting the distributed parameter line model instead, are addressed in Chapter 4.

When the relationships between phase and sequence voltages/currents are established through symmetrical component theory, we can use phase voltage magnitudes to solve the fault location problem. This will be discussed in Chapter 2.

Based on the same augmented bus impedance matrix, *Voltage and Current Relation* (VCR) are employed. Now the change of the current at any branch can be expressed as a function of the relevant fault current and the transfer impedance terms associated with the two ends of the branch. With this result, fault location algorithms based on either current phasors or phase current magnitudes are developed in this dissertation. A complete description of this subject is given in Chapter 3.

I have employed the distributed parameter line model for fault location in series-

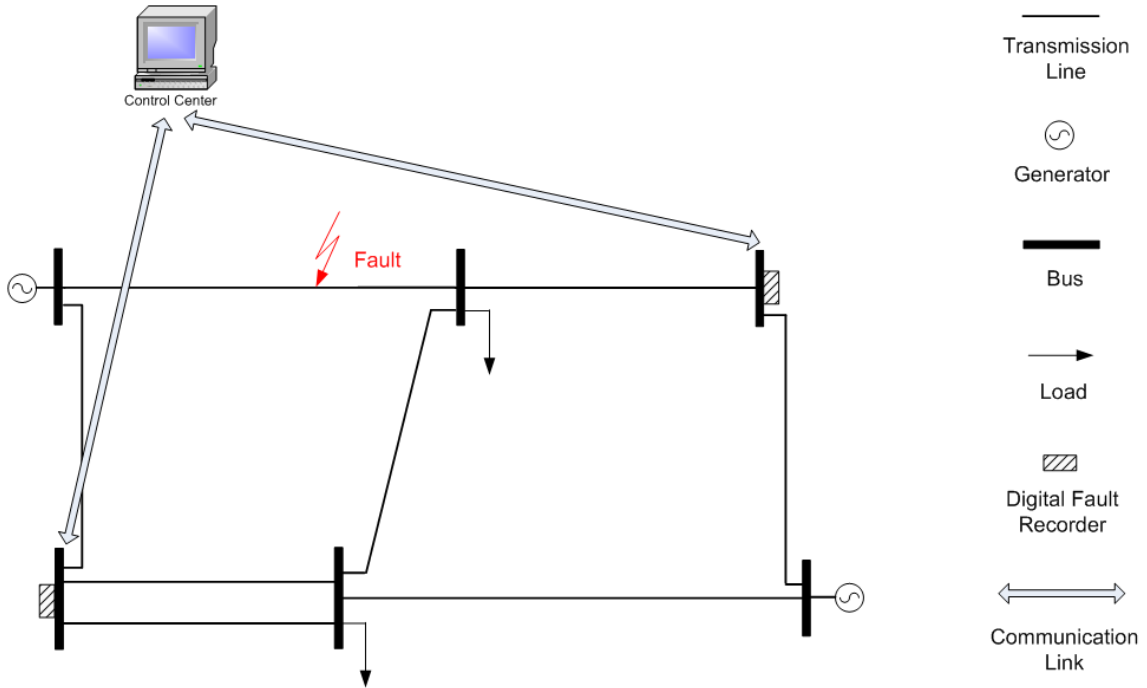


Figure 1.3: A sample wide area monitoring system.

compensated single-circuit lines. It takes fully into account the shunt capacitance. With different boundary conditions for the various fault types, the unknown fault location can be obtained by properly formulating the fault currents and voltages at the fault point. Two subroutines assuming that the fault occurs on either side of the series compensator are developed. A prescription to distinguish the correct fault location from the erroneous one is provided. The details of this topic are presented in Chapter 5.

1.4 Summary

In summary, prompt and accurate location of a fault is imperative to reduce power outage time, customer complaints, and loss of revenue for utility companies.

A major complication to these goals is that most existing fault location methods for single- and double-circuit transmission lines require measurements from one or two terminals of the faulted section itself. Some algorithms even necessitate data from all the terminals in the network. When faced with the real-life scenario that only sparse measurements are available, these methods are no longer qualified. As a solution to this discrepancy, this research has implemented fault location with sparse data for double-circuit transmission lines, with the bus impedance matrix technique at its heart. This work is an important application of Wide Area Monitoring Systems (WAMS) as shown in Fig. 1.3.

The fault location method proposed for series-compensated lines is ignorant of the

non-linearities of the SC and its MOV. This greatly improves the precision of fault location. Moreover, this approach does not demand synchronization of measurements of the two terminals, thus largely reducing the burden of network communication.

Chapter 2

Fault Location Using Sparse Voltage Measurements Based on Lumped Parameter Line Model

This chapter is outlined as follow. First of all, the proposed fault location method will be briefly introduced, followed by the fault location basis in Section 2.2. Next, the fault location method utilizing sparse voltage measurements based on lumped parameter line model is presented in Section 2.3. The proposed algorithms are examined in the simulation studies based on a 4-bus system in Section 2.4. At last, Section 2.5 completes this chapter with the concluding remarks.

2.1 Introduction

Diverse fault location algorithms on double-circuit lines have been developed in the past several decades. In general, existing algorithms require voltages and/or currents from one or two terminals of the faulted section or all the terminals of the network. For the scenario where only sparse measurements, which may be far away from the faulted section, are available, these methods are not suitable any more. Reference [57] has filled this gap by proposing a novel fault location method for single-circuit lines based on the bus impedance matrix technique. The distinctive characteristic of this method is that it only demands voltage measurements from one or two buses, which may be distant from the faulted line. As a supplement to the work in [57], the scenarios where only voltage magnitudes are available are addressed in [58].

Drawing on the bus impedance matrix technique adopted in [57, 58], this chapter further develops novel fault location algorithms for double-circuit lines based on the lumped parameter line model. Depending on the input of the method, fault location techniques utilizing voltage phasor measurements [59, 60] and phase voltage magnitudes [61] are implemented, respectively.

The measurements could be from one or more buses and do not need to be taken from the faulted line. The work is based on the assumption that the network data are known and the network is transposed. In addition, it is assumed that the faulted

section can be decided before hand based on relay operations. Fault type classification result, if necessary, is available. The proposed method is applicable for fundamental frequency phasors, to which all the voltage and current quantities refer throughout the dissertation.

2.2 Fault Location Basis

First of all, the common notations applicable to Chapter 2 and 3 are summarized as follows:

- n total number of buses of the pre-fault network;
- m unknown per-unit fault distance from bus p ;
- p, q buses of the faulted section;
- r fictitious bus representing the fault point and $r = n + 1$;
- i symmetrical component index; $i = 0, 1, 2$ for zero-, positive- and negative-sequence, respectively, put in parenthesis as a superscript throughout the work;
- $z_{j_1 j_2}^{(i)}$ i^{th} -sequence total self-series impedance of the single-circuit line between buses j_1 and j_2 ;
- $z_{j_1 j_2-1}^{(i)}$ i^{th} -sequence total self-series impedance of the first line of the parallel lines sharing two common terminals j_1 and j_2 ;
- $z_{j_1 j_2-2}^{(i)}$ i^{th} -sequence total self-series impedance of the second line of the parallel lines sharing two common terminals j_1 and j_2 ;
- $z_{j_1 j_2-m}^{(0)}$ zero-sequence total mutual-series impedance between the parallel lines sharing two common terminals j_1 and j_2 ;
- $Z_0^{(i)}$ bus impedance matrix of the pre-fault i^{th} -sequence network. It has the size n by n , whose element on the k_1^{th} row and k_2^{th} column is denoted as $Z_{0, k_1 k_2}^{(i)}$;
- $Z^{(i)}$ bus impedance matrix of the i^{th} -sequence network with the addition of fictitious fault bus r . It has a size of $n + 1$ by $n + 1$, whose element on the k_1^{th} row and k_2^{th} column is denoted by $Z_{k_1 k_2}^{(i)}$.

The bus impedance matrix of the pre-fault system, $Z_0^{(i)}$, can be built easily from network parameters [62, 63]. $Z^{(i)}$ is the function of unknown fault distance m and to be constructed upon $Z_0^{(i)}$ and network parameters. Suppose the fault occurs on the second branch of the parallel lines.

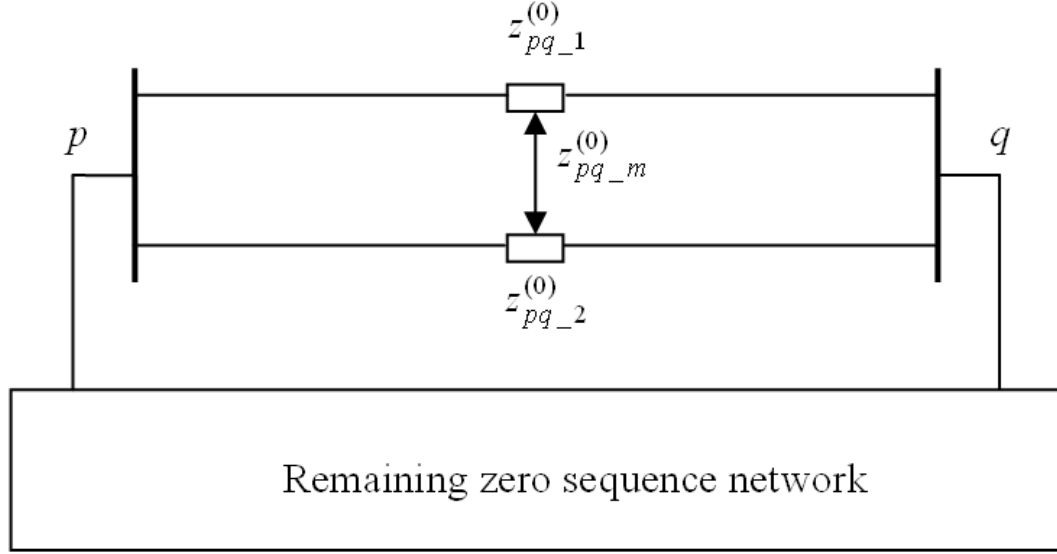


Figure 2.1: Pre-fault zero-sequence network.

2.2.1 Construction of Bus Impedance Matrix with Addition of the Fault Bus

The construction of bus impedance matrix with addition of the fault bus for zero-sequence network is first considered. The pre-fault zero-sequence network of a sample power system with the faulted section extracted is shown in Fig. 2.1, whose bus impedance matrix $Z_0^{(0)}$ is assumed to be already developed using well established techniques [62, 63]. The network with an additional fault bus on the faulted line is modeled as in Fig. 2.2, whose bus impedance matrix is $Z^{(0)}$.

To formulate $Z^{(0)}$, we first construct the bus impedance matrix $Z_1^{(0)}$ of the network in Fig. 2.3, which removes the branch with impedance $z_{pq_2}^{(0)}$ from Fig. 2.1. Note that the mutual impedance $z_{pq_m}^{(0)}$ between these two branches is removed as well. $Z_1^{(0)}$ can be constructed as follows [64]

$$Z_{1,kl}^{(0)} = Z_{0,kl}^{(0)} - \frac{L_0(k)L_0(l)}{Z_{c1}}, \quad k, l = 1, 2, \dots, n \quad (2.1)$$

where

$$\begin{bmatrix} y_a^{(0)} & y_m^{(0)} \\ y_m^{(0)} & y_b^{(0)} \end{bmatrix} = \begin{bmatrix} z_{pq_1}^{(0)} & z_{pq_m}^{(0)} \\ z_{pq_m}^{(0)} & z_{pq_2}^{(0)} \end{bmatrix}^{-1} \quad (2.2)$$

$$Z_{c1} = (Z_{0,pp}^{(0)} + Z_{0,qq}^{(0)} - 2Z_{0,pq}^{(0)}) \cdot [1 - z_{pq_m}^{(0)}(y_a^{(0)} + y_m^{(0)})]^2 - y_a^{(0)}(z_{pq_m}^{(0)})^2 - z_{pq_2}^{(0)} \quad (2.3)$$

$$L_0(k) = [1 - z_{pq_m}^{(0)}(y_a^{(0)} + y_m^{(0)})] \cdot (Z_{0,kp}^{(0)} - Z_{0,kq}^{(0)}), \quad k = 1, 2, \dots, n \quad (2.4)$$

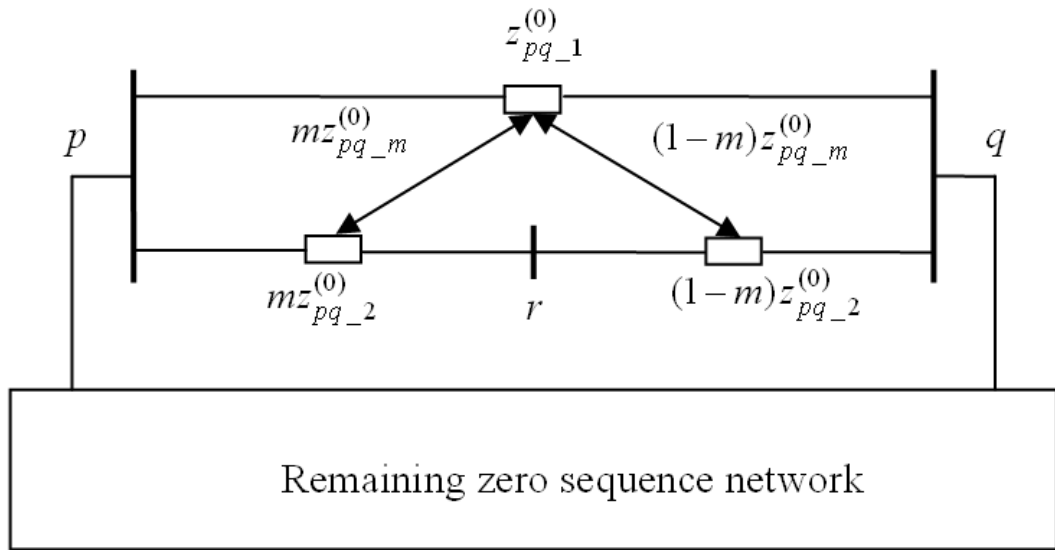


Figure 2.2: Zero-sequence network with an additional fault bus.

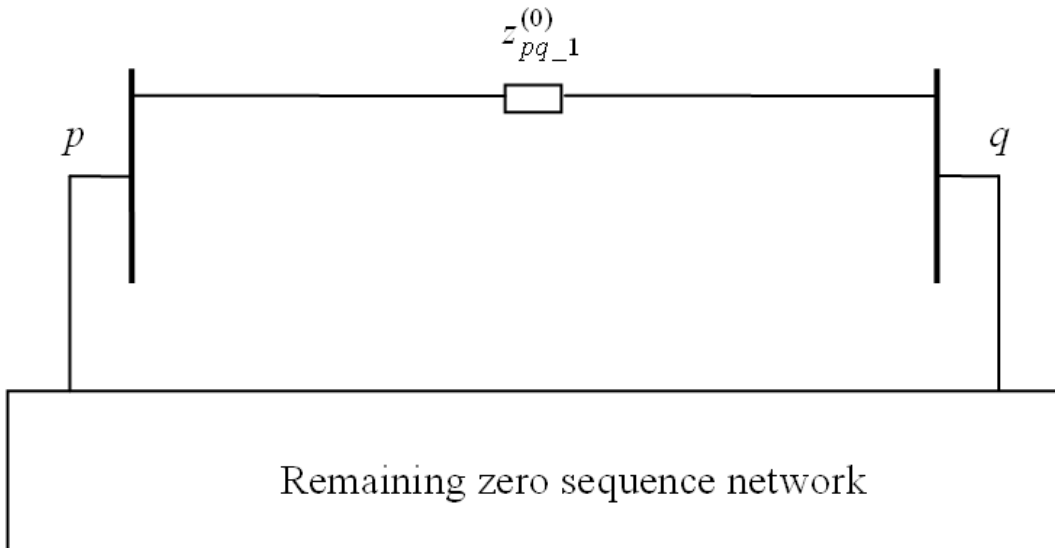


Figure 2.3: Zero-sequence network with a branch removed.

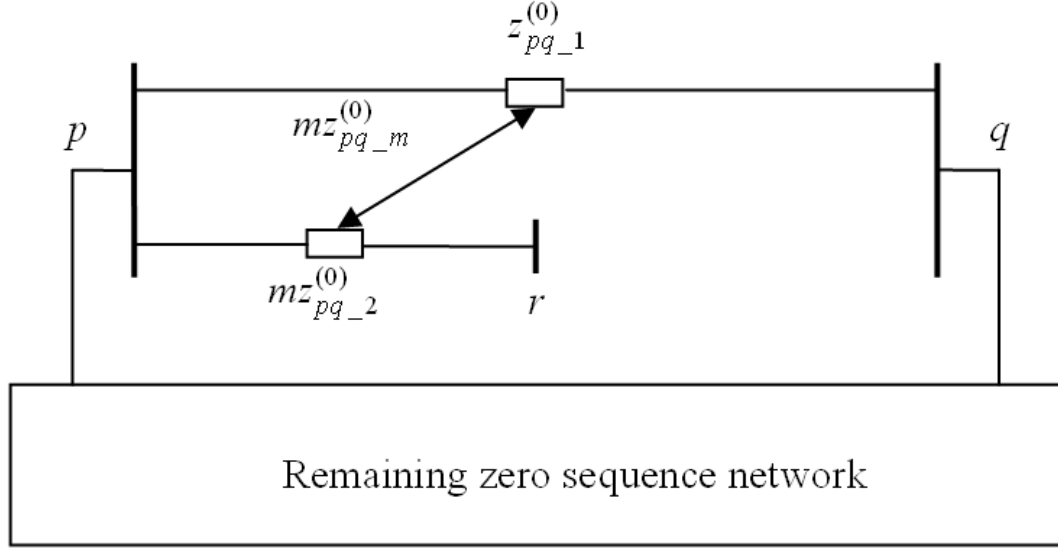


Figure 2.4: Zero-sequence network with addition of branch pr .

It can be seen that $Z_1^{(0)}$ is still a n by n matrix and is not a function of m . Next, we can add a new bus r to Fig. 2.3 and the self impedance of branch pr is $mz_{pq-2}^{(0)}$. The mutual impedance between pr and $pq-1$ is $mz_{pq-m}^{(0)}$ as shown in Fig. 2.4.

The bus impedance matrix of the network shown in Fig. 2.4 is $Z_2^{(0)}$, which has the following structure [64]

$$Z_2^{(0)} = \begin{bmatrix} Z_1^{(0)} & L_1 \\ L_1^T & Z_{2,rr}^{(0)} \end{bmatrix}_{(n+1)(n+1)} \quad (2.5)$$

where

$$L_1(k) = F_k + mG_k, \quad k = 1, 2, \dots, n$$

$$Z_{2,rr}^{(0)} = A_3 + A_4m + A_5m^2$$

$$F_k = Z_{1,kp}^{(0)}$$

$$G_k = \frac{z_{pq-m}^{(0)}}{z_{pq-1}^{(0)}} (Z_{1,kq}^{(0)} - Z_{1,kp}^{(0)})$$

$$A_3 = Z_{1,pp}^{(0)}$$

$$A_4 = \frac{2z_{pq-m}^{(0)}}{z_{pq-1}^{(0)}} (Z_{1,pq}^{(0)} - Z_{1,pp}^{(0)}) + z_{pq-2}^{(0)}$$

$$A_5 = \left(\frac{z_{pq-m}^{(0)}}{z_{pq-1}^{(0)}} \right)^2 (Z_{1,pp}^{(0)} + Z_{1,qq}^{(0)} - 2Z_{1,pq}^{(0)}) - \frac{(z_{pq-m}^{(0)})^2}{z_{pq-1}^{(0)}}$$

Upon Fig. 2.4, a branch qr with self impedance $(1-m)z_{pq-2}^{(0)}$ is added, and it has mutual impedance $(1-m)z_{pq-m}^{(0)}$ with the branch $pq-1$ as shown in Fig. 2.2. The bus impedance matrix of the network in Fig. 2.2, which is desired, can be constructed as follows

$$Z_{kl}^{(0)} = Z_{1,kl}^{(0)} - \frac{L_2(k)L_2(l)}{Z_{c2}}, \quad k, l = 1, 2, \dots, n \quad (2.6)$$

$$Z_{rk}^{(0)} = B_k^{(0)} + C_k^{(0)}m, \quad k = 1, 2, \dots, n \quad (2.7)$$

$$Z_{rr}^{(0)} = A_0^{(0)} + A_1^{(0)}m + A_2^{(0)}m^2 \quad (2.8)$$

where

$$L_2(k) = (Z_{1,kq}^{(0)} - Z_{1,kp}^{(0)}) \left(\frac{z_{pq-m}^{(0)}}{z_{pq-1}^{(0)}} - 1 \right), \quad k = 1, 2, \dots, n \quad (2.9)$$

$$Z_{c2} = \left(\frac{z_{pq-m}^{(0)}}{z_{pq-1}^{(0)}} - 1 \right)^2 (Z_{1,pp}^{(0)} + Z_{1,qq}^{(0)} - 2Z_{1,pq}^{(0)}) + z_{pq-2}^{(0)} - \frac{(z_{pq-m}^{(0)})^2}{z_{pq-1}^{(0)}} \quad (2.10)$$

$$B_k^{(0)} = F_k - \frac{A_6 L_2(k)}{Z_{c2}} \quad (2.11)$$

$$C_k^{(0)} = G_k - \frac{A_7 L_2(k)}{Z_{c2}} \quad (2.12)$$

$$A_0^{(0)} = A_3 - \frac{(A_6)^2}{Z_{c2}} \quad (2.13)$$

$$A_1^{(0)} = A_4 - \frac{2A_6 A_7}{Z_{c2}} \quad (2.14)$$

$$A_2^{(0)} = A_5 - \frac{(A_7)^2}{Z_{c2}} \quad (2.15)$$

$$A_6 = (Z_{1,pq}^{(0)} - Z_{1,pp}^{(0)}) \left(\frac{z_{pq-m}^{(0)}}{z_{pq-1}^{(0)}} - 1 \right) \quad (2.16)$$

$$A_7 = \frac{z_{pq-m}^{(0)}}{z_{pq-1}^{(0)}} \left(\frac{z_{pq-m}^{(0)}}{z_{pq-1}^{(0)}} - 1 \right) (Z_{1,pp}^{(0)} + Z_{1,qq}^{(0)} - 2Z_{1,pq}^{(0)}) + z_{pq-2}^{(0)} - \frac{(z_{pq-m}^{(0)})^2}{z_{pq-1}^{(0)}} \quad (2.17)$$

Now, let's consider the construction of bus impedance matrix with addition of a fictitious fault bus for positive-sequence networks. The positive-sequence network of a sample power system is shown in Fig. 2.5 and the network with an additional fault

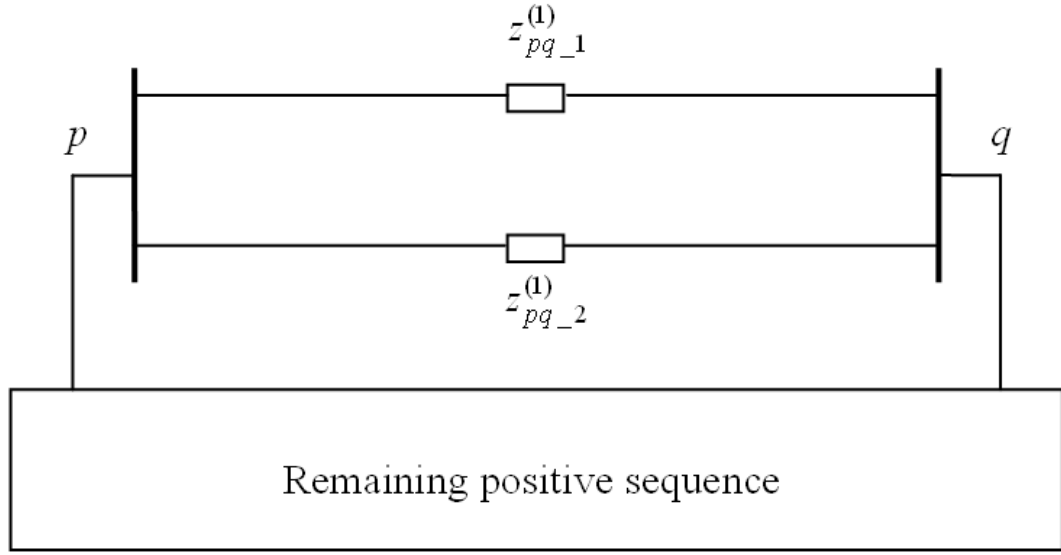


Figure 2.5: Pre-fault positive-sequence network.

bus is modeled in Fig. 2.6. Similarly, the bus impedance matrix of the network in Fig. 2.5 is denoted as $Z_0^{(1)}$ and can be readily developed. $Z^{(1)}$ is the bus impedance matrix for the network in Fig. 2.6 and can be constructed following the procedure for zero-sequence network. In fact, since there is no mutual coupling between the two parallel lines in the positive-sequence network, $Z^{(1)}$ can be constructed in the exact same way as that for a single-circuit line network shown in [57, 65]. $Z^{(1)}$ can be expressed as follows [65]

$$Z_{kl}^{(1)} = Z_{1,kl}^{(1)} - \frac{(Z_{1,kp}^{(1)} - Z_{1,kq}^{(1)})(Z_{1,lp}^{(1)} - Z_{1,lq}^{(1)})}{D^{(1)}}, \quad k, l = 1, 2, \dots, n \quad (2.18)$$

$$Z_{rk}^{(1)} = B_k^{(1)} + C_k^{(1)} m, \quad k = 1, 2, \dots, n \quad (2.19)$$

$$Z_{rr}^{(1)} = A_0^{(1)} + A_1^{(1)} m + A_2^{(1)} m^2 \quad (2.20)$$

where

$$B_k^{(1)} = Z_{1,kp}^{(1)} - \frac{(Z_{1,kp}^{(1)} - Z_{1,kq}^{(1)})(Z_{1,pp}^{(1)} - Z_{1,pq}^{(1)})}{D^{(1)}} \quad (2.21)$$

$$C_k^{(1)} = -\frac{(Z_{1,kp}^{(1)} - Z_{1,kq}^{(1)})z_{pq_2}^{(1)}}{D^{(1)}} \quad (2.22)$$

$$A_0^{(1)} = Z_{1,pp}^{(1)} - \frac{(Z_{1,pp}^{(1)} - Z_{1,pq}^{(1)})^2}{D^{(1)}} \quad (2.23)$$

$$A_1^{(1)} = z_{pq_2}^{(1)} \left[1 - \frac{2(Z_{1,pp}^{(1)} - Z_{1,pq}^{(1)})}{D^{(1)}} \right] \quad (2.24)$$

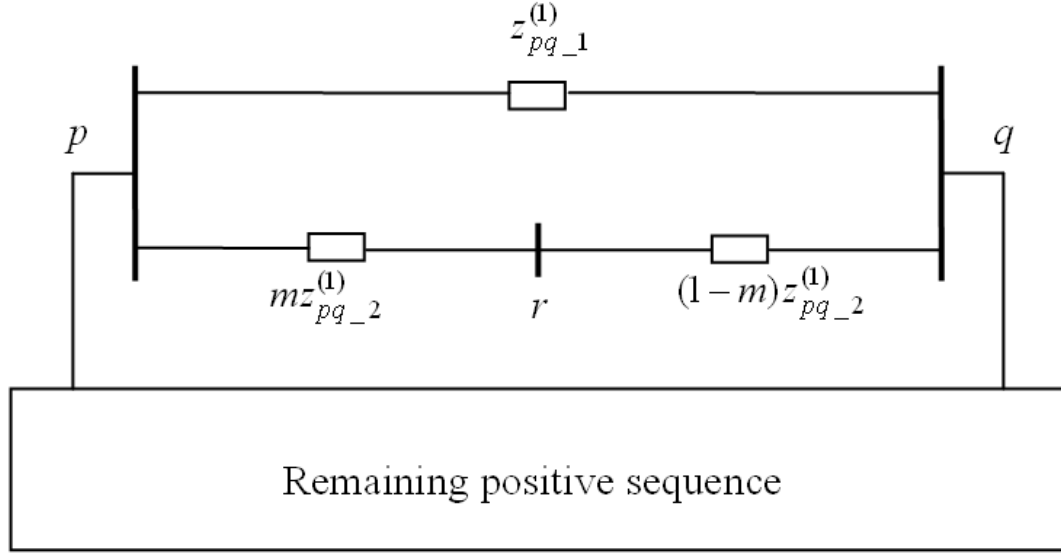


Figure 2.6: Positive-sequence network with an additional fault bus.

$$A_2^{(1)} = -\frac{(z_{pq_2}^{(1)})^2}{D^{(1)}} \quad (2.25)$$

$$D^{(1)} = Z_{1,pp}^{(1)} + Z_{1,qq}^{(1)} - 2Z_{1,pq}^{(1)} + z_{pq_2}^{(1)} \quad (2.26)$$

$$Z_{1,kl}^{(1)} = Z_{0,kl}^{(1)} - \frac{(Z_{0,kp}^{(1)} - Z_{0,kq}^{(1)})(Z_{0,lp}^{(1)} - Z_{0,lq}^{(1)})}{D_0^{(1)}}, \quad k, l = 1, 2, \dots, n \quad (2.27)$$

$$D_0^{(1)} = Z_{0,pp}^{(1)} + Z_{0,qq}^{(1)} - 2Z_{0,pq}^{(1)} - z_{pq_2}^{(1)} \quad (2.28)$$

It is assumed that the parameters are the same for positive- and negative-sequence networks, thus we have $Z^{(2)} = Z^{(1)}$. Here $Z^{(2)}$ represents the bus impedance matrix with an additional fault bus for the negative-sequence network.

It has been demonstrated that : (1) the first n by n sub-matrix of the bus impedance matrix $Z^{(i)}$ is determined by network parameters and has nothing to do with unknown fault location m ; (2) the expressions of the transfer impedance $Z_{kr}^{(i)}$ and the driving-point impedance $Z_{rr}^{(i)}$ for the zero-sequence network take on similar form as for the positive-sequence network, with the former being the linear function of unknown fault location m and the later being the quadratic function of m .

2.2.2 Alternative Way of Construction of Bus Impedance Matrix with Addition of the Fault Bus

A concept method to build the augmented bus impedance matrix has been proposed in [57] for single-circuit lines. In this part, similar idea has been adopted to investigate

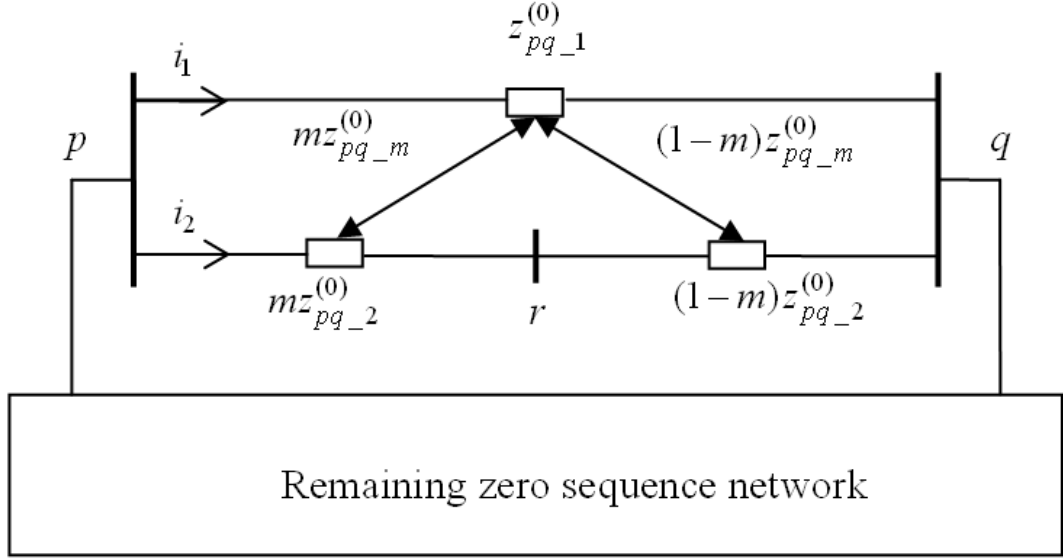


Figure 2.7: Zero-sequence network with 1 A injected to bus k .

the alternative way to build the bus impedance matrix with additional fictitious fault bus for double-circuit lines.

To formulate $Z^{(0)}$, we can inject a single current source into bus l ($l = 1, 2, \dots, n$), then the induced voltage at bus k ($k = 1, 2, \dots, n$) will be the same for the networks shown in Fig. 2.1 and Fig. 2.2. Based on the definition of bus impedance matrix, it is obtained that $Z_{kl}^{(0)} = Z_{0,kl}^{(0)}$, ($k, l = 1, 2, \dots, n$). Thus we have

$$Z^{(0)} = \begin{bmatrix} Z_{0,11}^{(0)} & \cdots & Z_{0,1l}^{(0)} & \cdots & Z_{0,1n}^{(0)} & Z_{1r}^{(0)} \\ \vdots & \ddots & \vdots & \ddots & \vdots & \vdots \\ Z_{0,k1}^{(0)} & \cdots & Z_{0,kl}^{(0)} & \cdots & Z_{0,kn}^{(0)} & Z_{kr}^{(0)} \\ \vdots & \ddots & \vdots & \ddots & \vdots & \vdots \\ Z_{0,n1}^{(0)} & \cdots & Z_{0,nl}^{(0)} & \cdots & Z_{0,nn}^{(0)} & Z_{nr}^{(0)} \\ Z_{r1}^{(0)} & \cdots & Z_{rl}^{(0)} & \cdots & Z_{rn}^{(0)} & Z_{rr}^{(0)} \end{bmatrix} \quad (2.29)$$

Therefore, to fully obtain $Z^{(0)}$, only its last row and column need to be calculated. In order to derive $Z_{kr}^{(0)}$, inject a current source of 1 Ampere into a single bus k ($k = 1, 2, \dots, n$) as shown in Fig. 2.7. i_1, i_2 denote the current flowing from bus p to q and r , respectively.

Making use of the bus impedance matrix in (2.29), the voltages at buses p, q and r in Fig. 2.7 will be

$$V_p = Z_{0,pk}^{(0)}, \quad V_q = Z_{0,qk}^{(0)}, \quad V_r = Z_{rk}^{(0)} \quad (2.30)$$

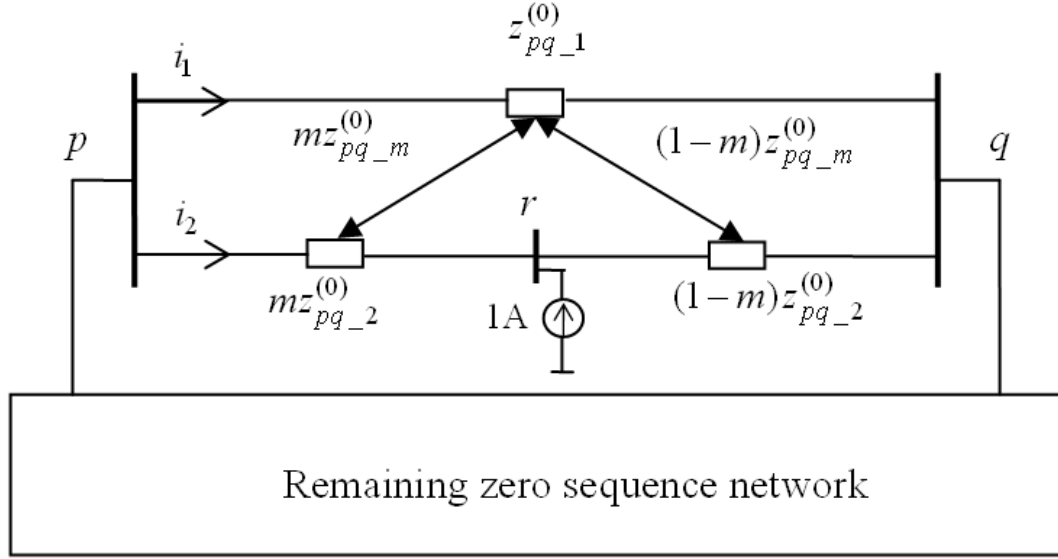


Figure 2.8: Zero-sequence network with 1 A injected into bus r .

From Fig. 2.7, the following three equations hold

$$V_p - V_r = mz_{pq-2}^{(0)}i_2 + mz_{pq-m}^{(0)}i_1 \quad (2.31)$$

$$V_r - V_q = (1-m)z_{pq-2}^{(0)}i_2 + (1-m)z_{pq-m}^{(0)}i_1 \quad (2.32)$$

$$V_p - V_q = z_{pq-1}^{(0)}i_1 + z_{pq-m}^{(0)}i_2 \quad (2.33)$$

Solving (2.31)-(2.33), the following arrives

$$V_r = V_p - m(V_p - V_q) \quad (2.34)$$

Substituting (2.30) into (2.34), it is obtained that

$$Z_{rk}^{(0)} = Z_{0,pk}^{(0)} - m(Z_{0,pk}^{(0)} - Z_{0,qk}^{(0)}), \quad k = 1, 2, \dots, n \quad (2.35)$$

Define

$$B_k^{(0)} = Z_{0,pk}^{(0)} \quad (2.36)$$

$$C_k^{(0)} = Z_{0,qk}^{(0)} - Z_{0,pk}^{(0)} \quad (2.37)$$

Then we have

$$Z_{rk}^{(0)} = B_k^{(0)} + C_k^{(0)}m, \quad k = 1, 2, \dots, n \quad (2.38)$$

For the derivation of $Z_{rr}^{(0)}$, inject one current source of 1 Ampere into bus r as shown in Fig. 2.8. Employing the bus impedance matrix in (2.29), the voltages at

buses p , q and r in Fig. 2.8 will be

$$V_p = Z_{pr}^{(0)}, \quad V_q = Z_{qr}^{(0)}, \quad V_r = Z_{rr}^{(0)} \quad (2.39)$$

From Fig. 2.8, the following equations hold

$$V_p - V_r = mz_{pq-2}^{(0)}i_2 + mz_{pq-m}^{(0)}i_1 \quad (2.40)$$

$$V_r - V_q = (1-m)z_{pq-2}^{(0)}(i_2 + 1) + (1-m)z_{pq-m}^{(0)}i_1 \quad (2.41)$$

$$V_p - V_q = z_{pq-1}^{(0)}i_1 + mz_{pq-m}^{(0)}i_2 + (1-m)z_{pq-m}^{(0)}(i_2 + 1) \quad (2.42)$$

Solving (2.40)-(2.42) results in

$$V_r = (1-m)V_p + mV_q + m(1-m)z_{pq-2}^{(0)} \quad (2.43)$$

Substituting (2.39) into (2.43), we have:

$$Z_{rr}^{(0)} = (1-m)Z_{pr}^{(0)} + mZ_{qr}^{(0)} + m(1-m)z_{pq-2}^{(0)} \quad (2.44)$$

where $Z_{pr}^{(0)}$ and $Z_{qr}^{(0)}$ can be obtained by letting k as p and q in (2.35). Thus we further have

$$Z_{rr}^{(0)} = Z_{0,pp}^{(0)} + m(2Z_{0,pq}^{(0)} - 2Z_{0,pp}^{(0)} + z_{pq-2}^{(0)}) + m^2(Z_{0,pp}^{(0)} + Z_{0,qq}^{(0)} - 2Z_{0,pq}^{(0)} - z_{pq-2}^{(0)}) \quad (2.45)$$

Define

$$A_0^{(0)} = Z_{0,pp}^{(0)} \quad (2.46)$$

$$A_1^{(0)} = 2Z_{0,pq}^{(0)} - 2Z_{0,pp}^{(0)} + z_{pq-2}^{(0)} \quad (2.47)$$

$$A_2^{(0)} = Z_{0,pp}^{(0)} + Z_{0,qq}^{(0)} - 2Z_{0,pq}^{(0)} - z_{pq-2}^{(0)} \quad (2.48)$$

Thus, we have

$$Z_{rr}^{(0)} = A_0^{(0)} + A_1^{(0)}m + A_2^{(0)}m^2 \quad (2.49)$$

For the positive/negative-sequence network, to formulate $Z^{(1)}$, injecting a single current source into bus l ($l = 1, 2, \dots, n$), then the induced voltages at bus k ($k = 1, 2, \dots, n$) will be the same for the networks shown in Fig. 2.5 and Fig. 2.6. Based on the definition of bus impedance matrix, it is obtained that $Z_{kl}^{(1)} = Z_{0,kl}^{(1)}$, ($k, l = 1, 2, \dots, n$). Thus we have

$$Z^{(1)} = \begin{bmatrix} Z_{0,11}^{(1)} & \cdots & Z_{0,1l}^{(1)} & \cdots & Z_{0,1n}^{(1)} & Z_{1r}^{(1)} \\ \vdots & \ddots & \vdots & \ddots & \vdots & \vdots \\ Z_{0,k1}^{(1)} & \cdots & Z_{0,kl}^{(1)} & \cdots & Z_{0,kn}^{(1)} & Z_{kr}^{(1)} \\ \vdots & \ddots & \vdots & \ddots & \vdots & \vdots \\ Z_{0,n1}^{(1)} & \cdots & Z_{0,nl}^{(1)} & \cdots & Z_{0,nn}^{(1)} & Z_{nr}^{(1)} \\ Z_{r1}^{(1)} & \cdots & Z_{rl}^{(1)} & \cdots & Z_{rn}^{(1)} & Z_{rr}^{(1)} \end{bmatrix} \quad (2.50)$$

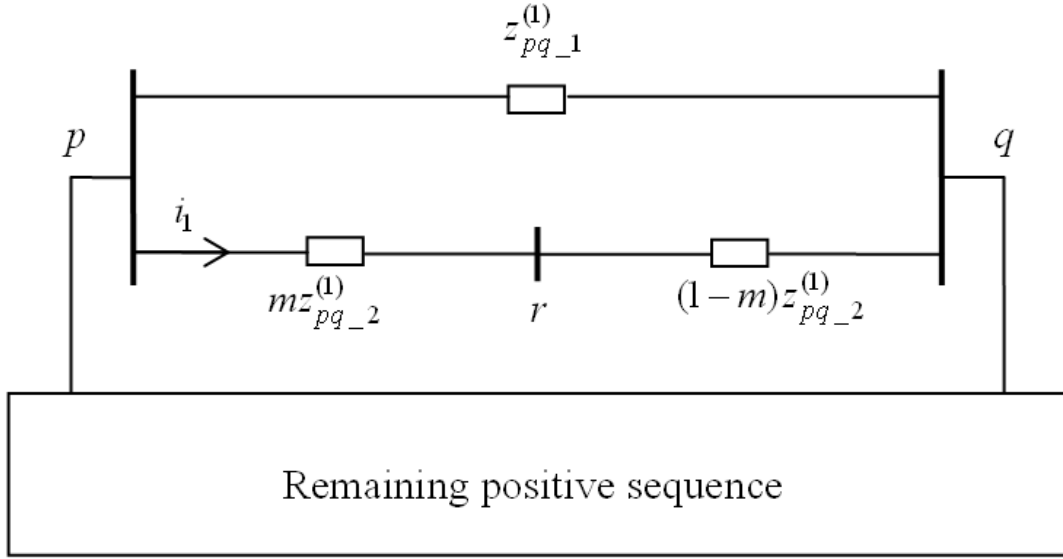


Figure 2.9: Positive-sequence network with 1 A injected to a single bus k .

In order to derive $Z_{kr}^{(1)}$, inject a current source of 1 Ampere into a single bus k , ($k = 1, 2, \dots, n$) as shown in Fig. 2.9. i_1 denotes the current flowing from bus p to r .

Making use of the bus impedance matrix in (2.50), the voltages at buses p , q and r in Fig. 2.9 will be

$$V_p = Z_{0,pk}^{(1)}, \quad V_q = Z_{0,qk}^{(1)}, \quad V_r = Z_{rk}^{(1)} \quad (2.51)$$

From Fig. 2.9, the following two equations hold

$$V_p - V_r = mz_{pq-2}^{(1)}i_1 \quad (2.52)$$

$$V_p - V_q = z_{pq-2}^{(1)}i_1 \quad (2.53)$$

Solving (2.52)-(2.53), the following arrives

$$V_r = V_p - m(V_p - V_q) \quad (2.54)$$

Substituting (2.51) into (2.54), it is obtained that

$$Z_{rk}^{(1)} = Z_{0,pk}^{(1)} - m(Z_{0,pk}^{(1)} - Z_{0,qk}^{(1)}), \quad k = 1, 2, \dots, n \quad (2.55)$$

Define

$$B_k^{(1)} = Z_{0,pk}^{(1)} \quad (2.56)$$

$$C_k^{(1)} = Z_{0,qk}^{(1)} - Z_{0,pk}^{(1)} \quad (2.57)$$

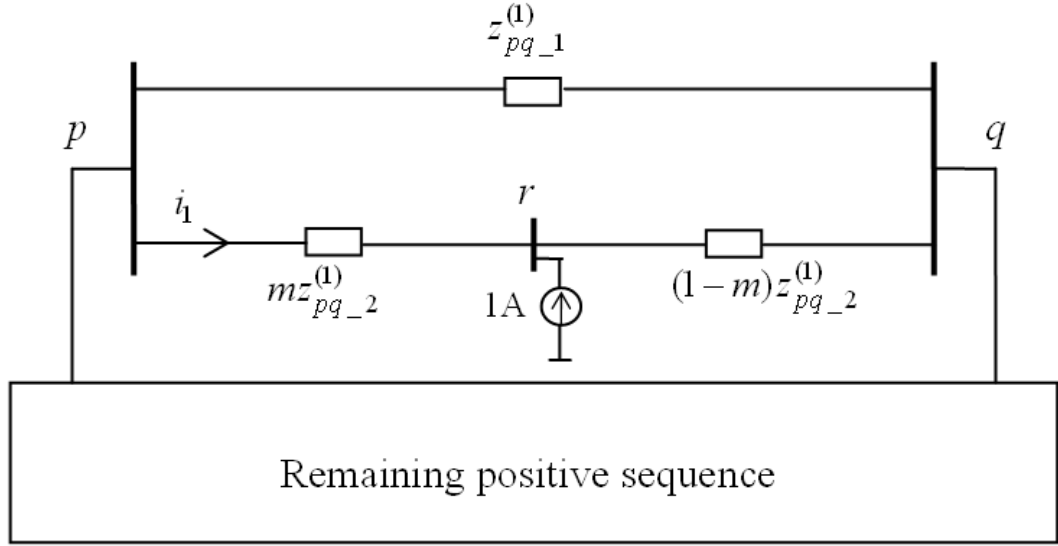


Figure 2.10: Positive-sequence network with 1 A injected to a single bus r .

Then we have

$$Z_{rk}^{(1)} = B_k^{(1)} + C_k^{(1)}m, \quad k = 1, 2, \dots, n \quad (2.58)$$

For the derivation of $Z_{rr}^{(0)}$, inject one current source of 1 Ampere into bus r as shown in Fig. 2.10. Employing the bus impedance matrix in (2.50), the voltages at buses p , q and r in Fig. 2.10 will be:

$$V_p = Z_{pr}^{(1)}, \quad V_q = Z_{qr}^{(1)}, \quad V_r = Z_{rr}^{(1)} \quad (2.59)$$

From Fig. 2.10, the following equations hold

$$V_p - V_r = mz_{pq_2}^{(1)}i_1 \quad (2.60)$$

$$V_r - V_q = (1 - m)z_{pq_2}^{(1)}(i_1 + 1) \quad (2.61)$$

Solving (2.60)-(2.61) results in

$$V_r = (1 - m)V_p + mV_q + m(1 - m)z_{pq_2}^{(1)} \quad (2.62)$$

Substituting (2.59) into (2.62), we have

$$Z_{rr}^{(1)} = (1 - m)Z_{pr}^{(1)} + mZ_{qr}^{(1)} + m(1 - m)z_{pq_2}^{(1)} \quad (2.63)$$

where $Z_{pr}^{(1)}$ and $Z_{qr}^{(1)}$ can be obtained by letting k as p and q in (2.55) as

$$Z_{rp}^{(1)} = Z_{0,pp}^{(1)} - m(Z_{0,pp}^{(1)} - Z_{0,qp}^{(1)}) \quad (2.64)$$

$$Z_{rq}^{(1)} = Z_{0,pq}^{(1)} - m(Z_{0,pq}^{(1)} - Z_{0,qq}^{(1)}) \quad (2.65)$$

Substituting (2.64) and (2.65) into (2.63) further results in

$$Z_{rr}^{(1)} = Z_{0,pp}^{(1)} + m(2Z_{0,pq}^{(1)} - 2Z_{0,pp}^{(1)} + z_{pq-2}^{(1)}) + m^2(Z_{0,pp}^{(1)} + Z_{0,qq}^{(1)} - 2Z_{0,pq}^{(1)} - z_{pq-2}^{(1)}) \quad (2.66)$$

Define

$$\begin{aligned} A_0^{(1)} &= Z_{0,pp}^{(1)} \\ A_1^{(1)} &= 2Z_{0,pq}^{(1)} - 2Z_{0,pp}^{(1)} + z_{pq-2}^{(1)} \\ A_2^{(1)} &= Z_{0,pp}^{(1)} + Z_{0,qq}^{(1)} - 2Z_{0,pq}^{(1)} - z_{pq-2}^{(1)} \end{aligned}$$

Thus, we have

$$Z_{rr}^{(1)} = A_0^{(1)} + A_1^{(1)}m + A_2^{(1)}m^2 \quad (2.67)$$

It is found that the expressions of elements of $Z^{(1)}$ are identical to $Z^{(0)}$. In summary, the bus impedance matrix with addition of a fictitious fault bus for zero-, positive-, or negative-sequence network can be written in a compact form as follows

$$Z_{kl}^{(i)} = Z_{0,kl}^{(i)}, \quad k, l = 1, 2, \dots, n \quad (2.68)$$

$$Z_{rk}^{(i)} = B_k^{(i)} + C_k^{(i)}m, \quad k = 1, 2, \dots, n \quad (2.69)$$

$$Z_{rr}^{(i)} = A_0^{(i)} + A_1^{(i)}m + A_2^{(i)}m^2 \quad (2.70)$$

where $i = 0, 1, 2$ and

$$B_k^{(i)} = Z_{0,pk}^{(i)} \quad (2.71)$$

$$C_k^{(i)} = Z_{0,qk}^{(i)} - Z_{0,pk}^{(i)} \quad (2.72)$$

$$A_0^{(i)} = Z_{0,pp}^{(i)} \quad (2.73)$$

$$A_1^{(i)} = 2Z_{0,pq}^{(i)} - 2Z_{0,pp}^{(i)} + z_{pq-2}^{(i)} \quad (2.74)$$

$$A_2^{(i)} = Z_{0,pp}^{(i)} + Z_{0,qq}^{(i)} - 2Z_{0,pq}^{(i)} - z_{pq-2}^{(i)} \quad (2.75)$$

$B_k^{(i)}$, $C_k^{(i)}$, $A_0^{(i)}$, $A_1^{(i)}$, and $A_2^{(i)}$ are all constants determined by network parameters.

Compared to the method of obtaining the bus impedance matrix with additional fictitious fault bus in Section 2.2.1 the approach shown in this section is very clear in concept and efficient in computation. We can deduce that the formulations of the driving-point impedance of the fault bus $Z_{rr}^{(i)}$ and the transfer impedance between this bus and any other bus $Z_{kr}^{(i)}$ as the functions of the fault location take on the same form for single-circuit and double-circuit lines [60]. This conclusion is based on the fact that the positive-sequence double-circuit line is the same as positive-, negative- or zero-sequence single-circuit line in the sense that there is no mutual coupling between parallel lines. Therefore, it can be concluded that (2.68)-(2.75) are applicable for both single-circuit and double-circuit structures.

2.2.3 Relation Between Voltage Change and Augmented Bus Impedance Matrix

At bus k ($k = 1, 2, \dots, n$), drawing on the definition of bus impedance matrix, the following hold [64]

$$E_k^{(1)} = E_k^{(1)0} - Z_{kr}^{(1)} I_f^{(1)} \quad (2.76)$$

$$E_k^{(2)} = -Z_{kr}^{(2)} I_f^{(2)} \quad (2.77)$$

$$E_k^{(0)} = -Z_{kr}^{(0)} I_f^{(0)} \quad (2.78)$$

where

$E_k^{(1)0}$ pre-fault positive-sequence voltage at bus k

$E_k^{(1)}, E_k^{(2)}, E_k^{(0)}$ positive-, negative-, zero-sequence voltage at bus k during the fault;

$I_f^{(1)}, I_f^{(2)}, I_f^{(0)}$ positive-, negative-, zero-sequence fault current at the fault point.

A note of value is that all the sequence voltages and currents are for phase A. It can be seen that the voltage change at any bus during the fault can be formulated with respect to the corresponding transfer impedance and fault current.

2.3 Proposed Fault Location Method

In Section 2.2, the sequence voltage change of any bus expressed in terms of the corresponding transfer impedance and fault current has been established. The formulations of the driving point impedance $Z_{rr}^{(i)}$ and the transfer impedance $Z_{kr}^{(i)}$ ($k = 1, 2, \dots, n$) with respect to the unknown fault location m have been found. With this foundation, we can proceed to derive fault location methods utilizing voltage phasors and phase voltage magnitudes, respectively. As a matter of fact, since $Z_{kr}^{(i)}$ ($k = 1, 2, \dots, n$) and $Z_{rr}^{(i)}$ take on the exactly same form for both single-circuit and double-circuit lines, it has been investigated that the overall fault location methods for double-circuit lines are the same as those for single-circuit lines [57, 58].

By manipulating the boundary conditions of different fault types, the fault location formulas utilizing voltage phasors can be obtained.

Further resorting to the relationships between phase voltages and sequence voltages, the fault location formula bridging the phase voltage magnitudes during the fault at any bus with unknown fault location can be derived [58, 61].

2.3.1 Fault Location Algorithms Utilizing Voltage Phasors

In this section, fault location formulas utilizing voltage phasors from one bus and two buses will be discussed.

2.3.1.1 Fault Scenarios with Measurements from Two Buses

First of all, fault location algorithms using both synchronized and unsynchronized measurements from two buses are dealt with.

1) Fault location with synchronized measurements from two buses

Suppose that synchronized pre-fault and fault voltage measurements at bus k and l ($k, l = 1, 2, \dots, n$) are available. For bus l , similar to (2.76)-(2.78), the following formulas exist

$$E_l^{(1)} = E_l^{(1)0} - Z_{lr}^{(1)} I_f^{(1)} \quad (2.79)$$

$$E_l^{(2)} = -Z_{lr}^{(1)} I_f^{(2)} \quad (2.80)$$

$$E_l^{(0)} = -Z_{lr}^{(0)} I_f^{(0)} \quad (2.81)$$

Eliminating $I_f^{(1)}$ from (2.76) and (2.79) and combining (2.69) results in

$$\frac{E_k^{(1)} - E_k^{(1)0}}{E_l^{(1)} - E_l^{(1)0}} = \frac{Z_{kr}^{(1)}}{Z_{lr}^{(1)}} = \frac{B_k^{(1)} + C_k^{(1)}m}{B_l^{(1)} + C_l^{(1)}m} \quad (2.82)$$

Let

$$d_{kl}^{(1)} = \frac{E_k^{(1)} - E_k^{(1)0}}{E_l^{(1)} - E_l^{(1)0}} \quad (2.83)$$

The fault location formula using positive-sequence measurements is derived as

$$m = \frac{B_k^{(1)} - d_{kl}^{(1)} B_l^{(1)}}{d_{kl}^{(1)} C_l^{(1)} - C_k^{(1)}} \quad (2.84)$$

Eliminating $I_f^{(2)}$ from (2.77) and (2.80) and combining (2.69) leads to

$$\frac{E_k^{(2)}}{E_l^{(2)}} = \frac{Z_{kr}^{(1)}}{Z_{lr}^{(1)}} = \frac{B_k^{(1)} + C_k^{(1)}m}{B_l^{(1)} + C_l^{(1)}m} \quad (2.85)$$

Let

$$d_{kl}^{(2)} = \frac{E_k^{(2)}}{E_l^{(2)}} \quad (2.86)$$

The fault location formula using negative-sequence measurements is derived as

$$m = \frac{B_k^{(1)} - d_{kl}^{(2)} B_l^{(1)}}{d_{kl}^{(2)} C_l^{(1)} - C_k^{(1)}} \quad (2.87)$$

Eliminating $I_f^{(0)}$ from (2.78) and (2.81) and combining (2.69) leads to

$$\frac{E_k^{(0)}}{E_l^{(0)}} = \frac{Z_{kr}^{(0)}}{Z_{lr}^{(0)}} = \frac{B_k^{(0)} + C_k^{(0)}m}{B_l^{(0)} + C_l^{(0)}m} \quad (2.88)$$

Let

$$d_{kl}^{(0)} = \frac{E_k^{(0)}}{E_l^{(0)}} \quad (2.89)$$

The fault location formula using zero-sequence measurements is derived as

$$m = \frac{B_k^{(0)} - d_{kl}^{(0)} B_l^{(0)}}{d_{kl}^{(0)} C_l^{(0)} - C_k^{(0)}} \quad (2.90)$$

On account of the fact only positive-sequence quantities exist for any kind of faults, positive-sequence quantities are preferred since in this case no fault type classification is needed.

The above fault location formulas are applicable only if there exists a path, which passes through the faulted line and does not pass any bus more than once, between buses k and l [57]. Otherwise, the voltage changes at these two buses will be constant or linearly dependent and independent of the fault location variable. Since most power network is interconnected, most combinations are able to produce fault location estimate.

2) Fault location with unsynchronized measurements from two buses

From (2.82) and (2.83), we can establish

$$\left| d_{kl}^{(1)} \right| = \left| \frac{B_k^{(1)} + C_k^{(1)} m}{B_l^{(1)} + C_l^{(1)} m} \right| \quad (2.91)$$

where $\left| \right|$ yields the magnitude of its argument. By separating the real and imaginary parts of (2.91), we can form two real equations with only one unknown variable m . Eliminating this variable from these two equations can lead to a 2^{nd} order polynomial of m . Two fault location estimates will be produced, and the one falls between 0 and 1 p.u. is retained as the actual fault location estimation.

2.3.1.2 Fault Scenarios with Measurements from a Single Bus

Suppose the voltage phasor measurements from a single bus k ($k, l = 1, 2, \dots, n$) are given, fault location algorithms for different fault types are derived in the following.

1) line to ground (LG) fault

For phase A to ground fault, the following boundary conditions are satisfied

$$I_f^{(0)} = I_f^{(1)} = I_f^{(2)} \quad (2.92)$$

$$I_f^{(1)} = \frac{E_r^{(1)0}}{Z_{rr}^{(0)} + Z_{rr}^{(1)} + Z_{rr}^{(2)} + 3R_f} \quad (2.93)$$

Eliminating $I_f^{(2)}$ and $I_f^{(0)}$ from (2.77) and (2.78) and combining (2.69) yields

$$\frac{E_k^{(2)}}{E_k^{(0)}} = \frac{Z_{kr}^{(1)}}{Z_{kr}^{(0)}} = \frac{B_k^{(1)} + C_k^{(1)}m}{B_k^{(0)} + C_k^{(0)}m} \quad (2.94)$$

Define

$$g = \frac{E_k^{(2)}}{E_k^{(0)}} \quad (2.95)$$

The fault location for AG fault is thus derived as

$$m = \frac{B_k^{(1)} - gB_k^{(0)}}{gC_k^{(0)} - C_k^{(1)}} \quad (2.96)$$

2) *line to line to ground (LLG) fault*

For phase B to C to ground fault, the following boundary conditions hold

$$\frac{I_f^{(2)}}{I_f^{(0)}} = \frac{Z_{rr}^{(0)} + 3R_f}{Z_{rr}^{(2)}} \quad (2.97)$$

$$I_f^{(1)} = \frac{E_r^{(1)0}}{Z_{rr}^{(1)} + \frac{Z_{rr}^{(2)}(Z_{rr}^{(0)} + 3R_f)}{Z_{rr}^{(0)} + Z_{rr}^{(2)} + 3R_f}} \quad (2.98)$$

$$I_f^{(2)} = -I_f^{(1)} \frac{Z_{rr}^{(0)} + 3R_f}{Z_{rr}^{(0)} + Z_{rr}^{(2)} + 3R_f} \quad (2.99)$$

$$I_f^{(0)} = -I_f^{(1)} \frac{Z_{rr}^{(2)}}{Z_{rr}^{(0)} + Z_{rr}^{(2)} + 3R_f} \quad (2.100)$$

Replacing $I_f^{(2)}$ and $I_f^{(0)}$ from (2.77) and (2.78) in (2.97), we have

$$\frac{E_k^{(2)}}{E_k^{(0)}} = \frac{Z_{kr}^{(1)}(Z_{rr}^{(0)} + 3R_f)}{Z_{kr}^{(0)} Z_{rr}^{(2)}} \quad (2.101)$$

Substituting (2.69) and (2.70) into (2.101) yields

$$g = \frac{(B_k^{(1)} + C_k^{(1)}m)(A_0^{(0)} + A_1^{(0)}m + A_2^{(0)}m^2 + 3R_f)}{(B_k^{(0)} + C_k^{(0)}m)(A_0^{(1)} + A_1^{(1)}m + A_2^{(1)}m^2)} \quad (2.102)$$

Equation (2.102) is a complex formula, which can be separated into real and imaginary parts to obtain two real formulations with both unknowns m and R_f . By eliminating the unknown variable R_f from these two real equations, a 4th order polynomial containing only one unknown variable m can be formed, from which the fault

location estimation can be solved. After m is obtained, the other unknown R_f can be calculated.

3) *line to line (LL) fault*

For phase B to C fault, the boundary conditions are stated as

$$I_f^{(2)} = -I_f^{(1)}, I_f^{(0)} = 0 \quad (2.103)$$

$$I_f^{(1)} = \frac{E_r^{(1)0}}{R_f + Z_{rr}^{(1)} + Z_{rr}^{(2)}} \quad (2.104)$$

Substituting (2.103) into (2.104) results in

$$I_f^{(2)} = -\frac{E_r^{(1)0}}{R_f + 2Z_{rr}^{(1)}} \quad (2.105)$$

Replacing $I_f^{(2)}$ in (2.105) with (2.77) leads to

$$E_k^{(2)} = \frac{Z_{kr}^{(1)} E_r^{(1)0}}{R_f + 2Z_{rr}^{(1)}} \quad (2.106)$$

Substituting (2.69) and (2.70) into (2.106)

$$E_k^{(2)} = \frac{(B_k^{(1)} + C_k^{(1)} m) E_r^{(1)0}}{R_f + 2A_0^{(1)} + 2A_1^{(1)} m + 2A_2^{(1)} m^2} \quad (2.107)$$

The unknowns in (2.107) include m and R_f and $E_r^{(1)0}$, therefore it is unsolvable. However, if we approximate $E_r^{(1)0}$ as 1.0 p.u. and separate (2.107) into real and imaginary parts to form two real equations, then m and R_f can be determined. m can be computed from solving a 2nd order polynomial and the other variable R_f can be solved afterwards. The assumption of a flat value for the pre-fault voltage at the fault bus may introduce certain error in fault location estimation.

4) *three phase symmetrical (LLL) fault*

For three phase symmetrical fault, the boundary conditions are as follows

$$I_f^{(0)} = I_f^{(2)} = 0 \quad (2.108)$$

$$I_f^{(1)} = \frac{E_r^{(1)0}}{R_f + Z_{rr}^{(1)}} \quad (2.109)$$

Replacing $I_f^{(1)}$ in (2.109) with (2.76) produces

$$E_k^{(1)} = E_k^{(1)0} - \frac{Z_{kr}^{(1)} E_r^{(1)0}}{R_f + Z_{rr}^{(1)}} \quad (2.110)$$

Substituting (2.69) and (2.70) into (2.110), we have

$$E_k^{(1)} = E_k^{(1)0} - \frac{(B_k^{(1)} + C_k^{(1)}m)E_r^{(1)0}}{R_f + A_0^{(1)} + A_1^{(1)}m + A_2^{(1)}m^2} \quad (2.111)$$

The unknowns m and R_f in (2.111) can be solved following a similar procedure as for (2.107).

One-bus fault location algorithms for other unsymmetrical faults involving other phases can be deduced and not shown here.

Note that for LLG, LL and LLL faults, multiple solutions can be obtained. A solution is defined as a pair of fault location estimate and fault resistance estimate. A solution could be a valid solution ($0 \leq m \leq 1$ and $R_f \geq 0$) or an invalid solution ($m < 0$ or $m > 1$ or $R_f < 0$). An invalid solution can be easily identified and removed. In cases where two or more valid solutions arise, one is the true solution and the others are erroneous solutions.

The fault location estimate for LLG fault is actually obtained by solving a 4th order polynomial function of m , and the corresponding fault resistance estimate can be solved afterwards. This way, four pairs of fault location and resistance estimates are produced. Any invalid solution if existing can be easily filtered out. It is still possible that two or even more valid solutions remain, where only one solution is true and the rest is erroneous. The erroneous solution can be identified by the following method. We can calculate the voltages of the bus with measurements from all the valid solutions by making use of the bus impedance matrix technique and compare them with the actual voltage measurements. The bus voltages computed from the erroneous solution differ from the original bus voltage measurements, and thus the erroneous solution can be recognized.

For both LL and LLL faults, a quadratic function with respect to m is formulated to solve for the fault location, which can be used to further calculate the corresponding fault resistance. Two solutions are produced as a result. If one of them is an invalid solution, a unique solution can be obtained. In case two valid solutions are yielded, one of them is an erroneous solution. The erroneous solution identification method proposed for LLG fault fails to distinguish between the two solutions since the computed bus voltages from both of them are the same as the actual bus voltage measurements. In this case, both fault location estimates will be treated as like estimates.

2.3.2 Fault Location Algorithms Utilizing Phase Voltage Magnitudes

At any bus k ($k = 1, 2, \dots, n$), suppose only the phase voltage magnitudes during the fault, $|E_{ka}|$, $|E_{kb}|$, and $|E_{kc}|$, are recorded by the recording device. Based on the symmetrical component theory

$$E_{ka} = E_k^{(0)} + E_k^{(1)} + E_k^{(2)} \quad (2.112)$$

$$E_{kb} = E_k^{(0)} + \alpha^2 E_k^{(1)} + \alpha E_k^{(2)} \quad (2.113)$$

$$E_{kc} = E_k^{(0)} + \alpha E_k^{(1)} + \alpha^2 E_k^{(2)} \quad (2.114)$$

where E_{ka} , E_{kb} , E_{kc} are the phase A, B, C voltage at bus k , respectively and $\alpha = e^{j120^\circ}$. Substituting (2.76), (2.77), and (2.78) into (2.112)-(2.114) gives rise to

$$E_{ka} = -Z_{kr}^{(0)} I_f^{(0)} + E_k^{(1)0} - Z_{kr}^{(1)} I_f^{(1)} - Z_{kr}^{(2)} I_f^{(2)} \quad (2.115)$$

$$E_{kb} = -Z_{kr}^{(0)} I_f^{(0)} + \alpha^2 (E_k^{(1)0} - Z_{kr}^{(1)} I_f^{(1)}) - \alpha Z_{kr}^{(2)} I_f^{(2)} \quad (2.116)$$

$$E_{kc} = -Z_{kr}^{(0)} I_f^{(0)} + \alpha (E_k^{(1)0} - Z_{kr}^{(1)} I_f^{(1)}) - \alpha^2 Z_{kr}^{(2)} I_f^{(2)} \quad (2.117)$$

2.3.2.1 Algorithms with Voltage Magnitudes from One Bus

In this section, fault location algorithms using measurements from one bus for different types of fault will be presented.

1) LG fault

For phase A to ground fault, from the boundary condition stated in (2.92), (2.115)-(2.117) can be simplified as follows

$$E_{ka} = E_k^{(1)0} - (Z_{kr}^{(0)} + 2Z_{kr}^{(1)}) I_f^{(1)} \quad (2.118)$$

$$E_{kb} = \alpha^2 E_k^{(1)0} - (Z_{kr}^{(0)} - Z_{kr}^{(1)}) I_f^{(1)} \quad (2.119)$$

$$E_{kc} = \alpha E_k^{(1)0} - (Z_{kr}^{(0)} - Z_{kr}^{(1)}) I_f^{(1)} \quad (2.120)$$

Substituting (2.69), (2.70) and (2.93) into (2.118)-(2.120) yields

$$|E_{ka}| = \left| E_k^{(1)0} - \left[(B_k^{(0)} + 2B_k^{(1)}) + (C_k^{(0)} + 2C_k^{(1)})m \right] I_f^{(1)} \right| \quad (2.121)$$

$$|E_{kb}| = \left| \alpha^2 E_k^{(1)0} - \left[(B_k^{(0)} - B_k^{(1)}) + (C_k^{(0)} - C_k^{(1)})m \right] I_f^{(1)} \right| \quad (2.122)$$

$$|E_{kc}| = \left| \alpha E_k^{(1)0} - \left[(B_k^{(0)} - B_k^{(1)}) + (C_k^{(0)} - C_k^{(1)})m \right] I_f^{(1)} \right| \quad (2.123)$$

where

$$I_f^{(1)} = \frac{E_r^{(1)0}}{(A_0^{(0)} + 2A_0^{(1)}) + (A_1^{(0)} + 2A_1^{(1)})m + (A_2^{(0)} + 2A_2^{(1)})m^2 + 3R_f} \quad (2.124)$$

Given $|E_{ka}|$, $|E_{kb}|$, and $|E_{kc}|$, it is needed to assume a certain value for $E_k^{(1)0}$ and $E_r^{(1)0}$ in order to estimate the fault location. A possible solution is: $E_k^{(1)0} = E_r^{(1)0} = 1.0$ p.u.. Then we will have three equations and two unknown variables m and R_f . The least squares approach can be utilized to obtain the solution, which is provided in Section 2.3.2.3. A initial value of 0.5 p.u. can be chosen for m and 0.1 p.u. for R_f .

2) LLG fault

For phase B to C to ground fault, from the boundary conditions in (2.98)-(2.100) and (2.115)-(2.117), the fault location formulations are obtained as

$$|E_{ka}| = \left| E_k^{(1)0} + \frac{Z_{rr}^{(2)}}{Z_{LLG}} (Z_{kr}^{(0)} - Z_{kr}^{(1)}) I_f^{(1)} \right| \quad (2.125)$$

$$|E_{kb}| = \left| \alpha^2 E_k^{(1)0} + \frac{Z_{kr}^{(0)} Z_{rr}^{(2)}}{Z_{LLG}} I_f^{(1)} - Z_{kr}^{(1)} \left(\alpha^2 - \alpha + \alpha \frac{Z_{rr}^{(2)}}{Z_{LLG}} \right) I_f^{(1)} \right| \quad (2.126)$$

$$|E_{kc}| = \left| \alpha E_k^{(1)0} + \frac{Z_{kr}^{(0)} Z_{rr}^{(2)}}{Z_{LLG}} I_f^{(1)} - Z_{kr}^{(1)} \left(\alpha - \alpha^2 + \alpha^2 \frac{Z_{rr}^{(2)}}{Z_{LLG}} \right) I_f^{(1)} \right| \quad (2.127)$$

where

$$Z_{LLG} = Z_{rr}^{(0)} + Z_{rr}^{(2)} + 3R_f \quad (2.128)$$

and $I_f^{(1)}$ can be obtained from (2.98). Substituting (2.69), (2.70) into (2.98), (2.128), (2.125), (2.126) and (2.127) can lead to the fault location formulations. Provided $|E_{ka}|$, $|E_{kb}|$, and $|E_{kc}|$, we can assume $E_k^{(1)0} = E_r^{(1)0} = 1.0$ p.u.. Then we will have three equations and two unknowns m and R_f , which can be solved similar to AG fault.

3) LL fault

For phase B to C fault, upon the boundary condition in (2.103), (2.115)-(2.117) can be reformatted as

$$E_{ka} = E_k^{(1)0} \quad (2.129)$$

$$E_{kb} = \alpha^2 E_k^{(1)0} + (\alpha - \alpha^2) Z_{kr}^{(1)} I_f^{(1)} \quad (2.130)$$

$$E_{kc} = \alpha E_k^{(1)0} - (\alpha - \alpha^2) Z_{kr}^{(1)} I_f^{(1)} \quad (2.131)$$

Substituting (2.69), (2.70) and (2.104) into (2.130)-(2.131) yields

$$|E_{kb}| = \left| \alpha^2 E_k^{(1)0} + (\alpha - \alpha^2) (B_k^{(1)} + C_k^{(1)} m) I_f^{(1)} \right| \quad (2.132)$$

$$|E_{kc}| = \left| \alpha E_k^{(1)0} - (\alpha - \alpha^2) (B_k^{(1)} + C_k^{(1)} m) I_f^{(1)} \right| \quad (2.133)$$

where

$$I_f^{(1)} = \frac{E_r^{(1)0}}{2A_0^{(1)} + 2A_1^{(1)} m + 2A_2^{(1)} m^2 + R_f} \quad (2.134)$$

With $|E_{kb}|$ and $|E_{kc}|$ being available, we can assume $E_k^{(1)0} = E_r^{(1)0} = 1.0$, p.u.. Then we will have two equations and two unknowns m and R_f , which can be solved by Newton-Raphson technique. The description of this technique is given in Section

2.3.2.3. Note that (2.129) does not contain unknown fault location or fault resistance and is not utilized in fault location estimation.

4) LLL fault

For three phase balanced fault, based on the boundary condition in (2.108), (2.115)-(2.117) can be reformatted as

$$E_{ka} = E_k^{(1)0} - Z_{kr}^{(1)} I_f^{(1)} \quad (2.135)$$

$$E_{kb} = \alpha^2 (E_k^{(1)0} - Z_{kr}^{(1)} I_f^{(1)}) \quad (2.136)$$

$$E_{kc} = \alpha (E_k^{(1)0} - Z_{kr}^{(1)} I_f^{(1)}) \quad (2.137)$$

where $I_f^{(1)}$ is from (2.109). Equations (2.135)-(2.137) contain the same information when absolute values are taken. Therefore, making use of (2.135) together with (2.69) and (2.70) will lead to the fault location formulation as

$$|E_{ka}| = \left| E_k^{(1)0} - \frac{(B_k^{(1)} + C_k^{(1)} m) E_r^{(1)0}}{A_0^{(1)} + A_1^{(1)} m + A_2^{(1)} m^2 + R_f} \right| \quad (2.138)$$

Given $|E_{ka}|$, other than assuming $E_k^{(1)0} = E_r^{(1)0} = 1.0$ p.u., R_f also needs to be known to solve for m . The fault resistance is normally very small for three phase faults, so a value close to zero can be assumed without causing significant errors. Then we will have one equation and one unknown m , the solution of which is similar to BC fault.

Formulas involving other phases for different kinds of fault can be deduced similarly.

2.3.2.2 Algorithms with Voltage Magnitudes from Multiple Buses

When the voltage measurements from any two buses bus k and l ($k, l = 1, 2, \dots, n$) are available, in addition to (2.115)-(2.117), we also have

$$E_{la} = -Z_{lr}^{(0)} I_f^{(0)} + E_l^{(1)0} - Z_{lr}^{(1)} I_f^{(1)} - Z_{lr}^{(2)} I_f^{(2)} \quad (2.139)$$

$$E_{lb} = -Z_{lr}^{(0)} I_f^{(0)} + \alpha^2 (E_l^{(1)0} - Z_{lr}^{(1)} I_f^{(1)}) - \alpha Z_{lr}^{(2)} I_f^{(2)} \quad (2.140)$$

$$E_{lc} = -Z_{lr}^{(0)} I_f^{(0)} + \alpha (E_l^{(1)0} - Z_{lr}^{(1)} I_f^{(1)}) - \alpha^2 Z_{lr}^{(2)} I_f^{(2)} \quad (2.141)$$

Dependent on the fault type, we will have six equations at most, with $|E_{ka}|$, $|E_{kb}|$, $|E_{kc}|$, $|E_{la}|$, $|E_{lb}|$, and $|E_{lc}|$ being known quantities and $E_k^{(1)0}$, $E_l^{(1)0}$, and $E_r^{(1)0}$ being unknowns. For LG and LLG faults, we have six equations; for LL fault, there will be four equations; for LLL fault, there will be two equations. Still, assuming a flat value of 1.0 p.u. for all the pre-fault voltages, m and R_f can be solved. Note that for three phase balanced faults, different from the single-bus algorithm, there is no need to assume any value for the fault resistance since we have one more equation now. In

general, the least squares based approach can be applied when multiple measurements are utilized.

In summary, for LG and LLG faults, a unique fault location estimate can be yielded. As for LL and LLL faults, in certain cases, multiple valid solutions might arise.

When multiple valid solutions are yielded, our studies indicate that it is not possible to tell which solution is the true solution and which one is the erroneous solution. This is because if the network is subject to the fault conditions as given by the valid solutions, by performing short-circuit analysis we will obtain the same voltage sags as the measured voltage sags. Hence, unless more information is available, there may be more than one likely fault location estimates.

2.3.2.3 Newton-Raphson Method and Least Squares Method

The well established Newton-Raphson approach [66] is as follows

$$X_{v+1} = X_v + \Delta X_v \quad (2.142)$$

$$\Delta X_v = -H_v^{-1} F(X_v) \quad (2.143)$$

$$H_v = \left. \frac{\partial F(X)}{\partial X} \right|_{X=X_v} \quad (2.144)$$

where

X_v the variable vector at v^{th} iteration;

X_{v+1} the variable vector after v^{th} iteration;

ΔX_v the variable update at v^{th} iteration.

$F(X_v)$ the function vector when $X = X_v$;

H_v the Jacobian matrix when $X = X_v$;

v the iteration number starting from 0.

When the variable update reaches within the specified tolerance, the iterative process can be terminated. Educated initial values for variable vector should be provided.

For least squares based method, the only difference lies in that the update variable ΔX_v is obtained as

$$\Delta X_v = -(H_v^T H_v)^{-1} [H_v^T F(X_v)] \quad (2.145)$$

When implementing the Newton-Raphson or least squares method, the Jacobian matrix needs to be calculated. There are two possible ways of doing this. One is to derive the analytical form of the Jacobian matrix. Let us take equation (2.121) as an example. The absolute sign on the right side of (2.121) can be eliminated by utilizing the following identity

$$|a + jb|^2 = a^2 + b^2 \quad (2.146)$$

Then, the Jacobian matrix can be readily obtained. The other method is based on numerical method, where the derivative of function $f(x_1, \dots)$ with respect to variable x_k is approximated by

$$\frac{f(x_1, \dots)}{x_k} = \frac{f(x_1, \dots, x_k + \delta, \dots) - f(x_1, \dots, x_k, \dots)}{\delta} \quad (2.147)$$

where δ is a small step used to calculate the derivative.

In this work, the second method is utilized because it obviates the need to derive the complicated analytical form of the derivatives of Jacobian matrix and still maintains high accuracy of fault location estimate.

2.4 Simulation Studies

This section presents the simulation results to evaluate the developed fault location algorithms. Electromagnetic Transients Program (EMTP) has been utilized to simulate the studied power system and generate transient waveforms for faults of different types, locations and fault resistances [67]. Discrete Fourier Transform is utilized to extract phasors from the waveforms of about 5th cycle after the fault inception to feed into the developed algorithms.

The studied power system is a 230 kV, 100 MVA, 50 Hz transmission line system. The system diagram is shown in Fig. 2.11. The system data are presented in Table 2.1 and 2.2. The system is modeled in EMTP based on lumped parameter line model. In this study, shunt capacitance of the line and load are not considered.

Table 2.1: Transmission line data

Line number	Line length (km)	Positive-sequence impedance (p.u.)	Zero-sequence impedance (p.u.)
1	178.5	0.015455 + j0.116066	0.098871 + j0.365188
2	110.2	0.096188 + j0.279293	0.243156 + j0.822918
3	193.0	0.022172 + j0.128174	0.099245 + j0.409333
4	193.0	0.022172 + j0.128174	0.099245 + j0.409333

Table 2.2: Generator data

Generator number	Positive-sequence impedance (p.u.)	Zero-sequence impedance (p.u.)
1	0.000600 + j0.037343	0.000540 + j0.016062
2	0.000900 + j0.054236	0.001300 + j0.045230
3	0.002200 + j0.096514	0.001300 + j0.045230

The zero-sequence mutual impedance between line 3 and 4 is: 0.079 + j0.2464 p.u..

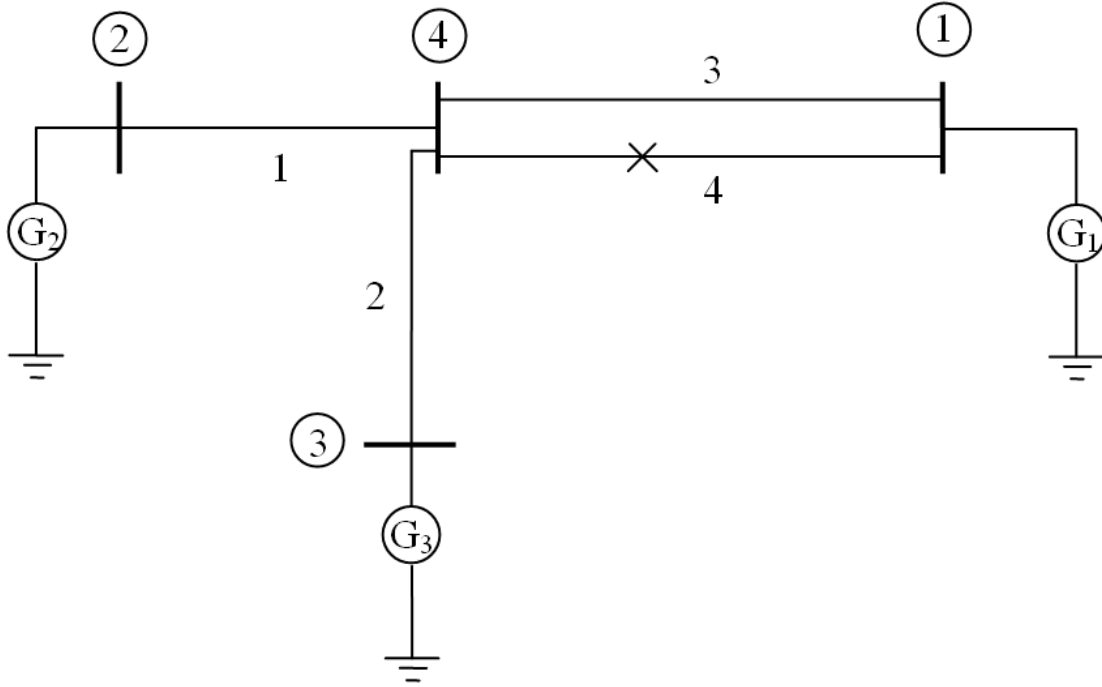


Figure 2.11: The studied 4-bus power system.

From Fig. 2.11, it can be observed that the section between bus 1 and 4 has the double-circuit line structure and the fault occurs on one of the parallel lines, with the cross denoting the fault point. For this particular system, we have $n = 4$, $p = 1$ and $q = 4$. The length of the faulted line is 193 km.

The estimation accuracy is evaluated by the percentage error calculated as

$$\%Error = \frac{|\text{Actual Location} - \text{Estimated Location}|}{\text{Total Length of Faulted Line}} \times 100 \quad (2.148)$$

where the location of the fault is defined as the distance between the fault point and bus p , which is 1 in our case.

Next, fault location algorithms utilizing voltage phasors and phase voltage magnitudes are studied, respectively.

2.4.1 Case Studies for Fault Location Using Voltage phasors

The developed fault location algorithms are tested under various fault conditions. Table 2.3 shows the fault location results produced by two-bus method. The first three columns represent the actual fault type, fault location and fault resistance, respectively. Columns 4-9 indicate the percentage errors of fault location estimate utilizing both synchronized and unsynchronized voltage measurements from two buses. In Table 2.3, positive-sequence voltage measurements are used to carry out two-bus fault location. It can be observed that quite close fault location estimates are produced

by using synchronized and unsynchronized data. The fault location results are quite satisfactory. In fact, when synchronized measurements are utilized, the fault location estimate contains an imaginary part, which represents the numerical round off error and is neglected directly. Notice that it is impossible to produce fault location estimate by employing voltage measurements from other bus combinations including 2 and 3, 2 and 4, and 3 and 4 on account of the reason explained in Section 2.3.1.1.

Table 2.3: Fault location results using voltage phasors at two buses

Fault type	Fault location (km)	Fault resistance (Ω)	Estimated error using voltages at two buses (%)					
			1&2		1&3		1&4	
			Syn.	Unsyn.	Syn.	Unsyn.	Syn.	Unsyn.
AG	30	1	0.040	0.074	0.15	0.20	0.0034	0.0017
		10	0.15	0.19	0.31	0.36	0.0025	0.0050
	90	1	0.051	0.077	0.22	0.26	0.024	0.031
		50	0.48	0.50	0.86	0.89	0.12	0.13
	150	10	0.066	0.078	0.26	0.28	0.094	0.11
		50	0.25	0.26	0.60	0.61	0.28	0.29
BC	30	1	0.0021	0.018	0.046	0.074	0.011	0.010
	90	1	0.0067	0.019	0.066	0.084	0.018	0.021
	150	1	0.0057	0.011	0.053	0.062	0.024	0.030
BCG	30	1	0.0013	0.018	0.038	0.060	0.012	0.011
		50	0.0088	0.029	0.055	0.082	0.014	0.012
	90	10	0.012	0.023	0.064	0.079	0.020	0.023
		50	0.016	0.028	0.074	0.091	0.023	0.025
	150	1	0.0052	0.0095	0.044	0.051	0.025	0.029
		10	0.0077	0.012	0.049	0.056	0.028	0.032
ABC	30	1	0.0015	0.011	0.028	0.041	0.0043	0.0041
	90	1	0.0052	0.011	0.037	0.046	0.0079	0.0098
	150	1	0.0037	0.0062	0.030	0.034	0.011	0.014

Table 2.4 presents the one-bus fault location results for AG and BCG faults. Columns 4-7 display the percentage errors of fault location estimate employing the voltage measurements from a single bus. It can be seen that the fault location estimates in Table 2.4 are quite accurate.

Table 2.5 exhibits the one-bus fault location results for BC and ABC faults. Columns 3-10 list the estimated fault location, fault resistance utilizing voltage measurements from a single bus. m is the estimated fault location (p.u.) and R_f is the estimated fault resistance (p.u.). The actual fault resistance is 1Ω and the base value of the impedance is 529Ω . The obtained fault location results are quite satisfactory.

In case two valid solutions are yielded, one of them is an erroneous solution designated as * in Table 2.5. As stated in Section 2.3.1.2, the erroneous solution can not be identified and both estimates will be treated as likely solutions. For example, for a BC fault with actual fault location of 30 km, based on voltages at bus 2, the

Table 2.4: Fault location results using voltage phasors at a single bus for AG and BCG faults

Fault type	Fault location (km)	Fault resistance (Ω)	Estimated error using voltage at a single bus (%)			
			1	2	3	4
AG	30	1	0.016	0.0027	0.0033	0.00034
		10	0.017	0.0026	0.0038	0.0012
	90	1	0.021	0.013	0.014	0.0035
		50	0.022	0.013	0.013	0.0049
	150	10	0.017	0.024	0.027	0.0081
		50	0.018	0.024	0.024	0.0086
BCG	30	1	0.014	0.018	0.017	0.019
		50	0.0028	0.047	0.11	0.031
	90	10	0.027	0.034	0.035	0.016
		50	0.017	0.014	0.048	0.00089
	150	1	0.026	0.14	0.055	0.024
		10	0.025	0.12	0.060	0.014

algorithm yields two valid solutions: (0.1554, 0.0019) p.u. and (0.3878, 0.0028) p.u.. The first element in the bracket represents the fault location estimate and the second one represents the fault resistance estimate. In this case, we have two possible fault location estimates: 0.1554 p.u. and 0.3878 p.u..

2.4.2 Case Studies for Fault Location Using Phase Voltage Magnitudes

Table 2.6 presents the fault location results under various faults. The first three columns list the actual fault type, fault location and fault resistance applied in EMTP. The fault location estimation errors utilizing phase voltage magnitudes from buses of different combinations are reported in the rest columns.

In Table 2.6, we assumed $R_f = 0.75 \Omega$ for single-bus ABC fault location algorithm. As can be seen, the fault location estimates are satisfactory.

It is shown, for three phase faults and phase to phase faults, that in certain cases, multiple valid solutions might arise, as indicated by *. For example, for a BC fault with actual fault location being 100 km and actual fault resistance being 1 Ω , using the phase voltage magnitudes at bus 2, we obtain the following two valid solutions: [0.5180, 0.0019] p.u. and [0.0671, 0.0011] p.u.

As reasoned in Section 2.3.2.2, when multiple valid solutions are yielded, our studies indicate that it is not possible to identify the erroneous solutions. Therefore, in this case, there are two possible fault location estimates: 0.5180 p.u. and 0.0671 p.u..

Table 2.5: Fault location results using voltage phasors at a single bus for BC and ABC faults

Fault type	Fault loca. (km)	Result using voltages at a single bus							
		1		2		3		4	
	m	R_f	m	R_f	m	R_f	m	R_f	
BC	30	0.1556	0.0019	0.1554	0.0019	0.1550	0.0019	0.1557	0.0019
				0.3878*	0.0028	0.3883*	0.0028	0.3875*	0.0028
	90	0.4665	0.0020	0.0994*	0.0011	0.0992*	0.0011	0.0994*	0.0011
				0.4663	0.0020	0.4667	0.0020	0.4663	0.0020
	150	0.7778	0.0020	0.7771	0.0020	0.7773	0.0020	0.7772	0.0020
		0.8785*	0.0017						
ABC	30	0.1556	0.0019	0.1570	0.0018	0.1584	0.0018	0.1559	0.0019
				0.3874*	0.0025	0.3856*	0.0025	0.3890*	0.0026
	90	0.4667	0.0019	0.1011*	0.0011	0.1018*	0.0011	0.1005*	0.0012
				0.4649	0.0018	0.4638	0.0017	0.4661	0.0019
	150	0.7801	0.0018	0.7767	0.0018	0.7763	0.0018	0.7771	0.0019
		0.8761*	0.0017						

2.5 Summary

In this chapter, fault location algorithms utilizing voltage phasors and phase voltage magnitudes based on the lumped parameter line model have been implemented. Thanks to the bus impedance matrix technique, the measurements can be taken from one or more buses, which are not restricted to the faulted line terminals. Simulation studies have shown that the fault location algorithms can yield quite accurate estimates under different fault conditions.

For the phasor-based method, we can summarize:

- Fault type classification is prerequisite for one-bus fault location algorithms and not required for two-bus algorithms using positive-sequence measurements;
- For one-bus algorithms, accurate fault location estimates can be provided for LG and LLG fault, while only approximate estimates for LL and LLL faults;
- One-bus algorithms for LL and LLL faults may yield two possible fault location estimates. Unless more information is available, the erroneous estimate can not be identified;
- Two-bus fault location algorithm is able to produce accurate fault location estimate without approximation but its application scope is subject to the network topology.

For the magnitude-based method, we have the following remarks:

- Fault type classification is required before performing fault location for both one-bus and multi-bus algorithms;

Table 2.6: Fault location results using voltage sag data

Fault type	Fault loca. (km)	Fault res. (Ω)	Fault location estimation error using voltage sags from different buses (%)				
			1	2	1&4	2&3	1&2&3
AG	40	10	0.0006	0.0211	0.0007	0.0198	0.0002
		50	0.0017	0.0095	0.0016	0.0069	0.0026
	100	1	0.0027	0.0704	0.0017	0.0361	0.0008
		50	0.0175	0.0439	0.0047	0.0564	0.0004
	140	1	0.0056	0.0803	0.0001	0.0078	0.0015
		10	0.0134	0.1248	0.0024	0.0504	0.0012
		100	0.6584	0.0542	0.0070	0.0747	0.0031
BC	40	1	0.0139	0.0075*	0.0144	0.0259*	0.0138
	100	1	0.0214	0.0135*	0.0077	0.0017*	0.0170
	140	1	0.0513*	0.0110	0.0012	0.0028	0.0024
BCG	40	1	0.0121	0.0051	0.0108	0.0024	0.0121
		10	0.0141	0.0020	0.0101	0.0039	0.0145
	100	10	0.0237	0.0187	0.0049	0.0071	0.0153
		50	0.0294	0.0182	0.0173	0.0004	0.0160
		100	0.0281	0.0186	0.0155	0.0033	0.0191
	140	1	0.0512	0.0152	0.0023	0.0077	0.0014
50		0.0739	0.0145	0.0107	0.0023	0.0049	
ABC	40	1	0.1751	1.8821*	0.0022	0.0772*	0.0046
	100	1	0.3182	0.3689*	0.0022	0.0262*	0.0032
	140	1	0.9498*	0.2203	0.0025	0.0163	0.0025

- All the algorithms using voltage sag data are iterative and only produce approximate estimation of fault location;
- For LG and LLG faults, a unique fault location estimate can be yielded;
- For LL and LLL faults, multiple valid solutions may be produced under certain fault conditions. Under this circumstance, we will have multiple fault location estimates.

Chapter 3

Fault Location Using Sparse Current Measurements Based on Lumped Parameter Line Model

In this chapter, fault location method utilizing sparse current measurements for double-circuit lines is presented. It is organized as follows. A brief introduction on the feature of the proposed method is given firstly in Section 3.1. Then, the fault location basis is derived in Section 3.2, upon which the fault location algorithms are provided in detail in Section 3.3. Next, the simulation studies in Section 3.4 report the fault location results, followed by the summary in Section 3.5.

3.1 Introduction

In Chapter 2, fault location method using sparse voltage measurements has been introduced. By taking advantage of the same bus impedance matrix technique, fault location algorithms for double-circuit lines using sparse current phasors [68] and current magnitudes [69] will be developed in this chapter. This work is extended from the fault location algorithms using sparse current measurements for single-circuit transmission lines [70].

Current measurements from one or more branches are taken as input, which can be far away from the faulted section. The faulted double-circuit line is modeled by the lumped parameter line model which ignores the shunt capacitance of the long lines. The following assumptions are utilized: (1) the network data are available; (2) the network is transposed; (3) the faulted section has been determined in advance; (4) fault type classification result is known.

3.2 Fault Location Basis

From Chapter 2, $Z^{(i)}$, the bus impedance matrix of the network with an additional fictitious fault bus, has been established and summarized as follows

$$Z_{kl}^{(i)} = Z_{0,kl}^{(i)}, \quad k, l = 1, 2, \dots, n \quad (3.1)$$

$$Z_{rk}^{(i)} = B_k^{(i)} + C_k^{(i)}m, \quad k = 1, 2, \dots, n \quad (3.2)$$

$$Z_{rr}^{(i)} = A_0^{(i)} + A_1^{(i)}m + A_2^{(i)}m^2 \quad (3.3)$$

where $i = 0, 1, 2$ and

$$B_k^{(i)} = Z_{0,pk}^{(i)} \quad (3.4)$$

$$C_k^{(i)} = Z_{0,qk}^{(i)} - Z_{0,pk}^{(i)} \quad (3.5)$$

$$A_0^{(i)} = Z_{0,pp}^{(i)} \quad (3.6)$$

$$A_1^{(i)} = 2Z_{0,pq}^{(i)} - 2Z_{0,pp}^{(i)} + z_{pq,2}^{(i)} \quad (3.7)$$

$$A_2^{(i)} = Z_{0,pp}^{(i)} + Z_{0,qq}^{(i)} - 2Z_{0,pq}^{(i)} - z_{pq,2}^{(i)} \quad (3.8)$$

and $Z_0^{(i)}$ can be readily built from network parameters.

At any bus k ($k = 1, 2, \dots, n$), the following formulas hold

$$E_k^{(1)} = E_k^{(1)0} - Z_{kr}^{(1)}I_f^{(1)} \quad (3.9)$$

$$E_k^{(2)} = -Z_{kr}^{(2)}I_f^{(2)} \quad (3.10)$$

$$E_k^{(0)} = -Z_{kr}^{(0)}I_f^{(0)} \quad (3.11)$$

In [70], (3.9)-(3.11) are utilized to formulate the sequence branch current with respect to the corresponding sequence fault current, based on which the fault location algorithms using branch current phasors are derived for single-circuit transmission lines. For double-circuit lines, with the same idea, we will derive the formulations of sequence branch current pertaining to the relevant sequence fault current [68].

The positive-, negative-, and zero-sequence currents between any bus k and l during the fault, $I_{kl}^{(1)}$, $I_{kl}^{(2)}$, $I_{kl}^{(0)}$ are calculated based on the following five categories.

Case 1: The currents of non-faulted single-circuit branch whose two terminals are j_1 and j_2

Making use of VCR and (3.9)-(3.11), the following relationships drawn from Fig. 3.1 hold

$$I_{j_1j_2}^{(1)} = \frac{E_{j_1}^{(1)} - E_{j_2}^{(1)}}{z_{j_1j_2}^{(1)}} = \frac{E_{j_1}^{(1)0} - Z_{j_1r}^{(1)}I_f^{(1)} - E_{j_2}^{(1)0} + Z_{j_2r}^{(1)}I_f^{(1)}}{z_{j_1j_2}^{(1)}} = I_{j_1j_2}^{(1)0} - \frac{Z_{j_1r}^{(1)} - Z_{j_2r}^{(1)}}{z_{j_1j_2}^{(1)}}I_f^{(1)} \quad (3.12)$$

$$I_{j_1j_2}^{(2)} = \frac{E_{j_1}^{(2)} - E_{j_2}^{(2)}}{z_{j_1j_2}^{(2)}} = \frac{-Z_{j_1r}^{(2)}I_f^{(2)} + Z_{j_2r}^{(2)}I_f^{(2)}}{z_{j_1j_2}^{(2)}} = -\frac{Z_{j_1r}^{(2)} - Z_{j_2r}^{(2)}}{z_{j_1j_2}^{(2)}}I_f^{(2)} \quad (3.13)$$

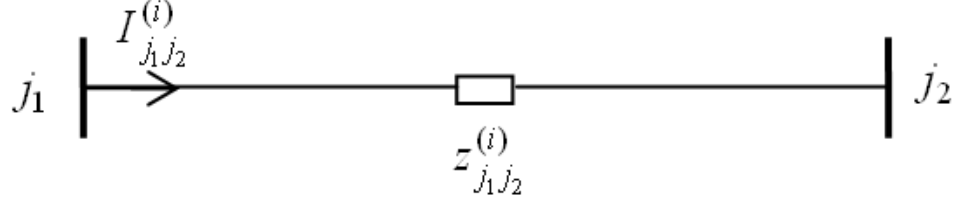


Figure 3.1: The i^{th} -sequence network of a single-circuit unfaulted line.

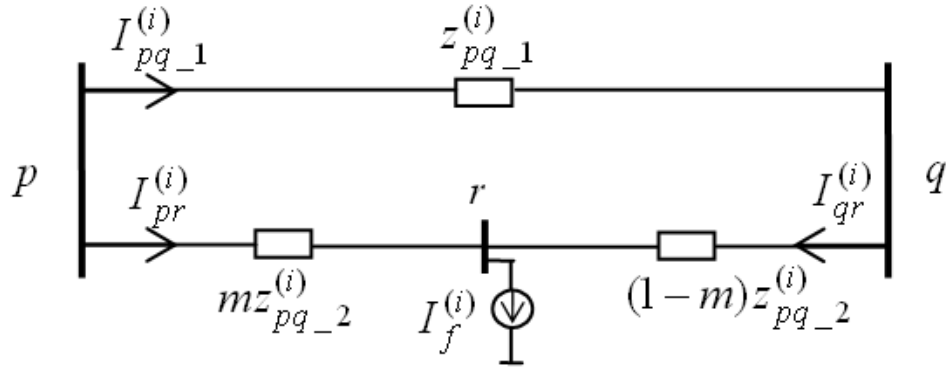


Figure 3.2: The positive/negative-sequence network of a double-circuit faulted line.

$$I_{j_1j_2}^{(0)} = \frac{E_{j_1}^{(0)} - E_{j_2}^{(0)}}{z_{j_1j_2}^{(0)}} = \frac{-Z_{j_1r}^{(0)}I_f^{(0)} + Z_{j_2r}^{(0)}I_f^{(0)}}{z_{j_1j_2}^{(0)}} = -\frac{Z_{j_1r}^{(0)} - Z_{j_2r}^{(0)}}{z_{j_1j_2}^{(0)}}I_f^{(0)} \quad (3.14)$$

where $I_{j_1j_2}^{(1)0}$ represents the positive-sequence pre-fault branch current.

Case 2 : The currents of the healthy circuit of the faulted double-circuit line whose two terminals are p and q

Since there is no mutual coupling between the parallel branches for positive- and negative-sequence networks as shown in Fig. 3.2, the positive- and negative-sequence currents of the healthy circuit of the faulted double-circuit line can be obtained similarly as in case 1.

$$I_{pq,1}^{(1)} = I_{pq,1}^{(1)0} - \frac{Z_{pr}^{(1)} - Z_{qr}^{(1)}}{z_{pq,1}^{(1)}}I_f^{(1)} \quad (3.15)$$

$$I_{pq,1}^{(2)} = -\frac{Z_{pr}^{(2)} - Z_{qr}^{(2)}}{z_{pq,1}^{(2)}}I_f^{(2)} \quad (3.16)$$

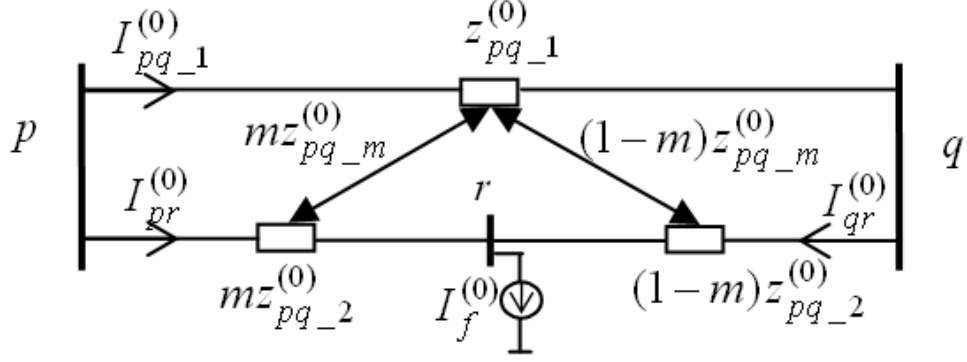


Figure 3.3: The zero-sequence network of a double-circuit faulted line.

For the derivation of $I_{pq-1}^{(0)}$, the following equations can be established from Fig. 3.3

$$I_{pq-1}^{(0)} z_{pq-1}^{(0)} + I_{pr}^{(0)} m z_{pq-m}^{(0)} - (I_{qr}^{(0)}) (1-m) z_{pq-m}^{(0)} = E_p^{(0)} - E_q^{(0)} \quad (3.17)$$

$$I_{pr}^{(0)} + I_{qr}^{(0)} = I_f^{(0)} \quad (3.18)$$

$$I_{pq-1}^{(0)} m z_{pq-m}^{(0)} + I_{pr}^{(0)} m z_{pq-2}^{(0)} = E_p^{(0)} - E_r^{(0)} \quad (3.19)$$

$$I_{qr}^{(0)} (1-m) z_{pq-2}^{(0)} - (I_{pq-1}^{(0)}) (1-m) z_{pq-m}^{(0)} = E_q^{(0)} - E_r^{(0)} \quad (3.20)$$

Substituting $I_{pr}^{(0)}$ from (3.18) into (3.17) gives rise to

$$I_{pq-1}^{(0)} z_{pq-1}^{(0)} + I_{pr}^{(0)} m z_{pq-m}^{(0)} - \left(I_f^{(0)} - I_{pr}^{(0)} \right) (1-m) z_{pq-m}^{(0)} = E_p^{(0)} - E_q^{(0)} \quad (3.21)$$

Replacing the voltage terms by (3.11), (3.21) can be further organized into

$$I_{pq-1}^{(0)} z_{pq-1}^{(0)} + I_{pr}^{(0)} z_{pq-m}^{(0)} = \left[-Z_{pr}^{(0)} + Z_{qr}^{(0)} + (1-m) z_{pq-m}^{(0)} \right] I_f^{(0)} \quad (3.22)$$

Substituting $I_{pr}^{(0)}$ from (3.18) into (3.20) yields

$$\left(I_f^{(0)} - I_{pr}^{(0)} \right) (1-m) z_{pq-2}^{(0)} - I_{pq-1}^{(0)} (1-m) z_{pq-m}^{(0)} = E_q^{(0)} - E_r^{(0)} \quad (3.23)$$

Subtracting (3.23) from (3.19), it is obtained

$$I_{pq-1}^{(0)} z_{pq-m}^{(0)} + I_{pr}^{(0)} z_{pq-2}^{(0)} - (1-m) z_{pq-2}^{(0)} I_f^{(0)} = E_p^{(0)} - E_q^{(0)} \quad (3.24)$$

Replacing the voltage terms by (3.11), (3.24) can be further organized into

$$I_{pq-1}^{(0)} z_{pq-m}^{(0)} + I_{pr}^{(0)} z_{pq-2}^{(0)} = \left[Z_{qr}^{(0)} - Z_{pr}^{(0)} + (1-m) z_{pq-2}^{(0)} \right] I_f^{(0)} \quad (3.25)$$

Then $I_{pq-1}^{(0)}$ and $I_{pr}^{(0)}$ can be solved from (3.22) and (3.25).

$$I_{pq-1}^{(0)} = -\frac{\left(Z_{pr}^{(0)} - Z_{qr}^{(0)}\right) \left(z_{pq,2}^{(0)} - z_{pq,m}^{(0)}\right)}{z_{pq,1}^{(0)} z_{pq,2}^{(0)} - \left(z_{pq,m}^{(0)}\right)^2} I_f^{(0)} \quad (3.26)$$

$$I_{pr}^{(0)} = -\left[\frac{\left(Z_{pr}^{(0)} - Z_{qr}^{(0)}\right) \left(z_{pq,m}^{(0)} - z_{pq,1}^{(0)}\right)}{\left(z_{pq,m}^{(0)}\right)^2 - z_{pq,1}^{(0)} z_{pq,2}^{(0)}} - 1 + m \right] I_f^{(0)} \quad (3.27)$$

From (3.17)-(3.20), we can derive another two equations

$$I_{pq-1}^{(0)} z_{pq,1}^{(0)} - I_{qr}^{(0)} z_{pq,m}^{(0)} = \left(-Z_{pr}^{(0)} + Z_{qr}^{(0)} - m z_{pq,m}^{(0)}\right) I_f^{(0)} \quad (3.28)$$

$$I_{pq-1}^{(0)} z_{pq,m}^{(0)} - I_{qr}^{(0)} z_{pq,2}^{(0)} = \left(-Z_{pr}^{(0)} + Z_{qr}^{(0)} - m z_{pq,2}^{(0)}\right) I_f^{(0)} \quad (3.29)$$

Eliminating $I_{pq-1}^{(0)}$ from (3.28) and (3.29) can derive the expression of $I_{qr}^{(0)}$

$$I_{qr}^{(0)} = -\left[\frac{\left(Z_{qr}^{(0)} - Z_{pr}^{(0)}\right) \left(z_{pq,m}^{(0)} - z_{pq,1}^{(0)}\right)}{\left(z_{pq,m}^{(0)}\right)^2 - z_{pq,1}^{(0)} z_{pq,2}^{(0)}} - m \right] I_f^{(0)} \quad (3.30)$$

Case 3: The currents of the faulted branch of the double-circuit line whose two terminals are p and r

From Fig. 3.2, we can build the following four equations for the positive- and negative-sequence networks

$$I_{pr}^{(1)} = \frac{E_p^{(1)} - E_r^{(1)}}{m z_{pq,2}^{(1)}} \quad (3.31)$$

$$I_{pr}^{(2)} = \frac{E_p^{(2)} - E_r^{(2)}}{m z_{pq,2}^{(2)}} \quad (3.32)$$

$$I_f^{(1)} - I_{pr}^{(1)} = \frac{E_q^{(1)} - E_r^{(1)}}{(1-m) z_{pq,2}^{(1)}} \quad (3.33)$$

$$I_f^{(2)} - I_{pr}^{(2)} = \frac{E_q^{(2)} - E_r^{(2)}}{(1-m) z_{pq,2}^{(2es.)}} \quad (3.34)$$

Eliminating $E_r^{(1)}$ from (3.31) and (3.33) leads to

$$E_p^{(1)} - E_q^{(1)} = I_{pr}^{(1)} m z_{pq,2}^{(1)} - (I_f^{(1)} - I_{pr}^{(1)}) (1-m) z_{pq,2}^{(1)} \quad (3.35)$$

Replacing the voltage terms by (3.9), we can obtain the expression of $I_{pr}^{(1)}$ as

$$I_{pr}^{(1)} = I_{pr}^{(1)0} - \left(\frac{Z_{pr}^{(1)} - Z_{qr}^{(1)}}{z_{pq.2}^{(1)}} - 1 + m \right) I_f^{(1)} \quad (3.36)$$

$I_{pr}^{(2)}$ can be similarly obtained from (3.32), (3.34) and (3.10) as

$$I_{pr}^{(2)} = - \left(\frac{Z_{pr}^{(2)} - Z_{qr}^{(2)}}{z_{pq.2}^{(2)}} - 1 + m \right) I_f^{(2)} \quad (3.37)$$

$I_{pr}^{(0)}$ can be found from case 2.

Case 4 : The currents of the faulted branch of the double-circuit line whose two terminals are q and r

$I_{qr}^{(1)}$ and $I_{qr}^{(2)}$ can be derived similar to $I_{pr}^{(1)}$ and $I_{pr}^{(2)}$ as shown in case 3 by using VCR for branch qr in Fig. 3.2.

$$I_{qr}^{(1)} = I_{qr}^{(1)0} - \left(\frac{Z_{qr}^{(1)} - Z_{pr}^{(1)}}{z_{pq.2}^{(1)}} - m \right) I_f^{(1)} \quad (3.38)$$

$$I_{qr}^{(2)} = - \left(\frac{Z_{qr}^{(2)} - Z_{pr}^{(2)}}{z_{pq.2}^{(2)}} - m \right) I_f^{(2)} \quad (3.39)$$

$I_{qr}^{(0)}$ can be found in case 2.

Case 5 : The currents of unfaulted double-circuit branches whose two terminals are k_1 and k_2

From Fig. 3.4, the currents of the branches k_1k_{2-1} and k_1k_{2-2} are calculated in the following

$$I_{k_1k_{2-1}}^{(1)0} = I_{k_1k_{2-1}}^{(1)0} - \frac{Z_{k_1r}^{(1)} - Z_{k_2r}^{(1)}}{z_{k_1k_{2-1}}^{(1)}} I_f^{(1)} \quad (3.40)$$

$$I_{k_1k_{2-1}}^{(2)} = - \frac{Z_{k_1r}^{(2)} - Z_{k_2r}^{(2)}}{z_{k_1k_{2-1}}^{(2)}} I_f^{(2)} \quad (3.41)$$

$$I_{k_1k_{2-2}}^{(1)0} = I_{k_1k_{2-2}}^{(1)0} - \frac{Z_{k_1r}^{(1)} - Z_{k_2r}^{(1)}}{z_{k_1k_{2-2}}^{(1)}} I_f^{(1)} \quad (3.42)$$

$$I_{k_1k_{2-2}}^{(2)} = - \frac{Z_{k_1r}^{(2)} - Z_{k_2r}^{(2)}}{z_{k_1k_{2-2}}^{(2)}} I_f^{(2)} \quad (3.43)$$

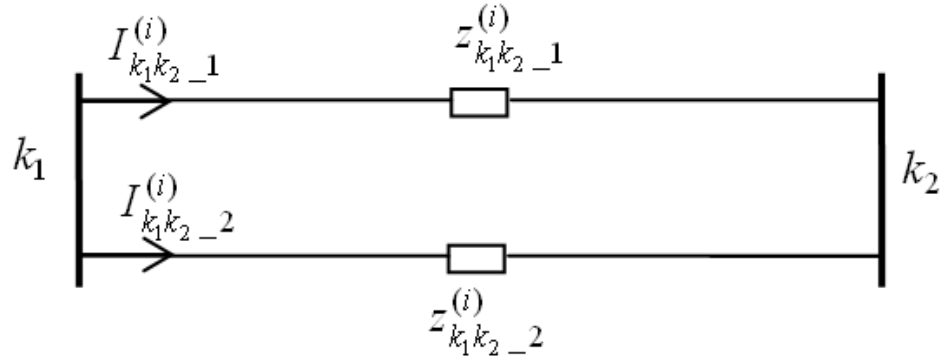


Figure 3.4: The positive/negative-sequence network of an unfaulted double-circuit line.

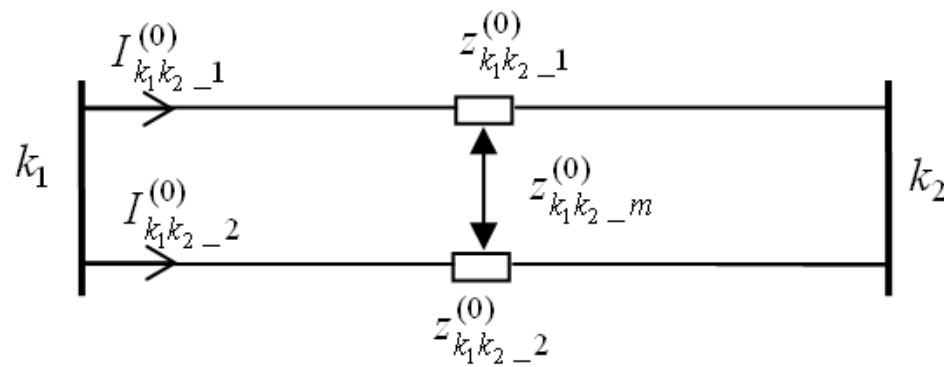


Figure 3.5: The zero-sequence network of an unfaulted double-circuit line.

Observing Fig. 3.5, we can write

$$I_{k_1 k_2-1}^{(0)} z_{k_1 k_2-1}^{(0)} + I_{k_1 k_2-2}^{(0)} z_{k_1 k_2-m}^{(0)} = E_{k_1}^{(0)} - E_{k_2}^{(0)} = (-Z_{k_1 r}^{(0)} + Z_{k_2 r}^{(0)}) I_f^{(0)} \quad (3.44)$$

$$I_{k_1 k_2-1}^{(0)} z_{k_1 k_2-m}^{(0)} + I_{k_1 k_2-2}^{(0)} z_{k_1 k_2-2}^{(0)} = E_{k_1}^{(0)} - E_{k_2}^{(0)} = (-Z_{k_1 r}^{(0)} + Z_{k_2 r}^{(0)}) I_f^{(0)} \quad (3.45)$$

Solving (3.44) and (3.45) can lead to

$$I_{k_1 k_2-1}^{(0)} = -\frac{z_{k_1 k_2-2}^{(0)} - z_{k_1 k_2-m}^{(0)}}{z_{k_1 k_2-1}^{(0)} z_{k_1 k_2-2}^{(0)} - \left(z_{k_1 k_2-m}^{(0)}\right)^2} \left(Z_{k_1 r}^{(0)} - Z_{k_2 r}^{(0)}\right) I_f^{(0)} \quad (3.46)$$

$$I_{k_1 k_2-2}^{(0)} = -\frac{z_{k_1 k_2-1}^{(0)} - z_{k_1 k_2-m}^{(0)}}{z_{k_1 k_2-1}^{(0)} z_{k_1 k_2-2}^{(0)} - \left(z_{k_1 k_2-m}^{(0)}\right)^2} \left(Z_{k_1 r}^{(0)} - Z_{k_2 r}^{(0)}\right) I_f^{(0)} \quad (3.47)$$

Let us observe (3.12)-(3.14), (3.15)-(3.16) and (3.26), (3.36)-(3.37) and (3.27), (3.38)-(3.39) and (3.30), (3.40)-(3.43), (3.46)-(3.47), and define

$$\beta_{j_1 j_2}^{(i)} = \frac{Z_{j_1 r}^{(i)} - Z_{j_2 r}^{(i)}}{z_{j_1 j_2}^{(i)}} = \frac{B_{j_1}^{(i)} - B_{j_2}^{(i)}}{z_{j_1 j_2}^{(i)}} + \frac{C_{j_1}^{(i)} - C_{j_2}^{(i)}}{z_{j_1 j_2}^{(i)}} m = B_{j_1 j_2}^{(i)} + C_{j_1 j_2}^{(i)} m, \quad i = 0, 1, 2 \quad (3.48)$$

$$\beta_{pq-1}^{(i)} = \frac{Z_{pr}^{(i)} - Z_{qr}^{(i)}}{z_{pq-1}^{(i)}} = \frac{B_p^{(i)} - B_q^{(i)}}{z_{pq-1}^{(i)}} + \frac{C_p^{(i)} - C_q^{(i)}}{z_{pq-1}^{(i)}} m = B_{pq-1}^{(i)} + C_{pq-1}^{(i)} m, \quad i = 1, 2 \quad (3.49)$$

$$\begin{aligned} \beta_{pq-1}^{(0)} &= \frac{\left(Z_{pr}^{(0)} - Z_{qr}^{(0)}\right) \left(z_{pq-2}^{(0)} - z_{pq-m}^{(0)}\right)}{z_{pq-1}^{(0)} z_{pq-2}^{(0)} - \left(z_{pq-m}^{(0)}\right)^2} = \frac{\left(B_p^{(0)} - B_q^{(0)}\right) \left(z_{pq-2}^{(0)} - z_{pq-m}^{(0)}\right)}{z_{pq-1}^{(0)} z_{pq-2}^{(0)} - \left(z_{pq-m}^{(0)}\right)^2} \\ &+ \frac{\left(C_p^{(0)} - C_q^{(0)}\right) \left(z_{pq-2}^{(0)} - z_{pq-m}^{(0)}\right)}{z_{pq-1}^{(0)} z_{pq-2}^{(0)} - \left(z_{pq-m}^{(0)}\right)^2} m = B_{pq-1}^{(0)} + C_{pq-1}^{(0)} m \end{aligned} \quad (3.50)$$

$$\begin{aligned} \beta_{pr}^{(i)} &= \frac{Z_{pr}^{(i)} - Z_{qr}^{(i)}}{z_{pq-2}^{(i)}} - 1 + m = \frac{B_p^{(i)} - B_q^{(i)} - z_{pq-2}^{(i)}}{z_{pq-2}^{(i)}} + \frac{C_p^{(i)} - C_q^{(i)} + z_{pq-2}^{(i)}}{z_{pq-2}^{(i)}} m \\ &= B_{pr}^{(i)} + C_{pr}^{(i)} m, \quad i = 1, 2 \end{aligned} \quad (3.51)$$

$$\begin{aligned} \beta_{pr}^{(0)} &= \frac{\left(Z_{pr}^{(0)} - Z_{qr}^{(0)}\right) \left(z_{pq-m}^{(0)} - z_{pq-1}^{(0)}\right)}{\left(z_{pq-m}^{(0)}\right)^2 - z_{pq-1}^{(0)} z_{pq-2}^{(0)}} - 1 + m \\ &= \frac{\left(B_p^{(0)} - B_q^{(0)}\right) \left(z_{pq-m}^{(0)} - z_{pq-1}^{(0)}\right) - \left(z_{pq-m}^{(0)}\right)^2 + z_{pq-1}^{(0)} z_{pq-2}^{(0)}}{\left(z_{pq-m}^{(0)}\right)^2 - z_{pq-1}^{(0)} z_{pq-2}^{(0)}} \end{aligned}$$

$$+ \frac{\left(C_p^{(0)} - C_q^{(0)}\right) \left(z_{pq-m}^{(0)} - z_{pq-1}^{(0)}\right) + \left(z_{pq-m}^{(0)}\right)^2 - z_{pq-1}^{(0)} z_{pq-2}^{(0)}}{\left(z_{pq-m}^{(0)}\right)^2 - z_{pq-1}^{(0)} z_{pq-2}^{(0)}} m = B_{pr}^{(0)} + C_{pr}^{(0)} m \quad (3.52)$$

$$\begin{aligned} \beta_{qr}^{(i)} &= \frac{Z_{qr}^{(i)} - Z_{pr}^{(i)}}{z_{pq-2}^{(i)}} - m = \frac{B_q^{(i)} - B_p^{(i)}}{z_{pq-2}^{(i)}} + \frac{C_q^{(i)} - C_p^{(i)} - z_{pq-2}^{(i)}}{z_{pq-2}^{(i)}} m \\ &= B_{qr}^{(i)} + C_{qr}^{(i)} m, \quad i = 1, 2 \end{aligned} \quad (3.53)$$

$$\begin{aligned} \beta_{qr}^{(0)} &= \frac{\left(Z_{qr}^{(0)} - Z_{pr}^{(0)}\right) \left(z_{pq-m}^{(0)} - z_{pq-1}^{(0)}\right)}{\left(z_{pq-m}^{(0)}\right)^2 - z_{pq-1}^{(0)} z_{pq-2}^{(0)}} - m = \frac{\left(B_q^{(0)} - B_p^{(0)}\right) \left(z_{pq-m}^{(0)} - z_{pq-1}^{(0)}\right)}{\left(z_{pq-m}^{(0)}\right)^2 - z_{pq-1}^{(0)} z_{pq-2}^{(0)}} \\ &+ \frac{\left(C_q^{(0)} - C_p^{(0)}\right) \left(z_{pq-m}^{(0)} - z_{pq-1}^{(0)}\right) - \left(z_{pq-m}^{(0)}\right)^2 + z_{pq-1}^{(0)} z_{pq-2}^{(0)}}{\left(z_{pq-m}^{(0)}\right)^2 - z_{pq-1}^{(0)} z_{pq-2}^{(0)}} m = B_{qr}^{(0)} + C_{qr}^{(0)} m \end{aligned} \quad (3.54)$$

$$\beta_{k_1 k_2-1}^{(i)} = \frac{Z_{k_1 r}^{(i)} - Z_{k_2 r}^{(i)}}{z_{k_1 k_2-1}^{(i)}} = \frac{B_{k_1}^{(i)} - B_{k_2}^{(i)}}{z_{k_1 k_2-1}^{(i)}} + \frac{C_{k_1}^{(i)} - C_{k_2}^{(i)}}{z_{k_1 k_2-1}^{(i)}} m = B_{k_1 k_2-1}^{(i)} + C_{k_1 k_2-1}^{(i)} m, \quad i = 1, 2 \quad (3.55)$$

$$\begin{aligned} \beta_{k_1 k_2-1}^{(0)} &= \frac{z_{k_1 k_2-2}^{(0)} - z_{k_1 k_2-m}^{(0)}}{z_{k_1 k_2-1}^{(0)} z_{k_1 k_2-2}^{(0)} - \left(z_{k_1 k_2-m}^{(0)}\right)^2} \left(Z_{k_1 r}^{(0)} - Z_{k_2 r}^{(0)}\right) \\ &= \frac{z_{k_1 k_2-2}^{(0)} - z_{k_1 k_2-m}^{(0)}}{z_{k_1 k_2-1}^{(0)} z_{k_1 k_2-2}^{(0)} - \left(z_{k_1 k_2-m}^{(0)}\right)^2} \left(B_{k_1}^{(0)} - B_{k_2}^{(0)}\right) \\ &+ \frac{z_{k_1 k_2-2}^{(0)} - z_{k_1 k_2-m}^{(0)}}{z_{k_1 k_2-1}^{(0)} z_{k_1 k_2-2}^{(0)} - \left(z_{k_1 k_2-m}^{(0)}\right)^2} \left(C_{k_1}^{(0)} - C_{k_2}^{(0)}\right) m = B_{k_1 k_2-1}^{(0)} + C_{k_1 k_2-1}^{(0)} m \end{aligned} \quad (3.56)$$

$$\beta_{k_1 k_2-2}^{(i)} = \frac{Z_{k_1 r}^{(i)} - Z_{k_2 r}^{(i)}}{z_{k_1 k_2-2}^{(i)}} = \frac{B_{k_1}^{(i)} - B_{k_2}^{(i)}}{z_{k_1 k_2-2}^{(i)}} + \frac{C_{k_1}^{(i)} - C_{k_2}^{(i)}}{z_{k_1 k_2-2}^{(i)}} m = B_{k_1 k_2-2}^{(i)} + C_{k_1 k_2-2}^{(i)} m, \quad i = 1, 2 \quad (3.57)$$

$$\beta_{k_1 k_2-2}^{(0)} = \frac{z_{k_1 k_1-1}^{(0)} - z_{k_1 k_2-m}^{(0)}}{z_{k_1 k_2-1}^{(0)} z_{k_1 k_2-2}^{(0)} - \left(z_{k_1 k_2-m}^{(0)}\right)^2} \left(Z_{k_1 r}^{(0)} - Z_{k_2 r}^{(0)}\right)$$

$$\begin{aligned}
&= \frac{z_{k_1 k_2-1}^{(0)} - z_{k_1 k_2-m}^{(0)}}{z_{k_1 k_2-1}^{(0)} z_{k_1 k_2-2}^{(0)} - \left(z_{k_1 k_2-m}^{(0)}\right)^2} \left(B_{k_1}^{(0)} - B_{k_2}^{(0)}\right) \\
&+ \frac{z_{k_1 k_2-1}^{(0)} - z_{k_1 k_2-m}^{(0)}}{z_{k_1 k_2-1}^{(0)} z_{k_1 k_2-2}^{(0)} - \left(z_{k_1 k_2-m}^{(0)}\right)^2} \left(C_{k_1}^{(0)} - C_{k_2}^{(0)}\right) m = B_{k_1 k_2-2}^{(0)} + C_{k_1 k_2-2}^{(0)} m \quad (3.58)
\end{aligned}$$

Then (3.12)-(3.14), (3.15)-(3.16) and (3.26), (3.36)-(3.37) and (3.27), (3.38)-(3.39) and (3.30), (3.40)-(3.43), (3.46)-(3.47) can be simplified into

$$I_{kl}^{(1)} = I_{kl}^{(1)0} - \beta_{kl}^{(1)} I_f^{(1)} \quad (3.59)$$

$$I_{kl}^{(2)} = -\beta_{kl}^{(2)} I_f^{(2)} \quad (3.60)$$

$$I_{kl}^{(0)} = -\beta_{kl}^{(0)} I_f^{(0)} \quad (3.61)$$

where

$$\beta_{kl}^{(i)} = B_{kl}^{(i)} + C_{kl}^{(i)} m, \quad i = 0, 1, 2 \quad (3.62)$$

Equations (3.59)-(3.61) hold for all the branches in the network during fault. Care should be taken that values of constants $B_{kl}^{(i)}$ and $C_{kl}^{(i)}$ depend on the specific branch and sequence network involved.

3.3 Proposed Fault Location Method

In Section 3.2, the sequence current change through any branch during the fault can be formulated with respect to the corresponding term $\beta_{kl}^{(i)}$ and fault current. $\beta_{kl}^{(i)}$ is related to the transfer impedance terms $Z_{kr}^{(i)}$ and $Z_{lr}^{(i)}$, which are associated to the two ends of the branch. Thus $\beta_{kl}^{(i)}$ can also be expressed in terms of m , the unknown fault location. In fact, (3.59)-(3.61) are applicable to both single-circuit lines and double-circuit lines [68]. Therefore, the fault location formulas proposed in [70] for single-circuit lines are directly applied for double-circuit lines.

Taking advantage of boundary conditions of different fault types and eliminating the sequence fault currents, the branch current measurements can be formulated as an analytical function of the unknown fault location. Then, the fault location can be obtained from the measured branch current phasors [68].

In addition, when the relationships between phase currents and sequence currents are employed, phase currents can be bridged with the unknown fault location variable, wherein the fault location algorithms using phase current magnitudes can be obtained [70].

3.3.1 Fault Location Algorithms Using Current Phasors

In this part, fault location algorithms employing current phasors from one branch and two branches are developed.

3.3.1.1 Fault Scenarios with Measurements from Two Branches

Suppose that synchronized current phasors through branches between bus k_1 and l_1 , and k_2 and l_2 are known. From (3.59), we have

$$I_{k_1 l_1}^{(1)} = I_{k_1 l_1}^{(1)0} - \beta_{k_1 l_1}^{(1)} I_f^{(1)} \quad (3.63)$$

$$I_{k_2 l_2}^{(1)} = I_{k_2 l_2}^{(1)0} - \beta_{k_2 l_2}^{(1)} I_f^{(1)} \quad (3.64)$$

Eliminating $I_f^{(1)}$ from (3.63) and (3.64), and applying (3.62) leads to

$$\frac{I_{k_1 l_1}^{(1)} - I_{k_1 l_1}^{(1)0}}{I_{k_2 l_2}^{(1)} - I_{k_2 l_2}^{(1)0}} = \frac{\beta_{k_1 l_1}^{(1)}}{\beta_{k_2 l_2}^{(1)}} = \frac{B_{k_1 l_1}^{(1)} + C_{k_1 l_1}^{(1)} m}{B_{k_2 l_2}^{(1)} + C_{k_2 l_2}^{(1)} m} \quad (3.65)$$

Define

$$d_{k_1 l_1 k_2 l_2}^{(1)} = \frac{I_{k_1 l_1}^{(1)} - I_{k_1 l_1}^{(1)0}}{I_{k_2 l_2}^{(1)} - I_{k_2 l_2}^{(1)0}} \quad (3.66)$$

The fault location is derived as

$$m = \frac{B_{k_1 l_1}^{(1)} - d_{k_1 l_1 k_2 l_2}^{(1)} B_{k_2 l_2}^{(1)}}{d_{k_1 l_1 k_2 l_2}^{(1)} C_{k_2 l_2}^{(1)} - C_{k_1 l_1}^{(1)}} \quad (3.67)$$

Note that no fault type classification is required for this algorithm. Negative-sequence or zero-sequence current phasors, where applicable, can also be exploited for fault location. However, positive-sequence currents are preferred, since they exist for any type of faults.

When the current changes due to the fault through two branches are linearly dependent to each other, it is impossible to carry out the fault location using the method above due to the reason explained in Section 2.3.1.1.

3.3.1.2 Fault Scenarios with Measurements from One Branch

In the following, fault location formulations using measurements from one branch have been derived for various types of fault.

(1) LG fault

For phase A to ground fault, based on the boundary condition in (2.97), we can eliminate $I_f^{(2)}$ and $I_f^{(0)}$ from (3.60) and (3.61) and combine (3.62) to reach

$$\frac{I_{kl}^{(2)}}{I_{kl}^{(0)}} = \frac{\beta_{kl}^{(2)}}{\beta_{kl}^{(0)}} = \frac{B_{kl}^{(2)} + C_{kl}^{(2)} m}{B_{kl}^{(0)} + C_{kl}^{(0)} m} \quad (3.68)$$

Define

$$g = \frac{I_{kl}^{(2)}}{I_{kl}^{(0)}}$$

The fault location for AG fault is then derived as

$$m = \frac{B_{kl}^{(2)} - gB_{kl}^{(0)}}{gC_{kl}^{(0)} - C_{kl}^{(2)}} \quad (3.69)$$

(2) *LLG fault*

For phase B to C to ground fault, from (2.98) and (2.99), we obtain

$$\frac{I_f^{(1)}}{I_f^{(2)}} = -\frac{Z_{rr}^{(0)} + Z_{rr}^{(2)} + 3R_f}{Z_{rr}^{(0)} + 3R_f} \quad (3.70)$$

By substituting (3.59) and (3.60) into (3.70) and using $\beta_{kl}^{(1)} = \beta_{kl}^{(2)}$, we have

$$\frac{I_{kl}^{(1)} - I_{kl}^{(1)0}}{I_{kl}^{(2)}} = -\frac{\beta_{kl}^{(1)} Z_{rr}^{(0)} + Z_{rr}^{(2)} + 3R_f}{\beta_{kl}^{(2)} Z_{rr}^{(0)} + 3R_f} = -\frac{Z_{rr}^{(0)} + Z_{rr}^{(2)} + 3R_f}{Z_{rr}^{(0)} + 3R_f} \quad (3.71)$$

Expanding (3.71) with (3.3) will lead to the fault location formula for BCG fault as follows

$$\frac{I_{kl}^{(1)} - I_{kl}^{(1)0}}{I_{kl}^{(2)}} = -\frac{\left(A_0^{(0)} + A_0^{(2)}\right) + \left(A_1^{(0)} + A_1^{(2)}\right)m + \left(A_2^{(0)} + A_2^{(2)}\right)m^2 + 3R_f}{A_0^{(0)} + A_1^{(0)}m + A_2^{(0)}m^2 + 3R_f} \quad (3.72)$$

The solution to (3.72) can be obtained by separating the complex equation into real and imaginary part, and solving the resulted real equations. Eliminating R_f from both equations will lead to a quadratic polynomial of m . The corresponding R_f can be calculated with any one of the real equations thereafter.

(3) *LL fault*

For phase B to C fault, from the boundary condition in (2.103), the expression of positive-sequence fault current in (2.104) and (3.60), we will derive

$$I_{kl}^{(2)} = \beta_{kl}^{(2)} \frac{E_r^{(1)0}}{Z_{rr}^{(1)} + Z_{rr}^{(2)} + R_f} \quad (3.73)$$

Substituting (3.3) and (3.62) into (3.73) will lead to the fault location formula for BC fault

$$I_{kl}^{(2)} = \frac{(B_{kl}^{(2)} + C_{kl}^{(2)}m)E_r^{(1)0}}{A_0^{(1)} + A_0^{(2)} + (A_1^{(1)} + A_1^{(2)})m + (A_2^{(1)} + A_2^{(2)})m^2 + R_f} \quad (3.74)$$

Assuming $E_r^{(1)0} = 1.0$, *p.u.*, (3.74) can be separated into two real equations. m can be calculated from a quadratic function first and then R_f can be solved from any of the two real equations. The assumption may bring about errors in fault location estimation.

(4) *LLL fault*

For three phase balanced fault, applying (3.59) into (2.109) can arrive at

$$I_{kl}^{(1)} = I_{kl}^{(1)0} - \frac{\beta_{kl}^{(1)} E_r^{(1)0}}{Z_{rr}^{(1)} + R_f} \quad (3.75)$$

Substituting (3.3) and (3.62) into (3.75) will reach the following ABC fault location formula

$$I_{kl}^{(1)} = I_{kl}^{(1)0} - \frac{(B_{kl}^{(1)} + C_{kl}^{(1)} m) E_r^{(1)0}}{A_0^{(1)} + A_1^{(1)} m + A_2^{(1)} m^2 + R_f} \quad (3.76)$$

Let $E_r^{(1)0} = 1.0, p.u.$, (3.76) can be similarly solved as BC fault. Assumption of one per unit for pre-fault voltage at the fault point may lead to errors in fault location estimate, which is related to the pre-fault load conditions in the network.

It should be noted that for LLG, LL and LLL one-bus fault location algorithms, two solutions are obtained, which may consist of either one valid solution ($0 \leq m \leq 1$ and $R_f \geq 0$) and one invalid solution ($m < 0$ or $m > 1$ or $R_f < 0$), or two valid solutions as defined in Section 2.3.1.2. In case there are one valid solution and one invalid solution, the invalid solution can be easily identified and removed and a unique solution arrives. In case there are two valid solutions, one is the true solution and the other is the erroneous solution.

For LLG fault, when two valid solutions are encountered, we can compute the currents of the branch with measurements from all the valid solutions by making use of the bus impedance matrix technique and compare them with the actual branch current measurements. The branch currents calculated from the erroneous solution differ from the branch current measurements and can therefore be identified.

For both LL and LLL faults, although it is natural to apply the same erroneous solution identification method proposed for LLG fault, it turns out that the calculated branch currents from both valid solutions are the same as the actual branch current measurements. Hence, the erroneous fault location estimate can not be distinguished this way and we will end up with two possible solutions.

3.3.2 Fault Location Algorithms Using Phase Current Magnitudes

In some cases, the recording devices only record the phase current magnitude during the fault. How to use these information to locate fault will be addressed in this sub-section.

At any branch kl , suppose only the phase current magnitudes during the fault, $|I_{kla}|$, $|I_{klb}|$, and $|I_{klc}|$, are recorded by the recording device. Based on the symmetrical component theory

$$I_{kla} = I_{kl}^{(0)} + I_{kl}^{(1)} + I_{kl}^{(2)} \quad (3.77)$$

$$I_{klb} = I_{kl}^{(0)} + \alpha^2 I_{kl}^{(1)} + \alpha I_{kl}^{(2)} \quad (3.78)$$

$$I_{klc} = I_{kl}^{(0)} + \alpha I_{kl}^{(1)} + \alpha^2 I_{kl}^{(2)} \quad (3.79)$$

where I_{kla} , I_{klb} , I_{klc} are the phase A, B, C current at branch kl , respectively. Substituting (3.59)-(3.61) into (3.77)-(3.79) leads to

$$I_{kla} = -\beta_{kl}^{(0)} I_f^{(0)} + I_{kl}^{(1)0} - \beta_{kl}^{(1)} I_f^{(1)} - \beta_{kl}^{(2)} I_f^{(2)} \quad (3.80)$$

$$I_{klb} = -\beta_{kl}^{(0)} I_f^{(0)} + \alpha^2 (I_{kl}^{(1)0} - \beta_{kl}^{(1)} I_f^{(1)}) - \alpha \beta_{kl}^{(2)} I_f^{(2)} \quad (3.81)$$

$$I_{klc} = -\beta_{kl}^{(0)} I_f^{(0)} + \alpha (I_{kl}^{(1)0} - \beta_{kl}^{(1)} I_f^{(1)}) - \alpha^2 \beta_{kl}^{(2)} I_f^{(2)} \quad (3.82)$$

3.3.2.1 Algorithms with Current Magnitudes from One Branch

Designed for the scenario where the measurements are only taken from one branch, we have the following one-branch algorithms.

1) LG fault

For phase A to ground fault, from the boundary condition stated in (2.92), (3.80)-(3.82) can be simplified as follows

$$I_{kla} = I_{kl}^{(1)0} - (\beta_{kl}^{(0)} + \beta_{kl}^{(1)} + \beta_{kl}^{(2)}) I_f^{(1)} \quad (3.83)$$

$$I_{klb} = \alpha^2 I_{kl}^{(1)0} - (\beta_{kl}^{(0)} + \alpha^2 \beta_{kl}^{(1)} + \alpha \beta_{kl}^{(2)}) I_f^{(1)} \quad (3.84)$$

$$I_{klc} = \alpha I_{kl}^{(1)0} - (\beta_{kl}^{(0)} + \alpha \beta_{kl}^{(1)} + \alpha^2 \beta_{kl}^{(2)}) I_f^{(1)} \quad (3.85)$$

Applying $\beta_{kl}^{(1)} = \beta_{kl}^{(2)}$, (3.83)-(3.85) can be simplified as

$$I_{kla} = I_{kl}^{(1)0} - (\beta_{kl}^{(0)} + 2\beta_{kl}^{(1)}) I_f^{(1)} \quad (3.86)$$

$$I_{klb} = \alpha^2 I_{kl}^{(1)0} - (\beta_{kl}^{(0)} - \beta_{kl}^{(1)}) I_f^{(1)} \quad (3.87)$$

$$I_{klc} = \alpha I_{kl}^{(1)0} - (\beta_{kl}^{(0)} - \beta_{kl}^{(1)}) I_f^{(1)} \quad (3.88)$$

Substituting (3.62), (3.3), and (2.93) into (3.86)-(3.88) can lead to the following fault location formulas

$$|I_{kla}| = \left| I_{kl}^{(1)0} - \left[(B_{kl}^{(0)} + 2B_{kl}^{(1)}) + (C_{kl}^{(0)} + 2C_{kl}^{(1)}) m \right] I_f^{(1)} \right| \quad (3.89)$$

$$|I_{klb}| = \left| \alpha^2 I_{kl}^{(1)0} - \left[(B_{kl}^{(0)} - B_{kl}^{(1)}) + (C_{kl}^{(0)} - C_{kl}^{(1)}) m \right] I_f^{(1)} \right| \quad (3.90)$$

$$|I_{klc}| = \left| \alpha I_{kl}^{(1)0} - \left[(B_{kl}^{(0)} - B_{kl}^{(1)}) + (C_{kl}^{(0)} - C_{kl}^{(1)}) m \right] I_f^{(1)} \right| \quad (3.91)$$

where

$$I_f^{(1)} = \frac{E_r^{(1)0}}{\left(A_0^{(0)} + 2A_0^{(1)} \right) + \left(A_1^{(0)} + 2A_1^{(1)} \right) m + \left(A_2^{(0)} + 2A_2^{(1)} \right) m^2 + 3R_f} \quad (3.92)$$

Given $|I_{kla}|$, $|I_{klb}|$ and $|I_{klc}|$ we can assume $I_{kl}^{(1)0} = 0$ and $E_r^{(1)0} = 1.0$ p.u. to solve two unknown variables m and R_f . With this assumption, it is realized that (3.90) and (3.91) contain the same information and can be treated as one function. Therefore, we have two equations and two unknowns, wherein Newton-Raphson approach can be utilized.

2) LLG fault

For phase B to C to ground fault, from the boundary condition in (2.98)-(2.100) and (3.80)-(3.82) the fault location formulations are obtained as

$$|I_{kla}| = \left| I_{kl}^{(1)0} + \frac{Z_{rr}^{(2)}}{Z_{LLG}} (\beta_{kl}^{(0)} - \beta_{kr}^{(1)}) I_f^{(1)} \right| \quad (3.93)$$

$$|I_{klb}| = \left| \alpha^2 I_{kl}^{(1)0} + \frac{\beta_{kl}^{(0)} Z_{rr}^{(2)}}{Z_{LLG}} I_f^{(1)} - \beta_{kl}^{(1)} (\alpha^2 - \alpha + \alpha \frac{Z_{rr}^{(2)}}{Z_{LLG}}) I_f^{(1)} \right| \quad (3.94)$$

$$|I_{klc}| = \left| \alpha I_{kl}^{(1)0} + \frac{\beta_{kl}^{(0)} Z_{rr}^{(2)}}{Z_{LLG}} I_f^{(1)} - \beta_{kl}^{(1)} (\alpha - \alpha^2 + \alpha^2 \frac{Z_{rr}^{(2)}}{Z_{LLG}}) I_f^{(1)} \right| \quad (3.95)$$

where

$$Z_{LLG} = Z_{rr}^{(0)} + Z_{rr}^{(2)} + 3R_f \quad (3.96)$$

and $I_f^{(1)}$ can be obtained from (2.98) and listed below

$$I_f^{(1)} = \frac{E_r^{(1)0}}{Z_{rr}^{(1)} + \frac{Z_{rr}^{(2)}(Z_{rr}^{(0)} + 3R_f)}{Z_{rr}^{(0)} + Z_{rr}^{(2)} + 3R_f}} \quad (3.97)$$

Substituting (3.62), (3.3) into (3.93)-(3.97) can lead to the fault location formulations. Provided $|I_{kla}|$, $|I_{klb}|$, and $|I_{klc}|$, we can assume $E_r^{(1)0} = 1.0$, p.u. and $I_{kl}^{(1)0} = 0$. Then we will have three equations and two unknowns m and R_f , which can be solved using least squares based approach.

3) LL fault

For phase B to C fault, upon the boundary condition in (2.103), (3.80)-(3.82) can be reformatted as

$$I_{kla} = I_{kl}^{(1)0} \quad (3.98)$$

$$I_{klb} = \alpha^2 I_{kl}^{(1)0} + (\alpha - \alpha^2) \beta_{kl}^{(1)} I_f^{(1)} \quad (3.99)$$

$$I_{klc} = \alpha I_{kl}^{(1)0} - (\alpha - \alpha^2) \beta_{kl}^{(1)} I_f^{(1)} \quad (3.100)$$

Applying (3.62), (3.3) and (2.104), (3.99)-(3.100) can be expanded as

$$|I_{klb}| = \left| \alpha^2 I_{kl}^{(1)0} + (\alpha - \alpha^2) (B_{kl}^{(1)} + C_{kl}^{(1)} m) I_f^{(1)} \right| \quad (3.101)$$

$$|I_{klc}| = \left| \alpha I_{kl}^{(1)0} - (\alpha - \alpha^2) \left(B_{kl}^{(1)} + C_{kl}^{(1)} m \right) I_f^{(1)} \right| \quad (3.102)$$

where

$$I_f^{(1)} = \frac{E_r^{(1)0}}{2A_0^{(1)} + 2A_1^{(1)}m + 2A_2^{(1)}m^2 + R_f} \quad (3.103)$$

With the assumption $I_{kl}^{(1)0} = 0$ and $E_r^{(1)0} = 1.0$ p.u., (3.101) and (3.102) are the same in essence. Therefore, we only have one equation. Further, we can presume a certain value for R_f to estimate the fault location m . Since the fault resistance is normally very small for double-phase fault, we can assign $R_f = 0.5 \Omega$ without causing significant errors. Newton-Raphson technique can be utilized to solve (3.101).

4) LLL fault

For three phase balanced fault, based on the boundary condition in (2.108), (3.80)-(3.82) can be reformatted as

$$I_{kla} = I_{kl}^{(1)0} - \beta_{kl}^{(1)} I_f^{(1)} \quad (3.104)$$

$$I_{klb} = \alpha^2 (I_{kl}^{(1)0} - \beta_{kl}^{(1)} I_f^{(1)}) \quad (3.105)$$

$$I_{klc} = \alpha (I_{kl}^{(1)0} - \beta_{kl}^{(1)} I_f^{(1)}) \quad (3.106)$$

where $I_f^{(1)}$ is from (2.109). Equations (3.104)-(3.106) contain the same information when absolute values are exercised. Therefore, making use of (3.104) together with (3.62) and (3.3) will lead to the fault location formulation as

$$|I_{kla}| = \left| I_{kl}^{(1)0} - \frac{(B_{kl}^{(1)} + C_{kl}^{(1)} m) E_r^{(1)0}}{A_0^{(1)} + A_1^{(1)} m + A_2^{(1)} m^2 + R_f} \right| \quad (3.107)$$

Given $|I_{kla}|$, other than assuming $I_{kl}^{(1)0} = 0$ and $E_r^{(1)0} = 1.0$ p.u., R_f also needs to be known to solve for m . The fault resistance is normally very small for three phase faults, so a value close to zero can be assumed without causing significant errors. Then we will have one equation and one unknown m , the solution of which is similar to LL fault.

Formulas involving other phases for different kinds of fault can be deduced similarly.

3.3.2.2 Algorithms with Current Magnitudes from Multiple Branches

When the current measurements from any two branches kl and k_1l_1 are available, in addition to (3.80)-(3.82), we also have

$$I_{k_1l_1a} = -\beta_{k_1l_1}^{(0)} I_f^{(0)} + I_{kl}^{(1)0} - \beta_{k_1l_1}^{(1)} I_f^{(1)} - \beta_{k_1l_1}^{(2)} I_f^{(2)} \quad (3.108)$$

$$I_{k_1l_1b} = -\beta_{k_1l_1}^{(0)} I_f^{(0)} + \alpha^2 (I_{kl}^{(1)0} - \beta_{k_1l_1}^{(1)} I_f^{(1)}) - \alpha \beta_{k_1l_1}^{(2)} I_f^{(2)} \quad (3.109)$$

$$I_{k_1l_1c} = -\beta_{k_1l_1}^{(0)} I_f^{(0)} + \alpha(I_{k_1l_1}^{(1)0} - \beta_{k_1l_1}^{(1)} I_f^{(1)}) - \alpha^2 \beta_{k_1l_1}^{(2)} I_f^{(2)} \quad (3.110)$$

Depending on the fault type, we will have six equations at most, with $|I_{kla}|$, $|I_{klb}|$, $|I_{klc}|$, $|I_{k_1l_1a}|$, $|I_{k_1l_1b}|$ and $|I_{k_1l_1c}|$ being known quantities and m , R_f , $I_{kl}^{(1)0}$, $I_{k_1l_1}^{(1)0}$ and $E_r^{(1)0}$ being unknowns. Still, assuming a flat value for all pre-fault voltages and currents, m and R_f can be solved. For LLG fault, there will be six equations. For LG fault, we will have four equations. For double-phase and three-phase balanced faults, there is no need to assume any value for the fault resistance since we have two equations now. In general, when multiple measurements are utilized. The least squares based technique can be adopted.

A note of value is that for LL and LLL faults, when the following relationship in (3.111) exists between any two or more branches, it is not possible to obtain any fault location estimation using these measurements.

$$\frac{B_{kl}^{(1)}}{C_{kl}^{(1)}} = \frac{B_{k_1l_1}^{(1)}}{C_{k_1l_1}^{(1)}} \quad (3.111)$$

This is because when (3.111) holds, the current measurements of these branches are linearly dependent and independent of m .

It should be pointed out that regardless of one-branch or multi-branch algorithms, for LG, LL and LLL faults, under certain fault conditions, multiple valid solutions might arise. When multiple valid solutions are yielded, our studies indicate that it is not possible to distinguish the true solution. This is because if the network is subject to the fault conditions as given by the valid solutions, by performing short-circuit analysis we will obtain the same current magnitudes as the measured current magnitudes. Hence, unless more information is available, there may be more than one fault location estimates.

3.4 Simulation Studies

In order to evaluate the developed fault location algorithms, simulation studies have been conducted and results will be shown in this section. The methodology is to simulate faults of different types, locations and fault resistances for the studied system with EMTP [67]. The current phasors extracted from the generated current waveforms using Discrete Fourier Transform are fed into the developed algorithms to calculate the fault location. The waveforms of about 8th cycle after fault inception are captured to obtain the phasors.

The sample 4-bus power system used in Section 2.4 is shown here again in Fig. 3.6. The possible current measurements and their flow directions for each branch are specified in Fig. 3.6. The system is modelled in EMTP based on the lumped parameter line model without considering load and shunt capacitance of the line. The location of the fault is defined as the distance between the fault point and bus 1. The fault location accuracy is evaluated by percentage error defined in equation (2.148).

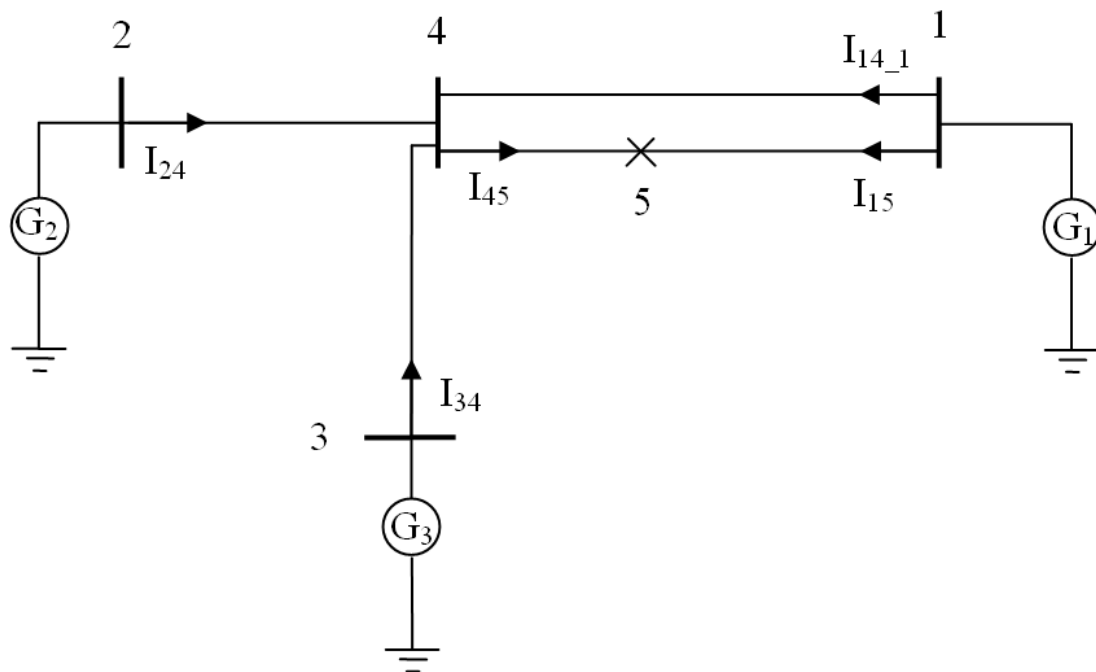


Figure 3.6: The diagram of studied 4-bus power system with current indicated.

Next, fault location results utilizing current phasors and phase current magnitudes are reported, respectively.

3.4.1 Case Studies for Fault Location Using Current Phasors

The algorithms have been tested under various fault conditions using current measurements from one or two branches. Table 3.1 shows the fault location results produced by synchronized current measurements from two branches. The first three columns represent the actual fault type, location and resistance respectively. Columns 4 and 5 list the errors of fault location estimate utilizing current measurements from branch (2, 4) and (1, 4, 1), and branch (1, 5) and (4, 5), respectively. Here, branch (2, 4) represents the circuit between bus 2 and 4. Branch (1, 4, 1) represents the first circuit of the double-circuit line between bus 1 and 4, where the third number in the bracket is used to distinguish between the two parallel branches. Other branches are named similarly.

The results in Table 3.1 are based on positive-sequence current measurements. It can be observed that the fault location estimate is quite accurate. In fact, the fault location estimate also contains an imaginary part, which represents the numerical round off error. Since we know the fault location estimate should be a real number, its imaginary part is neglected.

Quite accurate results have been obtained utilizing current measurements from other branch combinations such as (2, 4) & (1, 5), (2, 4) & (4, 5), (3, 4) & (1, 4, 1), (3, 4) & (1, 5), (3, 4) & (4, 5), (1, 4, 1) & (1, 5) and (1, 4, 1) & (4, 5). The

Table 3.1: Fault location results using current phasors from two branches

Fault type	Fault loca. (km)	Fault res. (Ω)	Est. err. using cur. from two branches (%)	
			(2,4) and (1,4,1)	(1,5) and (4,5)
AG	40	1	0.012	0.0082
		50	0.00014	0.00072
	100	1	0.011	0.0024
		50	0.00092	0.00023
	140	1	0.00042	0.000021
		50	0.00021	0.00020
BC	40	1	0.0028	0.00056
	100	1	0.0017	0.000030
	140	1	0.00022	0.00012
BCG	40	1	0.0021	0.0014
		50	0.0050	0.00013
	100	1	0.00081	0.00029
		50	0.0029	0.00016
	140	1	0.00024	0.000077
		50	0.00016	0.00014
ABC	40	1	0.013	0.0093
	100	1	0.010	0.0028
	140	1	0.00081	0.00041

above discussion equally applies to those branch combinations. The only exception is the combination (2, 4) & (3, 4), which does not produce any fault location estimate because the current changes from these two branches are linearly dependent.

Table 3.2: Fault location results using current phasors from one branch for AG fault

Fault location (km)	Fault res. (Ω)	Estimated error using current from one branch (%)		
		(2,4)	(1,4,1)	(1,5)
40	1	0.022	0.011	0.069
	10	0.0049	0.0019	0.016
100	1	0.015	0.011	0.015
	50	0.0014	0.00090	0.0014
140	10	0.000011	0.00069	0.00038
	50	0.000026	0.00061	0.00042

Table 3.2 presents the fault location results for AG fault utilizing the current measurements from one branch. Columns 3-5 display the percentage errors of fault location estimate employing current measurements from branch (2, 4), (1, 4, 1) and (1, 5), respectively. The fault location results in Table 3.2 are very satisfactory.

The fault location results for BCG fault using current measurements from branch (3, 4) are displayed in Table 3.3. Columns 3-4 exhibit the estimated fault resistance

and percentage fault location error. The base value of the impedance is 529Ω . Experiments shows that when fault resistance approaches a very high value, about 500Ω in our studies, erroneous solution may arise in some cases, which can be identified and removed by the proposed method earlier.

Table 3.3: Fault location results using current phasors from one branch for BCG fault

Fault location (km)	Fault res. (Ω)	Est. fault res. (p.u.)	Est. fault loca. error (%)
40	1	0.001904	0.0025
	10	0.01900	0.0043
100	10	0.01900	0.0027
	50	0.09450	0.0061
140	1	0.001901	0.0027
	50	0.09450	0.00021

Table 3.4 shows the fault location results utilizing current measurements of branch (2, 4) for BC and ABC faults. Column 3-5 list the estimated fault location, resistance and percentage fault location error. The actual fault resistance is 1Ω . Two valid solutions may be obtained with one of them being an erroneous one as indicated by N/A. For example, for a BC fault with fault location of 40 km, the algorithm with currents of branch (2, 4) as inputs yields two valid solutions, (0.2073, 0.001936) p.u. and (0.3240, 0.002361) p.u.. Therefore, we have two likely fault location estimates 0.2073 p.u. and 0.3240 p.u..

Table 3.4: Fault location results using current phasors from one branch for BC and ABC faults

Fault type	Fault location (km)	Est. fault loca. (p.u.)	Est. fault res. (p.u.)	Est. fault loca. err. (%)
BC	40	0.2073	0.001936	0.0046
		0.3240	0.002361	N/A
	100	0.06703	0.001153	N/A
		0.5183	0.001998	0.017
ABC	40	0.2053	0.001921	0.20
		0.3280	0.002297	N/A
	140	0.7254	0.001952	0.0011

In general, regardless of the fault type, when one branch current measurements are utilized, the fault location estimate is highly accurate as shown in Table 3.2, 3.3 and 3.4.

3.4.2 Case Studies for Fault Location Using Phase Current Magnitudes

Table 3.5 presents the fault location results using phase current magnitudes. The first three columns list the actual fault type, fault location and fault resistance utilized in EMTP. The percentage fault location estimation errors using phase current magnitudes from branches of different combinations are reported in the rest columns.

As can be seen, the accuracy of fault location estimates are quite satisfactory, with the biggest error being 0.9949% when using the measurements from a single bus for ABC and BC faults and 0.0292% for the rest. The bigger error of the first situation is on account of the approximation of the fault resistance. In certain cases, multiple valid solutions may arise designated by *. So far, our studies indicate that it is not possible to identify the true solution when only current magnitudes data are available.

Table 3.5: Fault location results using phase current magnitudes

Fault type	Fault loca. (km)	Fault res. (Ω)	Fault loca. est. error using phase current mag. from different branches (%)			
			(2,4)	(1,4,1)	(3,4) & (1,4,1)	(1,5) & (4,25)
AG	40	10	0.0049	0.0001*	0.0001	0.0012
BC	140	1	0.1070	0.0467*	0.0001	0.0001
BCG	100	50	0.0043	0.0009	0.0011	0.0003
ABC	40	1	0.9949*	0.0186*	0.0292	0.0183

3.5 Summary

In this chapter, fault location algorithms using sparse current phasors and phase current magnitudes based on the lumped parameter line model have been developed. Very accurate simulation study results have been obtained.

The phasor-based approach has the following characteristic

- Fault type classification is required before applying the one-branch fault location algorithm. While positive-sequence quantities are utilized to perform two-branch fault location algorithm, there is no need to exercise fault classification.
- Both two-branch algorithm and one-branch algorithms for LG and LLG faults are able to produce precise fault location. Whereas LL and LLL one-branch algorithms can only produce fault location approximation due to the assumption of flat value for the pre-fault voltage at the fault bus.
- Two-branch fault location algorithm has limited application determined by the network topology.

- For LL and LLL one-branch fault location algorithms, when two valid solutions are obtained, we will have two possible fault location estimates.

For the magnitude-based approach, we can sum up the following points

- Fault type classification is required before carrying out fault location for both one-branch and multi-branch algorithms.
- All the algorithms using phase current magnitudes are iterative and can only procure an approximate value of fault location.
- For LLG faults, regardless of one-branch or multi-branch algorithms, a unique fault location estimate can be yielded.
- For LL and LLL faults, the feasibility of the multi-branch fault location algorithms depends on the network topology.
- Erroneous fault location estimates may exist for one-branch or multi-branch algorithms for LG, LL and LLL faults. Without other information, such as voltage measurements, it is not possible to filter out the erroneous solution. Study on sufficiency of measurements for uniquely determining the true fault location for double-circuit lines is a complex problem and entails further research.

Chapter 4

Fault Location Utilizing Sparse Voltage Measurements Based on Distributed Parameter Line Model

In this chapter, the proposed fault location method is briefly given first. The zero-sequence equivalent π model of the double-circuit line is then derived in Section 4.2. Section 4.3 and 4.4 present the proposed fault location method. An optimal estimator able to detect and identify bad measurements is introduced in Section 4.5. Section 4.6 reports the simulation study results. Finally, Section 4.7 summarizes the chapter with concluding remarks.

4.1 Introduction

The fault location method proposed in Chapter 2 is based on the lumped parameter line model without considering the shunt capacitance. For long transmission lines, it may cause significant errors. This chapter has developed accurate fault location algorithms based on the distributed parameter line model, which fully takes the charging effect of the lines into consideration. Sparse voltage measurements are employed and no current measurements are required. The network data are assumed to be known and the network is transposed. The faulted section has been pinpointed in advance from relay operations. Also, the fault type classification, if needed, has been carried out before applying fault location algorithms.

4.2 Zero-Sequence Equivalent π Model of Double-Circuit Line

The positive-sequence equivalent π model for the double-circuit line is no different from the single-circuit line since there is no mutual coupling between the parallel lines, which is well described in classical textbooks [64]. However, the zero-sequence double-circuit line model based on the distributed parameter line model has not been

discussed in any textbooks due to its complexity. In reference [71], by decoupling the zero-sequence parallel lines into two independent modes, the equivalent π model for double-circuit lines having either identical or different line parameters is established. In this dissertation, a different approach purely in time-domain is provided. The constructed equivalent π model is the same as that of [71]. The proposed time-domain approach is only applicable to the scenario where the line parameters of the parallel lines are identical.

In this section, all the quantities refer to zero-sequence components unless otherwise specified. A schematic diagram of a zero-sequence double-circuit line is delineated in Fig. 4.1. The sending and receiving ends of the line are denoted as S and R .

V_{s1}, I_{s1} voltage and current at the sending end of line 1;

V_{r1}, I_{r1} voltage and current at the receiving end of line 1;

V_{s2}, I_{s2} voltage and current at the sending end of line 2;

V_{r2}, I_{r2} voltage and current at the receiving end of line 2;

x the distance between the considered point and the receiving end;

V_1, I_1 voltage and current of line 1 at the considered point;

V_2, I_2 voltage and current of line 2 at the considered point;

z self-series impedance of the line per unit length;

y self-shunt admittance of the line per unit length;

z_m mutual-series impedance between the parallel lines per unit length;

y_m mutual-shunt admittance between the parallel lines per unit length;

Given that the parameters of the lines are distributed uniformly throughout the length of the line, our objective is to derive the equivalent model that accounts for the distributed parameter effects. Suppose such an equivalent circuit exists as shown in Fig. 4.2, where we have Z and Z_m as the total equivalent self- and mutual-series impedance and Y and Y_m as the total equivalent self- and mutual-shunt admittance. The rest part of this section is devoted to the derivation of these equivalent parameters.

Based on Fig. 4.1, we write

$$dV_1 = I_1 z dx + I_2 z_m dx$$

$$dI_1 = V_1 y dx + (V_1 - V_2) y_m dx$$

From the above equations, we have

$$\frac{dV_1}{dx} = I_1 z + I_2 z_m \quad (4.1)$$

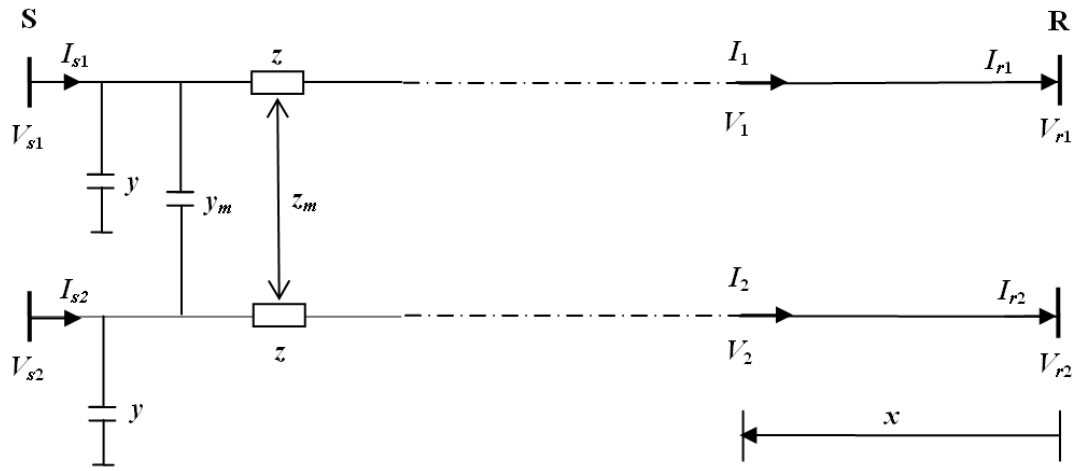


Figure 4.1: Mutually coupled zero-sequence networks of a parallel line.

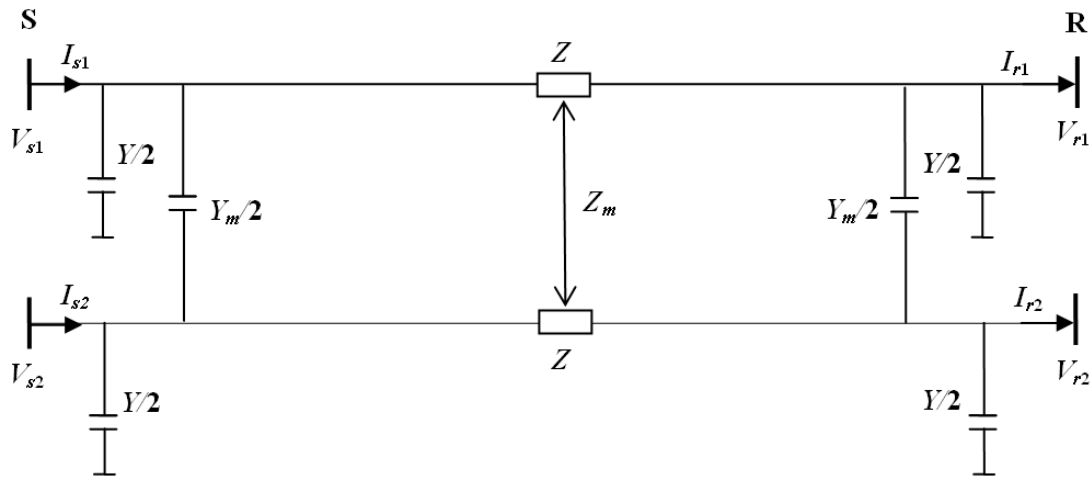


Figure 4.2: Equivalent π model of the zero-sequence double-circuit line.

$$\frac{dI_1}{dx} = V_1(y + y_m) - V_2y_m \quad (4.2)$$

Taking the derivative of (4.1) and (4.2) with respect to x , respectively, then we have

$$\frac{d^2V_1}{dx^2} = z\frac{dI_1}{dx} + z_m\frac{dI_2}{dx} \quad (4.3)$$

$$\frac{d^2I_1}{dx^2} = (y + y_m)\frac{dV_1}{dx} - y_m\frac{dV_2}{dx} \quad (4.4)$$

Referring to Fig. 4.1, for the second line the following equations hold

$$dV_2 = I_2 z dx + I_1 z_m dx$$

$$dI_2 = V_2 y dx + (V_2 - V_1)y_m dx$$

From the above two equations we can derive

$$\frac{dV_2}{dx} = I_2 z + I_1 z_m \quad (4.5)$$

$$\frac{dI_2}{dx} = V_2(y + y_m) - V_1 y_m \quad (4.6)$$

Then taking the derivative of (4.5) and (4.6) with respect to x , respectively, we have

$$\frac{d^2V_2}{dx^2} = z\frac{dI_2}{dx} + z_m\frac{dI_1}{dx} \quad (4.7)$$

$$\frac{d^2I_2}{dx^2} = (y + y_m)\frac{dV_2}{dx} - y_m\frac{dV_1}{dx} \quad (4.8)$$

Substituting (4.2) and (4.6) into (4.3), then

$$\begin{aligned} \frac{d^2V_1}{dx^2} &= z[V_1(y + y_m) - V_2y_m] + z_m[V_2(y + y_m) - V_1y_m] \\ &= (zy + zy_m - z_my_m)V_1 + (z_my + z_my_m - zy_m)V_2 \end{aligned} \quad (4.9)$$

Substituting (4.1) and (4.5) into (4.4), then

$$\begin{aligned} \frac{d^2I_1}{dx^2} &= (y + y_m)(I_1 z + I_2 z_m) - y_m(I_2 z + I_1 z_m) \\ &= (zy + zy_m - z_my_m)I_1 + (z_my + z_my_m - zy_m)I_2 \end{aligned} \quad (4.10)$$

Substituting (4.2) and (4.6) into (4.7), then

$$\begin{aligned} \frac{d^2V_2}{dx^2} &= z[V_2(y + y_m) - V_1y_m] + z_m[V_1(y + y_m) - V_2y_m] \\ &= (zy + zy_m - z_my_m)V_2 + (z_my + z_my_m - zy_m)V_1 \end{aligned} \quad (4.11)$$

Substituting (4.1) and (4.5) into (4.8), then

$$\begin{aligned}\frac{d^2 I_2}{dx^2} &= (y + y_m)(I_2 z + I_1 z_m) - y_m(I_1 z + I_2 z_m) \\ &= (zy + zy_m - z_m y_m)I_2 + (z_m y + z_m y_m - zy_m)I_1\end{aligned}\quad (4.12)$$

From (4.10), we can obtain the expression of I_2

$$I_2 = \frac{1}{z_m y + z_m y_m - zy_m} \left[\frac{d^2 I_1}{dx^2} - (zy + zy_m - z_m y_m)I_1 \right] \quad (4.13)$$

$$\frac{dI_2}{dx} = \frac{1}{z_m y + z_m y_m - zy_m} \left[\frac{d^3 I_1}{dx^3} - (zy + zy_m - z_m y_m) \frac{dI_1}{dx} \right] \quad (4.14)$$

$$\frac{d^2 I_2}{dx^2} = \frac{1}{z_m y + z_m y_m - zy_m} \left[\frac{d^4 I_1}{dx^4} - (zy + zy_m - z_m y_m) \frac{d^2 I_1}{dx^2} \right] \quad (4.15)$$

Substituting (4.13) and (4.15) into (4.12), we obtain

$$\begin{aligned}\frac{1}{z_m y + z_m y_m - zy_m} \left[\frac{d^4 I_1}{dx^4} - (zy + zy_m - z_m y_m) \frac{d^2 I_1}{dx^2} \right] = \\ \frac{zy + zy_m - z_m y_m}{z_m y + z_m y_m - zy_m} \left[\frac{d^2 I_1}{dx^2} - (zy + zy_m - z_m y_m)I_1 \right] + (z_m y + z_m y_m - zy_m)I_1\end{aligned}$$

which can be rearranged into the following form

$$\begin{aligned}\frac{d^4 I_1}{dx^4} - 2(zy + zy_m - z_m y_m) \frac{d^2 I_1}{dx^2} \\ + [(zy + zy_m - z_m y_m)^2 - (z_m y + z_m y_m - zy_m)^2] I_1 = 0\end{aligned}\quad (4.16)$$

The characteristic equation of (4.16) is

$$\lambda^4 - 2(zy + zy_m - z_m y_m)\lambda^2 + [(zy + zy_m - z_m y_m)^2 - (z_m y + z_m y_m - zy_m)^2] = 0$$

The roots of the above equation are

$$\begin{aligned}\lambda^2 &= \frac{2(zy + zy_m - z_m y_m)}{2} \\ &\pm \frac{\sqrt{4(zy + zy_m - z_m y_m)^2 - 4[(zy + zy_m - z_m y_m)^2 - (z_m y + z_m y_m - zy_m)^2]}}{2} \\ &= (zy + zy_m - z_m y_m) \pm (z_m y + z_m y_m - zy_m) \\ &= \begin{cases} (z + z_m)y \\ (z - z_m)(y + 2y_m) \end{cases}\end{aligned}$$

Then, the solution of λ is

$$\lambda_1 = \sqrt{y(z + z_m)}$$

$$\begin{aligned}\lambda_2 &= -\sqrt{y(z+z_m)} \\ \lambda_3 &= \sqrt{(z-z_m)(y+2y_m)} \\ \lambda_4 &= -\sqrt{(z-z_m)(y+2y_m)}\end{aligned}$$

Therefore the solution of (4.16) is

$$I_1 = A_1 e^{\lambda_1 x} + A_2 e^{\lambda_2 x} + A_3 e^{\lambda_3 x} + A_4 e^{\lambda_4 x}$$

which is

$$I_1 = A_1 e^{\sqrt{y(z+z_m)}x} + A_2 e^{-\sqrt{y(z+z_m)}x} + A_3 e^{\sqrt{(z-z_m)(y+2y_m)}x} + A_4 e^{-\sqrt{(z-z_m)(y+2y_m)}x} \quad (4.17)$$

Define

$$\gamma_{m1} = \sqrt{(z-z_m)(y+2y_m)} \quad (4.18)$$

$$\gamma_{m2} = \sqrt{(z+z_m)y} \quad (4.19)$$

Then (4.17) becomes

$$I_1 = A_1 e^{\gamma_{m2}x} + A_2 e^{-\gamma_{m2}x} + A_3 e^{\gamma_{m1}x} + A_4 e^{-\gamma_{m1}x} \quad (4.20)$$

From (4.12), we have

$$I_1 = \frac{1}{z_m y + z_m y_m - z y_m} \left[\frac{d^2 I_2}{dx^2} - (z y + z y_m - z_m y_m) I_2 \right] \quad (4.21)$$

$$\frac{d^2 I_1}{dx^2} = \frac{1}{z_m y + z_m y_m - z y_m} \left[\frac{d^4 I_2}{dx^4} - (z y + z y_m - z_m y_m) \frac{d^2 I_2}{dx^2} \right] \quad (4.22)$$

Substituting (4.21) and (4.22) into (4.10) and rearranging leads to

$$\begin{aligned}\frac{d^4 I_2}{dx^4} - 2(z y + z y_m - z_m y_m) \frac{d^2 I_2}{dx^2} \\ + [(z y + z y_m - z_m y_m)^2 - (z_m y + z_m y_m - z y_m)^2] I_2 = 0\end{aligned} \quad (4.23)$$

The solution of (4.23) can be extracted from that of (4.16), which is shown as follows

$$I_2 = A_5 e^{\sqrt{y(z+z_m)}x} + A_6 e^{-\sqrt{y(z+z_m)}x} + A_7 e^{\sqrt{(z-z_m)(y+2y_m)}x} + A_8 e^{-\sqrt{(z-z_m)(y+2y_m)}x} \quad (4.24)$$

Using (4.18) and (4.19), (4.24) is formulated as

$$I_2 = A_5 e^{\gamma_{m2}x} + A_6 e^{-\gamma_{m2}x} + A_7 e^{\gamma_{m1}x} + A_8 e^{-\gamma_{m1}x} \quad (4.25)$$

From (4.2) and (4.6), V_1 and V_2 with respect to I_1 and I_2 can be found

$$V_1 = \frac{1}{y(y+2y_m)} \left[\frac{dI_1}{dx}(y+y_m) + \frac{dI_2}{dx}y_m \right] \quad (4.26)$$

$$V_2 = \frac{1}{y(y+2y_m)} \left[\frac{dI_1}{dx} y_m + \frac{dI_2}{dx} (y+y_m) \right] \quad (4.27)$$

Substituting the respective derivatives of I_1 and I_2 over x from (4.20) and (4.25) into (4.26) and (4.27), we can derive

$$V_1 = \frac{1}{y(y+2y_m)} \left\{ [A_1(y+y_m) + A_5y_m] \gamma_{m2} e^{\gamma_{m2}x} - [A_2(y+y_m) + A_6y_m] \gamma_{m2} e^{-\gamma_{m2}x} \right. \\ \left. + [A_3(y+y_m) + A_7y_m] \gamma_{m1} e^{\gamma_{m1}x} - [A_4(y+y_m) + A_8y_m] \gamma_{m1} e^{-\gamma_{m1}x} \right\} \quad (4.28)$$

$$V_2 = \frac{1}{y(y+2y_m)} \left\{ [A_1y_m + A_5(y+y_m)] \gamma_{m2} e^{\gamma_{m2}x} - [A_2y_m + A_6(y+y_m)] \gamma_{m2} e^{-\gamma_{m2}x} \right. \\ \left. + [A_3y_m + A_7(y+y_m)] \gamma_{m1} e^{\gamma_{m1}x} - [A_4y_m + A_8(y+y_m)] \gamma_{m1} e^{-\gamma_{m1}x} \right\} \quad (4.29)$$

The derivative of (4.28) with respect to x is

$$\frac{dV_1}{dx} = \frac{1}{y(y+2y_m)} \left\{ [A_1(y+y_m) + A_5y_m] \gamma_{m2}^2 e^{\gamma_{m2}x} + [A_2(y+y_m) + A_6y_m] \gamma_{m2}^2 e^{-\gamma_{m2}x} \right. \\ \left. + [A_3(y+y_m) + A_7y_m] \gamma_{m1}^2 e^{\gamma_{m1}x} + [A_4(y+y_m) + A_8y_m] \gamma_{m1}^2 e^{-\gamma_{m1}x} \right\} \quad (4.30)$$

Based on (4.20) and (4.25), we have

$$I_1z + I_2z_m = A_1ze^{\gamma_{m2}x} + A_2ze^{-\gamma_{m2}x} + A_3ze^{\gamma_{m1}x} + A_4ze^{-\gamma_{m1}x} \\ + A_5z_me^{\gamma_{m2}x} + A_6z_me^{-\gamma_{m2}x} + A_7z_me^{\gamma_{m1}x} + A_8z_me^{-\gamma_{m1}x} \\ = (A_1z + A_5z_m)e^{\gamma_{m2}x} + (A_2z + A_6z_m)e^{-\gamma_{m2}x} \\ + (A_3z + A_7z_m)e^{\gamma_{m1}x} + (A_4z + A_8z_m)e^{-\gamma_{m1}x} \quad (4.31)$$

Since $dV_1/dx = I_1z + I_2z_m$ holds from (4.1), by comparing (4.30) and (4.31), the following exist

$$\frac{\gamma_{m2}^2}{y(y+2y_m)} [A_1(y+y_m) + A_5y_m] = A_1z + A_5z_m \\ \frac{\gamma_{m2}^2}{y(y+2y_m)} [A_2(y+y_m) + A_6y_m] = A_2z + A_6z_m \\ \frac{\gamma_{m1}^2}{y(y+2y_m)} [A_3(y+y_m) + A_7y_m] = A_3z + A_7z_m \\ \frac{\gamma_{m1}^2}{y(y+2y_m)} [A_4(y+y_m) + A_8y_m] = A_4z + A_8z_m \quad (4.32)$$

The derivative of (4.29) with respect to x is

$$\frac{dV_2}{dx} = \frac{1}{y(y+2y_m)} \left\{ [A_1y_m + A_5(y+y_m)] \gamma_{m2}^2 e^{\gamma_{m2}x} + [A_2y_m + A_6(y+y_m)] \gamma_{m2}^2 e^{-\gamma_{m2}x} \right.$$

$$+ [A_3y_m + A_7(y + y_m)]\gamma_{m1}^2 e^{\gamma_{m1}x} + [A_4y_m + A_8(y + y_m)]\gamma_{m1}^2 e^{-\gamma_{m1}x} \} \quad (4.33)$$

Based on (4.20) and (4.25), we have

$$\begin{aligned} I_1z_m + I_2z &= A_1z_me^{\gamma_{m2}x} + A_2z_me^{-\gamma_{m2}x} + A_3z_me^{\gamma_{m1}x} + A_4z_me^{-\gamma_{m1}x} \\ &\quad + A_5ze^{\gamma_{m2}x} + A_6ze^{-\gamma_{m2}x} + A_7ze^{\gamma_{m1}x} + A_8ze^{-\gamma_{m1}x} \\ &= (A_1z_m + A_5z)e^{\gamma_{m2}x} + (A_2z_m + A_6z)e^{-\gamma_{m2}x} \\ &\quad + (A_3z_m + A_7z)e^{\gamma_{m1}x} + (A_4z_m + A_8z)e^{-\gamma_{m1}x} \end{aligned} \quad (4.34)$$

Since $dV_2/dx = I_2z + I_1z_m$ holds from (4.5), by comparing (4.33) and (4.34), the following exist

$$\begin{aligned} \frac{\gamma_{m2}^2}{y(y + 2y_m)} [A_1y_m + A_5(y + y_m)] &= A_1z_m + A_5z \\ \frac{\gamma_{m2}^2}{y(y + 2y_m)} [A_2y_m + A_6(y + y_m)] &= A_2z_m + A_6z \\ \frac{\gamma_{m1}^2}{y(y + 2y_m)} [A_3y_m + A_7(y + y_m)] &= A_3z_m + A_7z \\ \frac{\gamma_{m1}^2}{y(y + 2y_m)} [A_4y_m + A_8(y + y_m)] &= A_4z_m + A_8z \end{aligned} \quad (4.35)$$

Solving either (4.34) or (4.35) can reach the following relationships

$$\begin{aligned} A_5 &= \frac{\gamma_{m2}^2(y + y_m) - zy(y + 2y_m)}{z_my(y + 2y_m) - \gamma_{m2}^2y_m} A_1 \\ A_6 &= \frac{\gamma_{m2}^2(y + y_m) - zy(y + 2y_m)}{z_my(y + 2y_m) - \gamma_{m2}^2y_m} A_2 \\ A_7 &= \frac{\gamma_{m1}^2(y + y_m) - zy(y + 2y_m)}{z_my(y + 2y_m) - \gamma_{m1}^2y_m} A_3 \\ A_8 &= \frac{\gamma_{m1}^2(y + y_m) - zy(y + 2y_m)}{z_my(y + 2y_m) - \gamma_{m1}^2y_m} A_4 \end{aligned} \quad (4.36)$$

Replacing γ_{m1} and γ_{m2} from (4.18) and (4.19), (4.36) can be simplified into

$$\begin{aligned} A_5 &= A_1 \\ A_6 &= A_2 \\ A_7 &= -A_3 \\ A_8 &= -A_4 \end{aligned} \quad (4.37)$$

Let's define

$$\sqrt{\frac{z + z_m}{y}} = Z_{cm2} \quad (4.38)$$

$$\sqrt{\frac{z - z_m}{y + 2y_m}} = Z_{cm1} \quad (4.39)$$

Using (4.37), (4.38) and (4.39), the coefficients of V_1 and V_2 in (4.28) and (4.29) can be simplified into

$$\begin{aligned} \frac{A_1(y + y_m) + A_5y_m}{y(y + 2y_m)}\gamma_{m2} &= A_1\frac{\gamma_{m2}}{y} = A_1\sqrt{\frac{z + z_m}{y}} = A_1Z_{cm2} \\ -\frac{A_2(y + y_m) + A_6y_m}{y(y + 2y_m)}\gamma_{m2} &= -A_2\frac{\gamma_{m2}}{y} = -A_2\sqrt{\frac{z + z_m}{y}} = -A_2Z_{cm2} \\ \frac{A_3(y + y_m) + A_7y_m}{y(y + 2y_m)}\gamma_{m1} &= A_3\frac{\gamma_{m1}}{y + 2y_m} = A_3\sqrt{\frac{z - z_m}{y + 2y_m}} = A_3Z_{cm1} \\ -\frac{A_4(y + y_m) + A_8y_m}{y(y + 2y_m)}\gamma_{m1} &= -A_4\frac{\gamma_{m1}}{y + 2y_m} = -A_4\sqrt{\frac{z - z_m}{y + 2y_m}} = -A_4Z_{cm1} \\ \frac{A_1y_m + A_5(y + y_m)}{y(y + 2y_m)}\gamma_{m2} &= A_1\frac{\gamma_{m2}}{y} = A_1\sqrt{\frac{z + z_m}{y}} = A_1Z_{cm2} \\ -\frac{A_2y_m + A_6(y + y_m)}{y(y + 2y_m)}\gamma_{m2} &= -A_2\frac{\gamma_{m2}}{y} = -A_2\sqrt{\frac{z + z_m}{y}} = -A_2Z_{cm2} \\ \frac{A_3y_m + A_7(y + y_m)}{y(y + 2y_m)}\gamma_{m1} &= -A_3\frac{\gamma_{m1}}{y + 2y_m} = -A_3\sqrt{\frac{z - z_m}{y + 2y_m}} = -A_3Z_{cm1} \\ -\frac{A_4y_m + A_8(y + y_m)}{y(y + 2y_m)}\gamma_{m1} &= A_4\frac{\gamma_{m1}}{y + 2y_m} = A_4\sqrt{\frac{z - z_m}{y + 2y_m}} = A_4Z_{cm1} \end{aligned} \quad (4.40)$$

Finally, (4.28) and (4.29) can be simplified into

$$V_1 = A_1Z_{cm2}e^{\gamma_{m2}x} - A_2Z_{cm2}e^{-\gamma_{m2}x} + A_3Z_{cm1}e^{\gamma_{m1}x} - A_4Z_{cm1}e^{-\gamma_{m1}x} \quad (4.41)$$

$$V_2 = A_1Z_{cm2}e^{\gamma_{m2}x} - A_2Z_{cm2}e^{-\gamma_{m2}x} - A_3Z_{cm1}e^{\gamma_{m1}x} + A_4Z_{cm1}e^{-\gamma_{m1}x} \quad (4.42)$$

Thus far, we have established the formulations of I_1 , I_2 , V_1 , and V_2 as shown in (4.20), (4.25), (4.41) and (4.42). The unknown coefficients A_1 , A_2 , A_3 and A_4 are to be determined by boundary conditions. At $x = 0$, we have the boundary condition

$$\begin{aligned} V_1 &= V_{r1} \\ V_2 &= V_{r2} \\ I_1 &= I_{r1} \\ I_2 &= I_{r2} \end{aligned} \quad (4.43)$$

Thus, at $x = 0$, (4.20), (4.25), (4.41) and (4.42) become

$$I_{r1} = A_1 + A_2 + A_3 + A_4 \quad (4.44)$$

$$I_{r2} = A_1 + A_2 - A_3 - A_4 \quad (4.45)$$

$$V_{r1} = A_1 Z_{cm2} - A_2 Z_{cm2} + A_3 Z_{cm1} - A_4 Z_{cm1} \quad (4.46)$$

$$V_{r2} = A_1 Z_{cm2} - A_2 Z_{cm2} - A_3 Z_{cm1} + A_4 Z_{cm1} \quad (4.47)$$

From (4.44)-(4.47), we can obtain the coefficients as follows

$$A_1 = \frac{1}{4}(I_{r1} + I_{r2}) + \frac{1}{4Z_{cm2}}(V_{r1} + V_{r2}) \quad (4.48)$$

$$A_2 = \frac{1}{4}(I_{r1} + I_{r2}) - \frac{1}{4Z_{cm2}}(V_{r1} + V_{r2}) \quad (4.49)$$

$$A_3 = \frac{1}{4}(I_{r1} - I_{r2}) + \frac{1}{4Z_{cm1}}(V_{r1} - V_{r2}) \quad (4.50)$$

$$A_4 = \frac{1}{4}(I_{r1} - I_{r2}) - \frac{1}{4Z_{cm1}}(V_{r1} - V_{r2}) \quad (4.51)$$

Substituting (4.48)-(4.51) into (4.20) leads to

$$\begin{aligned} I_1 &= A_1 [\cosh(\gamma_{m2}x) + \sinh(\gamma_{m2}x)] + A_2 [\cosh(\gamma_{m2}x) - \sinh(\gamma_{m2}x)] \\ &\quad + A_3 [\cosh(\gamma_{m1}x) + \sinh(\gamma_{m1}x)] + A_4 [\cosh(\gamma_{m1}x) - \sinh(\gamma_{m1}x)] \\ &= (A_1 + A_2) \cosh(\gamma_{m2}x) + (A_1 - A_2) \sinh(\gamma_{m2}x) \\ &\quad + (A_3 + A_4) \cosh(\gamma_{m1}x) + (A_3 - A_4) \sinh(\gamma_{m1}x) \\ &= \frac{I_{r1} + I_{r2}}{2} \cosh(\gamma_{m2}x) + \frac{V_{r1} + V_{r2}}{2Z_{cm2}} \sinh(\gamma_{m2}x) \\ &\quad + \frac{I_{r1} - I_{r2}}{2} \cosh(\gamma_{m1}x) + \frac{V_{r1} - V_{r2}}{2Z_{cm1}} \sinh(\gamma_{m1}x) \end{aligned} \quad (4.52)$$

Similarly, (4.25), (4.41) and (4.42) are formulated as

$$\begin{aligned} I_2 &= \frac{I_{r1} + I_{r2}}{2} \cosh(\gamma_{m2}x) + \frac{V_{r1} + V_{r2}}{2Z_{cm2}} \sinh(\gamma_{m2}x) \\ &\quad - \frac{I_{r1} - I_{r2}}{2} \cosh(\gamma_{m1}x) - \frac{V_{r1} - V_{r2}}{2Z_{cm1}} \sinh(\gamma_{m1}x) \end{aligned} \quad (4.53)$$

$$\begin{aligned} V_1 &= \frac{V_{r1} + V_{r2}}{2} \cosh(\gamma_{m2}x) + \frac{I_{r1} + I_{r2}}{2} Z_{cm2} \sinh(\gamma_{m2}x) \\ &\quad + \frac{V_{r1} - V_{r2}}{2} \cosh(\gamma_{m1}x) + \frac{I_{r1} - I_{r2}}{2} Z_{cm1} \sinh(\gamma_{m1}x) \end{aligned} \quad (4.54)$$

$$\begin{aligned} V_2 &= \frac{V_{r1} + V_{r2}}{2} \cosh(\gamma_{m2}x) + \frac{I_{r1} + I_{r2}}{2} Z_{cm2} \sinh(\gamma_{m2}x) \\ &\quad - \frac{V_{r1} - V_{r2}}{2} \cosh(\gamma_{m1}x) - \frac{I_{r1} - I_{r2}}{2} Z_{cm1} \sinh(\gamma_{m1}x) \end{aligned} \quad (4.55)$$

Let $x = l$, we have the boundary condition

$$V_1 = V_{s1}$$

$$\begin{aligned}
V_2 &= V_{s2} \\
I_1 &= I_{s1} \\
I_2 &= I_{s2}
\end{aligned} \tag{4.56}$$

Applying (4.56), (4.52)-(4.55) can be formulated as

$$\begin{aligned}
I_{s1} &= \frac{V_{r1}}{2} \left[\frac{\sinh(\gamma_{m2}l)}{Z_{cm2}} + \frac{\sinh(\gamma_{m1}l)}{Z_{cm1}} \right] + \frac{V_{r2}}{2} \left[\frac{\sinh(\gamma_{m2}l)}{Z_{cm2}} - \frac{\sinh(\gamma_{m1}l)}{Z_{cm1}} \right] \\
&+ \frac{I_{r1}}{2} [\cosh(\gamma_{m2}l) + \cosh(\gamma_{m1}l)] + \frac{I_{r2}}{2} [\cosh(\gamma_{m2}l) - \cosh(\gamma_{m1}l)]
\end{aligned} \tag{4.57}$$

$$\begin{aligned}
I_{s2} &= \frac{V_{r1}}{2} \left[\frac{\sinh(\gamma_{m2}l)}{Z_{cm2}} - \frac{\sinh(\gamma_{m1}l)}{Z_{cm1}} \right] + \frac{V_{r2}}{2} \left[\frac{\sinh(\gamma_{m2}l)}{Z_{cm2}} + \frac{\sinh(\gamma_{m1}l)}{Z_{cm1}} \right] \\
&+ \frac{I_{r1}}{2} [\cosh(\gamma_{m2}l) - \cosh(\gamma_{m1}l)] + \frac{I_{r2}}{2} [\cosh(\gamma_{m2}l) + \cosh(\gamma_{m1}l)]
\end{aligned} \tag{4.58}$$

$$\begin{aligned}
V_{s1} &= \frac{V_{r1}}{2} [\cosh(\gamma_{m2}l) + \cosh(\gamma_{m1}l)] + \frac{V_{r2}}{2} [\cosh(\gamma_{m2}l) - \cosh(\gamma_{m1}l)] \\
&+ \frac{I_{r1}}{2} [Z_{cm2} \sinh(\gamma_{m2}l) + Z_{cm1} \sinh(\gamma_{m1}l)] \\
&+ \frac{I_{r2}}{2} [Z_{cm2} \sinh(\gamma_{m2}l) - Z_{cm1} \sinh(\gamma_{m1}l)]
\end{aligned} \tag{4.59}$$

$$\begin{aligned}
V_{s2} &= \frac{V_{r1}}{2} [\cosh(\gamma_{m2}l) - \cosh(\gamma_{m1}l)] + \frac{V_{r2}}{2} [\cosh(\gamma_{m2}l) + \cosh(\gamma_{m1}l)] \\
&+ \frac{I_{r1}}{2} [Z_{cm2} \sinh(\gamma_{m2}l) - Z_{cm1} \sinh(\gamma_{m1}l)] \\
&+ \frac{I_{r2}}{2} [Z_{cm2} \sinh(\gamma_{m2}l) + Z_{cm1} \sinh(\gamma_{m1}l)]
\end{aligned} \tag{4.60}$$

On the other hand, from Fig. 4.2, we can derive

$$\begin{aligned}
V_{s1} &= V_{r1} + \left[V_{r1} \frac{Y}{2} + (V_{r1} - V_{r2}) \frac{Y_m}{2} + I_{r1} \right] Z \\
&+ \left[V_{r2} \frac{Y}{2} + (V_{r2} - V_{r1}) \frac{Y_m}{2} + I_{r2} \right] Z_m \\
&= V_{r1} \left(1 + \frac{YZ}{2} + \frac{Y_m Z}{2} - \frac{Y_m Z_m}{2} \right) + V_{r2} \left(\frac{YZ_m}{2} + \frac{Y_m Z_m}{2} - \frac{Y_m Z}{2} \right) \\
&+ I_{r1} Z + I_{r2} Z_m
\end{aligned} \tag{4.61}$$

Comparing and equating the coefficients of V_{r1} , V_{r2} , I_{r1} and I_{r2} from (4.59) and (4.61), respectively, we can write

$$Z = \frac{1}{2} [Z_{cm2} \sinh(\gamma_{m2}l) + Z_{cm1} \sinh(\gamma_{m1}l)] \tag{4.62}$$

$$Z_m = \frac{1}{2} [Z_{cm2} \sinh(\gamma_{m2}l) - Z_{cm1} \sinh(\gamma_{m1}l)] \quad (4.63)$$

$$Y = \frac{2 \tanh\left(\frac{\gamma_{m2}l}{2}\right)}{Z_{cm2}} \quad (4.64)$$

$$Y_m = \frac{\tanh\left(\frac{\gamma_{m1}l}{2}\right)}{Z_{cm1}} - \frac{\tanh\left(\frac{\gamma_{m2}l}{2}\right)}{Z_{cm2}} \quad (4.65)$$

Referring to Fig. 4.2, we can also write the formulations of V_{s2} , I_{s1} and I_{s2} . It has been verified that (4.62)-(4.65) also hold for these expressions. Thus far, the equivalent π model for zero-sequence double-circuit lines sharing identical parameters is established, based on which we can proceed to the fault location basis.

4.3 Fault Location Basis

The basic methodology of the proposed fault location method is to add a fictitious bus where the fault occurs to the original network, and then the driving point impedance of the fault bus and the transfer impedances between this bus and other buses are revealed as functions of unknown fault distance. According to the definition of bus impedance matrix, the sequence voltage change during the fault at any bus can be formulated with respect to the corresponding transfer impedance and sequence fault current. In association with the boundary conditions of different fault types, fault current terms can be canceled out and the fault location can be obtained.

In this section, our objective is to decouple the original network into three independent sequence component networks and construct the bus impedance matrix with additional buses for each sequence network, separately.

First of all, the notations used in this chapter are summarized as follows

n total number of buses of the pre-fault network;

p, q buses of the faulted section;

r fictitious bus representing the fault point and $r = n + 2$;

s fictitious bus and $s = n + 1$;

m unknown per unit fault distance from bus p ;

l length of the line between buses p and q ;

i symmetrical component index; $i = 0, 1, 2$ for zero-, positive- and negative-sequence, respectively, put in parenthesis as a superscript throughout the chapter;

- $z_{j_1 j_2}^{(i)}$ i^{th} -sequence total equivalent self-series impedance of the branch between buses j_1 and j_2 ; in case of a double-circuit line sharing both terminals j_1 and j_2 , an extra subscript is used to distinguish the first and second parallel lines, i.e. $z_{j_1 j_2-1}^{(i)}, z_{j_1 j_2-2}^{(i)}$;
- $z_{j_1 j_2-m}^{(0)}$ zero-sequence total equivalent mutual-series impedance of the branches of the double-circuit line sharing both terminals j_1 and j_2 ;
- $y_{j_1 j_2}^{(i)}$ i^{th} -sequence total equivalent self-shunt admittance of the branch between buses j_1 and j_2 ; in case of a double-circuit line sharing both terminals j_1 and j_2 , an extra subscript is used to distinguish the first and second parallel lines, i.e. $y_{j_1 j_2-1}^{(i)}, y_{j_1 j_2-2}^{(i)}$;
- $z_{1m}^{(0)}, y_{1m}^{(0)}$ zero-sequence total equivalent mutual-series impedance and mutual-shunt admittance between branches ps and pr , respectively;
- $z_{2m}^{(0)}, y_{2m}^{(0)}$ zero-sequence total equivalent mutual-series impedance and mutual-shunt admittance between branches qs and qr , respectively;
- $Z_0^{(i)}$ bus impedance matrix of the pre-fault i^{th} -sequence network. It has a size n by n , whose element on the k_1^{th} row and k_2^{th} column is denoted as $Z_{0, k_1 k_2}^{(i)}$;
- $Z^{(i)}$ bus impedance matrix of the i^{th} -sequence network with the addition of fictitious buses s and r . It has a size of $n + 2$ by $n + 2$, whose element on the k_1^{th} row and k_2^{th} column is denoted by $Z_{k_1 k_2}^{(i)}$.

4.3.1 Construction of Zero-Sequence Augmented Bus Impedance Matrix

The construction of bus impedance matrix with addition of the fault bus for the zero-sequence network is first considered. The pre-fault zero-sequence network of a sample power system is shown in Fig. 4.3, whose bus impedance matrix $Z_0^{(0)}$ can be developed using well established techniques [64]. Note that the studied parallel lines in our work share identical parameters, i.e. $z_{pq-1}^{(0)} = z_{pq-2}^{(0)}, y_{pq-1}^{(0)} = y_{pq-2}^{(0)}$. The parameters in Fig. 4.3 are as follows as obtained in Section 4.2

$$z_{pq-1}^{(0)} = \frac{1}{2} \left[Z_{cm2}^{(0)} \sinh \left(\gamma_{m2}^{(0)} l \right) + Z_{cm1}^{(0)} \sinh \left(\gamma_{m1}^{(0)} l \right) \right] \quad (4.66)$$

$$y_{pq-1}^{(0)} = \frac{2 \tanh \left(\frac{1}{2} \gamma_{m2}^{(0)} l \right)}{Z_{cm2}^{(0)}} \quad (4.67)$$

$$z_{pq-m}^{(0)} = \frac{1}{2} \left[Z_{cm2}^{(0)} \sinh \left(\gamma_{m2}^{(0)} l \right) - Z_{cm1}^{(0)} \sinh \left(\gamma_{m1}^{(0)} l \right) \right] \quad (4.68)$$

$$y_{pq-m}^{(0)} = \frac{\tanh \left(\frac{1}{2} \gamma_{m1}^{(0)} l \right)}{Z_{cm1}^{(0)}} - \frac{\tanh \left(\frac{1}{2} \gamma_{m2}^{(0)} l \right)}{Z_{cm2}^{(0)}} \quad (4.69)$$

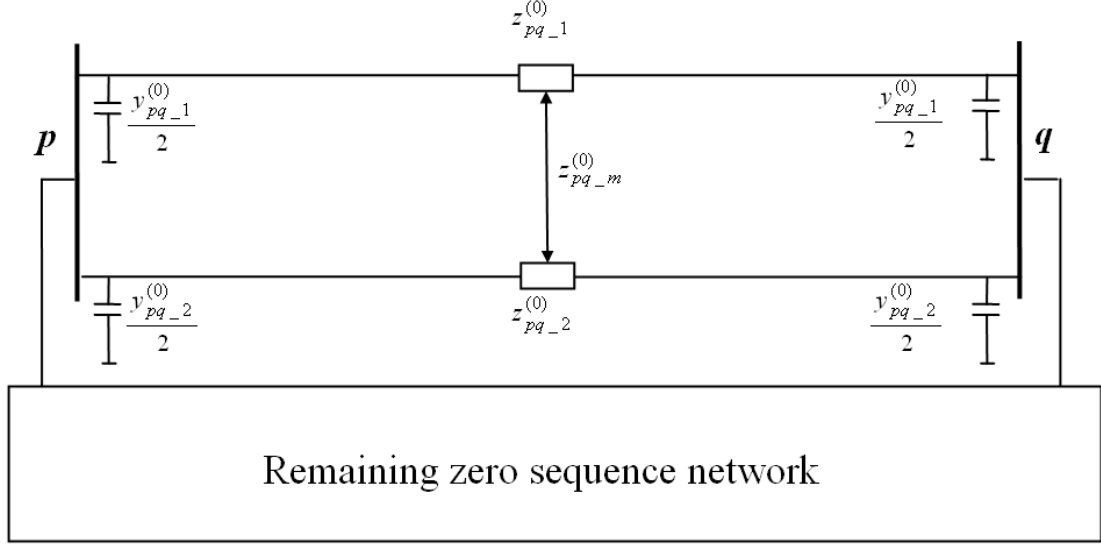


Figure 4.3: Pre-fault zero-sequence network.

A note of worth is that $y_{pq-m}^{(0)}$ is not shown in Fig. 4.3, which is the total equivalent mutual-shunt admittance between the parallel lines sharing two common terminals p and q . Because of the common terminals of the double-circuit line, the mutual shunt admittance disappears. Supposing the fault occurs on the second branch of the parallel lines, Fig. 4.4 depicts the zero-sequence network with addition of two fictitious buses s and r . From Fig. 4.4, we have $z_{ps}^{(0)} = z_{pr}^{(0)}$, $z_{qs}^{(0)} = z_{qr}^{(0)}$, $y_{ps}^{(0)} = y_{pr}^{(0)}$ and $y_{qs}^{(0)} = y_{qr}^{(0)}$. The parameters in terms of m are as follows

$$z_{pr}^{(0)} = \frac{1}{2} \left[Z_{cm2}^{(0)} \sinh \left(\gamma_{m2}^{(0)} ml \right) + Z_{cm1}^{(0)} \sinh \left(\gamma_{m1}^{(0)} ml \right) \right] \quad (4.70)$$

$$z_{qr}^{(0)} = \frac{1}{2} \left\{ Z_{cm2}^{(0)} \sinh \left[\gamma_{m2}^{(0)} (1-m) l \right] + Z_{cm1}^{(0)} \sinh \left[\gamma_{m1}^{(0)} (1-m) l \right] \right\} \quad (4.71)$$

$$y_{pr}^{(0)} = \frac{2 \tanh \left(\frac{1}{2} \gamma_{m2}^{(0)} ml \right)}{Z_{cm2}^{(0)}} \quad (4.72)$$

$$y_{qr}^{(0)} = \frac{2 \tanh \left[\frac{1}{2} \gamma_{m2}^{(0)} (1-m) l \right]}{Z_{cm2}^{(0)}} \quad (4.73)$$

$$z_{1m}^{(0)} = \frac{1}{2} \left[Z_{cm2}^{(0)} \sinh \left(\gamma_{m2}^{(0)} ml \right) - Z_{cm1}^{(0)} \sinh \left(\gamma_{m1}^{(0)} ml \right) \right] \quad (4.74)$$

$$z_{2m}^{(0)} = \frac{1}{2} \left\{ Z_{cm2}^{(0)} \sinh \left[\gamma_{m2}^{(0)} (1-m) l \right] - Z_{cm1}^{(0)} \sinh \left[\gamma_{m1}^{(0)} (1-m) l \right] \right\} \quad (4.75)$$

$$y_{1m}^{(0)} = \frac{\tanh \left(\frac{1}{2} \gamma_{m1}^{(0)} ml \right)}{Z_{cm1}^{(0)}} - \frac{\tanh \left(\frac{1}{2} \gamma_{m2}^{(0)} ml \right)}{Z_{cm2}^{(0)}} \quad (4.76)$$

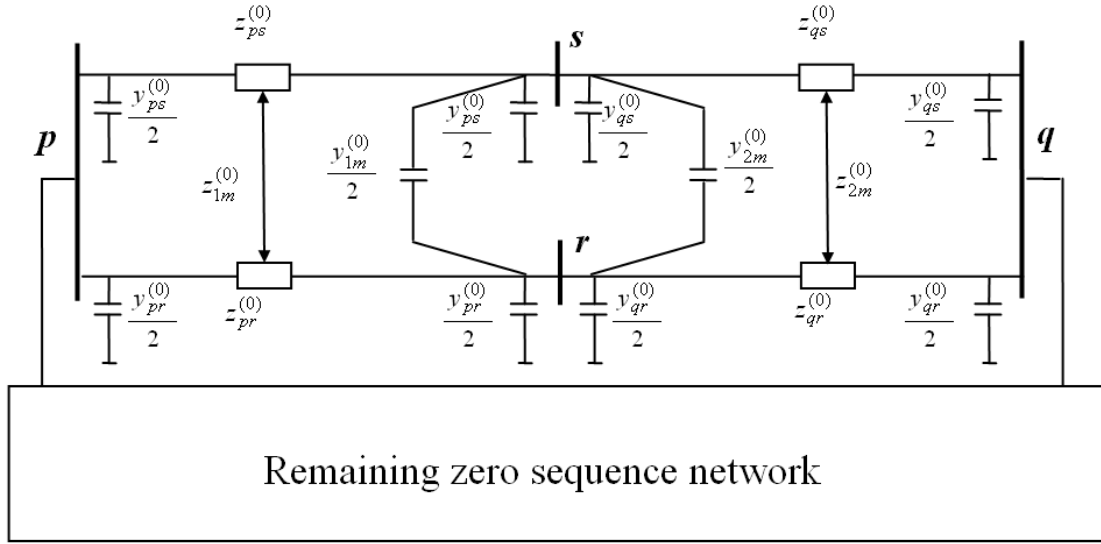


Figure 4.4: Zero-sequence network with two additional fictitious buses.

$$y_{2m}^{(0)} = \frac{\tanh \left[\frac{1}{2} \gamma_{m1}^{(0)} (1-m) l \right]}{Z_{cm1}^{(0)}} - \frac{\tanh \left[\frac{1}{2} \gamma_{m2}^{(0)} (1-m) l \right]}{Z_{cm2}^{(0)}} \quad (4.77)$$

where

$$Z_{cm1}^{(0)} = \sqrt{\frac{z^{(0)} - z_m^{(0)}}{y^{(0)} + 2y_m^{(0)}}}$$

$$Z_{cm2}^{(0)} = \sqrt{\frac{z^{(0)} + z_m^{(0)}}{y^{(0)}}}$$

$$\gamma_{m1}^{(0)} = \sqrt{\left(z^{(0)} - z_m^{(0)} \right) \left(y^{(0)} + 2y_m^{(0)} \right)}$$

$$\gamma_{m2}^{(0)} = \sqrt{\left(z^{(0)} + z_m^{(0)} \right) y^{(0)}}$$

and

$z^{(0)}$ zero-sequence per-unit length self-series impedance (Ω/mile) of the line between buses p and q ,

$y^{(0)}$ zero-sequence per-unit length self-shunt admittance (S/mile) of the line between buses p and q ,

$z_m^{(0)}$ zero-sequence per-unit length mutual-series impedance (Ω/mile) between the two lines of buses p and q ,

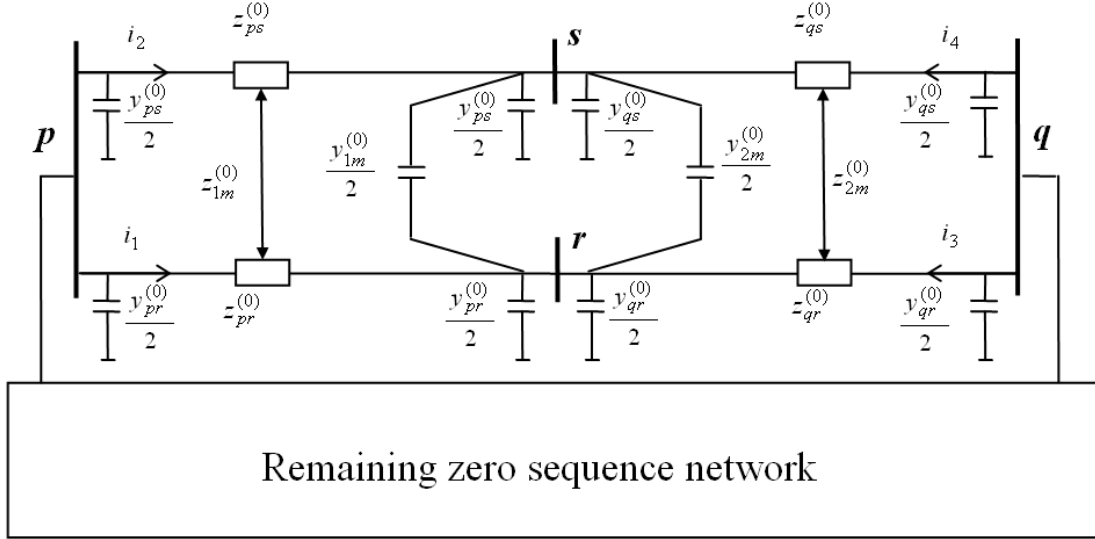


Figure 4.5: Zero-sequence network with 1 A injected to a single bus k .

$y_m^{(0)}$ zero-sequence per-unit length mutual-shunt admittance (S/mile) between the two lines of buses p and q .

To formulate $Z^{(0)}$, suppose there is only one current source injected into a single bus j ($j = 1, 2, \dots, n$), then the resulted voltages at bus k ($k = 1, 2, \dots, n$) will be the same for the networks shown in Fig. 4.3 and Fig. 4.4. According to the definition of bus impedance matrix, it is obtained that $Z_{jk}^{(0)} = Z_{0,jk}^{(0)}$, $j, k = 1, 2, \dots, n$. We have

$$Z^{(0)} = \begin{bmatrix} Z_{0,11}^{(0)} & \cdots & Z_{0,1p}^{(0)} & Z_{0,1q}^{(0)} & \cdots & Z_{0,1n}^{(0)} & Z_{1s}^{(0)} & Z_{1r}^{(0)} \\ \vdots & \ddots & \vdots & \vdots & \ddots & \vdots & \vdots & \vdots \\ Z_{0,p1}^{(0)} & \cdots & Z_{0,pp}^{(0)} & Z_{0,pq}^{(0)} & \cdots & Z_{0,pn}^{(0)} & Z_{ps}^{(0)} & Z_{pr}^{(0)} \\ Z_{0,q1}^{(0)} & \cdots & Z_{0,qp}^{(0)} & Z_{0,qq}^{(0)} & \cdots & Z_{0,qn}^{(0)} & Z_{qs}^{(0)} & Z_{qr}^{(0)} \\ \vdots & \ddots & \vdots & \vdots & \ddots & \vdots & \vdots & \vdots \\ Z_{0,n1}^{(0)} & \cdots & Z_{0,np}^{(0)} & Z_{0,nq}^{(0)} & \cdots & Z_{0,nn}^{(0)} & Z_{ns}^{(0)} & Z_{nr}^{(0)} \\ Z_{s1}^{(0)} & \cdots & Z_{sp}^{(0)} & Z_{sq}^{(0)} & \cdots & Z_{sn}^{(0)} & Z_{ss}^{(0)} & Z_{sr}^{(0)} \\ Z_{r1}^{(0)} & \cdots & Z_{rp}^{(0)} & Z_{rq}^{(0)} & \cdots & Z_{rn}^{(0)} & Z_{rs}^{(0)} & Z_{rr}^{(0)} \end{bmatrix} \quad (4.78)$$

Let's inject a current source of 1 Ampere to a single bus k ($k = 1, 2, \dots, n$) as shown in Fig. 4.5. i_1, i_2 denote the currents flowing from bus p to r and s respectively; i_3, i_4 denote the currents flowing from bus q to r and s respectively. Making use of the bus impedance matrix in (4.78), we obtain

$$V_p = Z_{0,pk}^{(0)}, \quad V_q = Z_{0,qk}^{(0)}, \quad V_r = Z_{rk}^{(0)} \quad (4.79)$$

It follows from Fig. 4.5 that

$$V_p - V_r = i_1 z_{pr}^{(0)} + i_2 z_{1m}^{(0)} \quad (4.80)$$

$$V_q - V_r = i_3 z_{qr}^{(0)} + i_4 z_{2m}^{(0)} \quad (4.81)$$

$$i_1 + i_3 = V_r \left(\frac{y_{pr}^{(0)}}{2} + \frac{y_{qr}^{(0)}}{2} \right) + (V_r - V_s) \left(\frac{y_{1m}^{(0)}}{2} + \frac{y_{2m}^{(0)}}{2} \right) \quad (4.82)$$

$$V_p - V_s = i_1 z_{1m}^{(0)} + i_2 z_{pr}^{(0)} \quad (4.83)$$

$$V_q - V_s = i_3 z_{2m}^{(0)} + i_4 z_{qr}^{(0)} \quad (4.84)$$

$$i_2 + i_4 = V_s \left(\frac{y_{pr}^{(0)}}{2} + \frac{y_{qr}^{(0)}}{2} \right) + (V_s - V_r) \left(\frac{y_{1m}^{(0)}}{2} + \frac{y_{2m}^{(0)}}{2} \right) \quad (4.85)$$

Based on (4.80)-(4.85), there are six unknowns $i_1, i_2, i_3, i_4, V_r, V_s$ and six equations, from which V_r can be solved as follows

$$V_r = \frac{aV_p + bV_q}{d} \quad (4.86)$$

where

$$a = \frac{1}{\left(z_{1m}^{(0)}\right)^2 - \left(z_{pr}^{(0)}\right)^2} + \frac{1}{z_{1m}^{(0)} + z_{pr}^{(0)}} \left(\frac{1}{z_{2m}^{(0)} - z_{qr}^{(0)}} - y_{1m}^{(0)} - y_{2m}^{(0)} - \frac{y_{pr}^{(0)}}{2} - \frac{y_{qr}^{(0)}}{2} \right) \quad (4.87)$$

$$b = \frac{1}{\left(z_{2m}^{(0)}\right)^2 - \left(z_{qr}^{(0)}\right)^2} + \frac{1}{z_{2m}^{(0)} + z_{qr}^{(0)}} \left(\frac{1}{z_{1m}^{(0)} - z_{pr}^{(0)}} - y_{1m}^{(0)} - y_{2m}^{(0)} - \frac{y_{pr}^{(0)}}{2} - \frac{y_{qr}^{(0)}}{2} \right) \quad (4.88)$$

$$d = \left(\frac{1}{z_{1m}^{(0)} + z_{pr}^{(0)}} + \frac{1}{z_{2m}^{(0)} + z_{qr}^{(0)}} + \frac{y_{pr}^{(0)}}{2} + \frac{y_{qr}^{(0)}}{2} \right) \times \left(\frac{1}{z_{1m}^{(0)} - z_{pr}^{(0)}} + \frac{1}{z_{2m}^{(0)} - z_{qr}^{(0)}} - y_{1m}^{(0)} - y_{2m}^{(0)} - \frac{y_{pr}^{(0)}}{2} - \frac{y_{qr}^{(0)}}{2} \right) \quad (4.89)$$

Substituting (4.79) into (4.86) will result in

$$Z_{rk}^{(0)} = \frac{aZ_{0,pk}^{(0)} + bZ_{0,qk}^{(0)}}{d} \quad (4.90)$$

To derive $Z_{rr}^{(0)}$, let us inject one current source of 1 Ampere into bus r as shown in Fig. 4.6. Based on the bus impedance matrix in (4.78), the voltages at buses p, q and r in Fig. 4.6 are

$$V_p = Z_{pr}^{(0)}, \quad V_q = Z_{qr}^{(0)}, \quad V_r = Z_{rr}^{(0)} \quad (4.91)$$

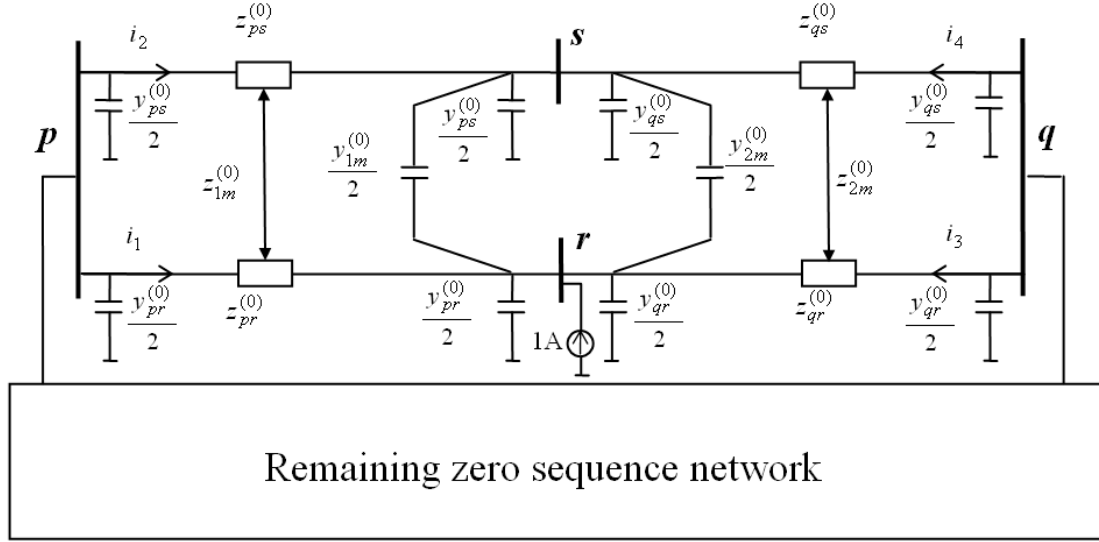


Figure 4.6: Zero-sequence network with 1 A injected to bus r .

From Fig. 4.6, the following equations hold

$$V_p - V_r = i_1 z_{pr}^{(0)} + i_2 z_{1m}^{(0)} \quad (4.92)$$

$$V_q - V_r = i_3 z_{qr}^{(0)} + i_4 z_{2m}^{(0)} \quad (4.93)$$

$$i_1 + i_3 + 1 = V_r \left(\frac{y_{pr}^{(0)}}{2} + \frac{y_{qr}^{(0)}}{2} \right) + (V_r - V_s) \left(\frac{y_{1m}^{(0)}}{2} + \frac{y_{2m}^{(0)}}{2} \right) \quad (4.94)$$

$$V_p - V_s = i_1 z_{1m}^{(0)} + i_2 z_{pr}^{(0)} \quad (4.95)$$

$$V_q - V_s = i_3 z_{2m}^{(0)} + i_4 z_{qr}^{(0)} \quad (4.96)$$

$$i_2 + i_4 = V_s \left(\frac{y_{pr}^{(0)}}{2} + \frac{y_{qr}^{(0)}}{2} \right) + (V_s - V_r) \left(\frac{y_{1m}^{(0)}}{2} + \frac{y_{2m}^{(0)}}{2} \right) \quad (4.97)$$

With six unknown variables $i_1, i_2, i_3, i_4, V_r, V_s$, solving (4.92)-(4.97) reaches the expression of V_r as follows

$$V_r = \frac{aV_p + bV_q + c}{d} \quad (4.98)$$

where

$$c = \frac{z_{pr}^{(0)}}{\left(z_{1m}^{(0)} \right)^2 - \left(z_{pr}^{(0)} \right)^2} + \frac{z_{qr}^{(0)}}{\left(z_{2m}^{(0)} \right)^2 - \left(z_{qr}^{(0)} \right)^2} - \frac{y_{pr}^{(0)}}{2} - \frac{y_{qr}^{(0)}}{2} - \frac{y_{1m}^{(0)}}{2} - \frac{y_{2m}^{(0)}}{2} \quad (4.99)$$

Substituting (4.91) into (4.98) yields

$$Z_{rr}^{(0)} = \frac{aZ_{rp}^{(0)} + bZ_{rq}^{(0)} + c}{d} \quad (4.100)$$

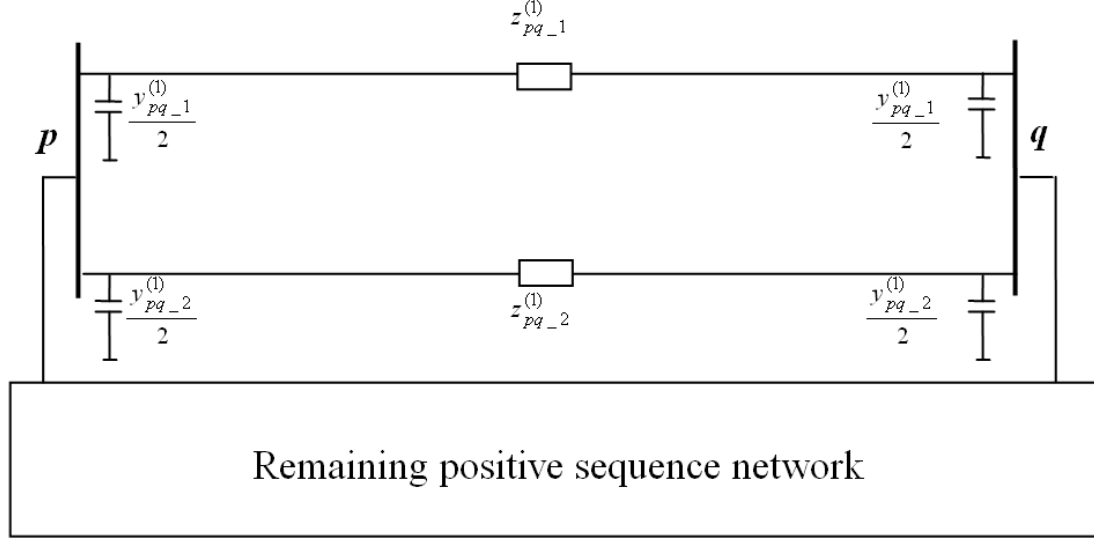


Figure 4.7: Pre-fault positive-sequence network.

where $Z_{rp}^{(0)}$ and $Z_{rq}^{(0)}$ in (4.100) can be obtained by letting $k = p$ and $k = q$ in (4.90) as follows

$$Z_{rp}^{(0)} = \frac{aZ_{0,pp}^{(0)} + bZ_{0,qp}^{(0)}}{d} \quad (4.101)$$

$$Z_{rq}^{(0)} = \frac{aZ_{0,pq}^{(0)} + bZ_{0,qq}^{(0)}}{d} \quad (4.102)$$

Note a , b , c and d are formulated with $z_{pr}^{(0)}$, $z_{qr}^{(0)}$, $y_{pr}^{(0)}$, $y_{qr}^{(0)}$, $z_{1m}^{(0)}$, $z_{2m}^{(0)}$, $y_{1m}^{(0)}$, and $y_{2m}^{(0)}$.

4.3.2 Construction of Positive-Sequence Augmented Bus Impedance Matrix

In this sub-section, we consider the construction of bus impedance matrix with addition of the fault bus for the positive-sequence network. The pre-fault positive-sequence network of a sample power system is shown in Fig. 4.7, whose bus impedance matrix $Z_0^{(1)}$ can be established. Fig. 4.8 delineates the positive-sequence network with two fictitious buses s and r . The parameters in Fig. 4.8 in terms of m are as follows

$$z_{pr}^{(1)} = Z_c^{(1)} \sinh(m\gamma^{(1)}l) \quad (4.103)$$

$$z_{qr}^{(1)} = Z_c^{(1)} \sinh[(1-m)\gamma^{(1)}l] \quad (4.104)$$

$$y_{pr}^{(1)} = \frac{2}{Z_c^{(1)}} \tanh\left(\frac{1}{2}m\gamma^{(1)}l\right) \quad (4.105)$$

$$y_{qr}^{(1)} = \frac{2}{Z_c^{(1)}} \tanh\left[\frac{1}{2}(1-m)\gamma^{(1)}l\right] \quad (4.106)$$

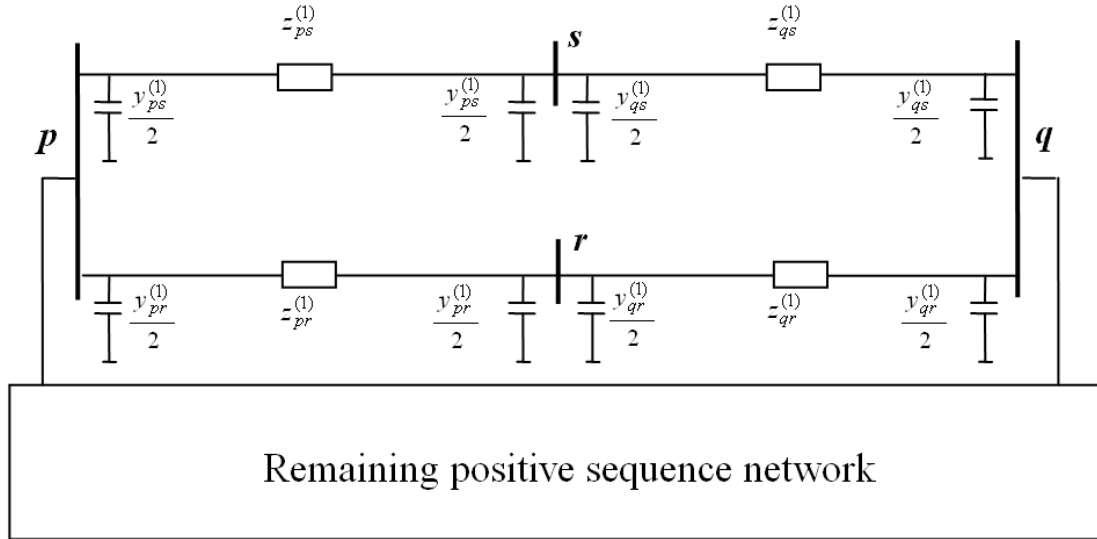


Figure 4.8: Positive-sequence network with additional fictitious buses.

where

$$Z_c^{(1)} = \sqrt{\frac{z^{(1)}}{y^{(1)}}}$$

$$\gamma^{(1)} = \sqrt{z^{(1)}y^{(1)}}$$

and

$z^{(1)}$ positive-sequence per-unit length self-series impedance (Ω/mile) of the line between buses p and q ,

$y^{(1)}$ positive-sequence per-unit length self-shunt admittance (S/mile) of the line between buses p and q .

To formulate $Z^{(1)}$, suppose there is only one current source injected into a single bus j ($j = 1, 2, \dots, n$), then the resulted voltages at bus k ($k = 1, 2, \dots, n$) will be the same for the networks shown in Fig. 4.7 and Fig. 4.8. According to the definition of

bus impedance matrix, it is obtained that $Z_{jk}^{(1)} = Z_{0,jk}^{(1)}$, $j, k = 1, 2, \dots, n$. We have

$$Z^{(1)} = \begin{bmatrix} Z_{0,11}^{(1)} & \cdots & Z_{0,1p}^{(1)} & Z_{0,1q}^{(1)} & \cdots & Z_{0,1n}^{(1)} & Z_{1s}^{(1)} & Z_{1r}^{(1)} \\ \vdots & \ddots & \vdots & \vdots & \ddots & \vdots & \vdots & \vdots \\ Z_{0,p1}^{(1)} & \cdots & Z_{0,pp}^{(1)} & Z_{0,pq}^{(1)} & \cdots & Z_{0,pn}^{(1)} & Z_{ps}^{(1)} & Z_{pr}^{(1)} \\ Z_{0,q1}^{(1)} & \cdots & Z_{0,qp}^{(1)} & Z_{0,qq}^{(1)} & \cdots & Z_{0,qn}^{(1)} & Z_{qs}^{(1)} & Z_{qr}^{(1)} \\ \vdots & \ddots & \vdots & \vdots & \ddots & \vdots & \vdots & \vdots \\ Z_{0,n1}^{(1)} & \cdots & Z_{0,np}^{(1)} & Z_{0,nq}^{(1)} & \cdots & Z_{0,nn}^{(1)} & Z_{ns}^{(1)} & Z_{nr}^{(1)} \\ Z_{s1}^{(1)} & \cdots & Z_{sp}^{(1)} & Z_{sq}^{(1)} & \cdots & Z_{sn}^{(1)} & Z_{ss}^{(1)} & Z_{sr}^{(1)} \\ Z_{r1}^{(1)} & \cdots & Z_{rp}^{(1)} & Z_{rq}^{(1)} & \cdots & Z_{rn}^{(1)} & Z_{rs}^{(1)} & Z_{rr}^{(1)} \end{bmatrix} \quad (4.107)$$

Injecting a single current source of 1 Ampere into any bus k ($k = 1, 2, \dots, n$), from (4.107) we have

$$V_p = Z_{0,pk}^{(1)}, \quad V_q = Z_{0,qk}^{(1)}, \quad V_r = Z_{rk}^{(1)} \quad (4.108)$$

Then the following equation can be derived from Fig. 4.8,

$$\frac{V_p - V_r}{z_{pr}^{(1)}} + \frac{V_q - V_r}{z_{qr}^{(1)}} = V_r \frac{y_{pr}^{(1)}}{2} + V_r \frac{y_{qr}^{(1)}}{2} \quad (4.109)$$

Further rearranging (4.109), we obtain

$$V_r = \frac{2z_{qr}^{(1)}V_p + 2z_{pr}^{(1)}V_q}{(y_{pr}^{(1)} + y_{qr}^{(1)})z_{pr}^{(1)}z_{qr}^{(1)} + 2(z_{pr}^{(1)} + z_{qr}^{(1)})} \quad (4.110)$$

Substituting (4.108) into (4.110), we have

$$Z_{rk}^{(1)} = \frac{2(Z_{0,pk}^{(1)}z_{qr}^{(1)} + Z_{0,qk}^{(1)}z_{pr}^{(1)})}{(y_{pr}^{(1)} + y_{qr}^{(1)})z_{pr}^{(1)}z_{qr}^{(1)} + 2(z_{pr}^{(1)} + z_{qr}^{(1)})} \quad (4.111)$$

Further substituting the expressions of (4.103)-(4.106) into (4.111), we have

$$Z_{rk}^{(1)} = \frac{\frac{Z_{0,pk}^{(1)}}{\sinh(m\gamma^{(1)}l)} + \frac{Z_{0,qk}^{(1)}}{\sinh[(1-m)\gamma^{(1)}l]}}{\frac{1}{\sinh(m\gamma^{(1)}l)} + \frac{1}{\sinh[(1-m)\gamma^{(1)}l]} + \tanh\left(\frac{m\gamma^{(1)}l}{2}\right) + \tanh\left[\frac{\gamma^{(1)}l(1-m)}{2}\right]} \quad (4.112)$$

For the derivation of $Z_{rr}^{(1)}$, we can inject a current source of 1 Ampere into bus r as shown in Fig. 4.9. Again, resorting to (4.107) yields

$$V_p = Z_{pr}^{(1)}, \quad V_q = Z_{qr}^{(1)}, \quad V_r = Z_{rr}^{(1)}. \quad (4.113)$$

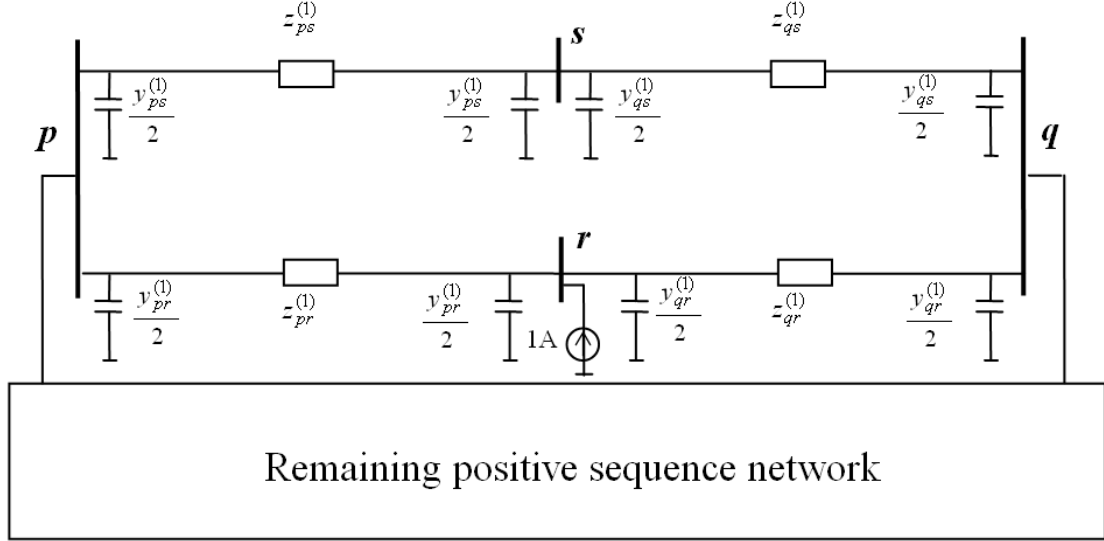


Figure 4.9: Positive-sequence network with 1 A injected to bus r .

Drawing on Fig. 4.9, the following equation is satisfied

$$\frac{V_p - V_r}{z_{pr}^{(1)}} + \frac{V_q - V_r}{z_{qr}^{(1)}} + 1 = V_r \frac{y_{pr}^{(1)}}{2} + V_r \frac{y_{qr}^{(1)}}{2} \quad (4.114)$$

Further organizing (4.114) leads to

$$V_r = \frac{2z_{qr}^{(1)}V_p + 2z_{pr}^{(1)}V_q + 2z_{pr}^{(1)}z_{qr}^{(1)}}{(y_{pr}^{(1)} + y_{qr}^{(1)})z_{pr}^{(1)}z_{qr}^{(1)} + 2(z_{pr}^{(1)} + z_{qr}^{(1)})} \quad (4.115)$$

Substituting (4.113) into (4.115) results in

$$Z_{rr}^{(1)} = \frac{2z_{qr}^{(1)}Z_{pr}^{(1)} + 2z_{pr}^{(1)}Z_{qr}^{(1)} + 2z_{pr}^{(1)}z_{qr}^{(1)}}{(y_{pr}^{(1)} + y_{qr}^{(1)})z_{pr}^{(1)}z_{qr}^{(1)} + 2(z_{pr}^{(1)} + z_{qr}^{(1)})} \quad (4.116)$$

where $Z_{rp}^{(1)}$ and $Z_{rq}^{(1)}$ can be obtained from (4.111) by letting k as p and q as follows

$$Z_{pr}^{(1)} = \frac{2(Z_{0,pp}^{(1)}z_{qr}^{(1)} + Z_{0,qp}^{(1)}z_{pr}^{(1)})}{(y_{pr}^{(1)} + y_{qr}^{(1)})z_{pr}^{(1)}z_{qr}^{(1)} + 2(z_{pr}^{(1)} + z_{qr}^{(1)})} \quad (4.117)$$

$$Z_{qr}^{(1)} = \frac{2(Z_{0,pq}^{(1)}z_{qr}^{(1)} + Z_{0,qq}^{(1)}z_{pr}^{(1)})}{(y_{pr}^{(1)} + y_{qr}^{(1)})z_{pr}^{(1)}z_{qr}^{(1)} + 2(z_{pr}^{(1)} + z_{qr}^{(1)})} \quad (4.118)$$

Substituting (4.117) and (4.118) into (4.116) gives

$$Z_{rr}^{(1)} = \frac{4z_{qr}^{(1)}(Z_{0,pp}^{(1)}z_{qr}^{(1)} + Z_{0,qp}^{(1)}z_{pr}^{(1)}) + 4z_{pr}^{(1)}(Z_{0,pq}^{(1)}z_{qr}^{(1)} + Z_{0,qq}^{(1)}z_{pr}^{(1)})}{[(y_{pr}^{(1)} + y_{qr}^{(1)})z_{pr}^{(1)}z_{qr}^{(1)} + 2(z_{pr}^{(1)} + z_{qr}^{(1)})]^2}$$

$$+ \frac{2z_{pr}^{(1)}z_{qr}^{(1)}}{(y_{pr}^{(1)} + y_{qr}^{(1)})z_{pr}^{(1)}z_{qr}^{(1)} + 2(z_{pr}^{(1)} + z_{qr}^{(1)})} \quad (4.119)$$

Finally, by making use of (4.103)-(4.106), we will reach

$$Z_{rr}^{(1)} = \frac{\frac{Z_{0,pp}^{(1)}}{\sinh^2(m\gamma^{(1)}l)} + \frac{2Z_{0,pq}^{(1)}}{\sinh(m\gamma^{(1)}l)\sinh[(1-m)\gamma^{(1)}l]} + \frac{Z_{0,qq}^{(1)}}{\sinh^2[(1-m)\gamma^{(1)}l]}}{\left\{ \frac{1}{\sinh[(1-m)\gamma^{(1)}l]} + \frac{1}{\sinh(m\gamma^{(1)}l)} + \tanh\left(\frac{m\gamma^{(1)}l}{2}\right) + \tanh\left[\frac{(1-m)\gamma^{(1)}l}{2}\right] \right\}^2} + \frac{Z_c^{(1)}}{\frac{1}{\sinh[(1-m)\gamma^{(1)}l]} + \frac{1}{\sinh(m\gamma^{(1)}l)} + \tanh\left(\frac{m\gamma^{(1)}l}{2}\right) + \tanh\left[\frac{(1-m)\gamma^{(1)}l}{2}\right]} \quad (4.120)$$

It is assumed that the parameters are the same for positive- and negative-sequence networks, thus we have $Z^{(2)} = Z^{(1)}$.

4.4 Proposed Fault Location Method

In this section, fault location algorithms employing voltage measurements from one bus or two buses are derived. Based on the definition of bus impedance matrix, at bus k ($k = 1, 2, \dots, n$), the following formulas hold

$$E_k^{(1)} = E_k^{(1)0} - Z_{kr}^{(1)} I_f^{(1)} \quad (4.121)$$

$$E_k^{(2)} = -Z_{kr}^{(2)} I_f^{(2)} \quad (4.122)$$

$$E_k^{(0)} = -Z_{kr}^{(0)} I_f^{(0)} \quad (4.123)$$

Note that all the sequence voltages and currents are for phase A.

4.4.1 Two-Bus Fault Location Algorithms

1) *Fault location with synchronized measurements from two buses*

Suppose the voltage measurements at buses k and j ($k, j = 1, 2, \dots, n$) are available. For bus j , similar to (4.121)-(4.123), the following formulas exist

$$E_j^{(1)} = E_j^{(1)0} - Z_{jr}^{(1)} I_f^{(1)} \quad (4.124)$$

$$E_j^{(2)} = -Z_{jr}^{(2)} I_f^{(2)} \quad (4.125)$$

$$E_j^{(0)} = -Z_{jr}^{(0)} I_f^{(0)} \quad (4.126)$$

Eliminating $I_f^{(1)}$ from (4.121) and (4.124) results in

$$\frac{E_k^{(1)} - E_k^{(1)0}}{E_j^{(1)} - E_j^{(1)0}} = \frac{Z_{kr}^{(1)}}{Z_{jr}^{(1)}} \quad (4.127)$$

Defining

$$d_{kj} = \frac{E_k^{(1)} - E_k^{(1)0}}{E_j^{(1)} - E_j^{(1)0}} \quad (4.128)$$

and substituting (4.112) into (4.127) gives

$$d_{kj} = \frac{Z_{0,pk}^{(1)} \sinh [(1-m)\gamma^{(1)}l] + Z_{0,qk}^{(1)} \sinh (m\gamma^{(1)}l)}{Z_{0,pj}^{(1)} \sinh [(1-m)\gamma^{(1)}l] + Z_{0,qj}^{(1)} \sinh (m\gamma^{(1)}l)} \quad (4.129)$$

Fault location is obtained by simplifying (4.129) based on the identity $\sinh \theta = (e^\theta - e^{-\theta})/2$ as shown in [57]

$$m = \frac{1}{2\gamma^{(1)}l} \ln \left[\frac{\left(d_{kj} Z_{0,qj}^{(1)} - Z_{0,qk}^{(1)} \right) - \left(d_{kj} Z_{0,pj}^{(1)} - Z_{0,pk}^{(1)} \right) e^{\gamma^{(1)}l}}{\left(d_{kj} Z_{0,qj}^{(1)} - Z_{0,qk}^{(1)} \right) - \left(d_{kj} Z_{0,pj}^{(1)} - Z_{0,pk}^{(1)} \right) e^{-\gamma^{(1)}l}} \right] \quad (4.130)$$

The above fault location formula is applicable only if there exists a path, which passes through the faulted line and does not pass any bus more than once, between buses k and j . Otherwise, the ratio of voltage changes at these two buses will be constant and independent of the fault location variable. Since most power network is interconnected, most combinations are able to produce fault location estimate.

Negative-sequence or zero-sequence voltage measurements, where applicable, can also be employed for fault location. However, positive-sequence voltages are preferred due to the fact that no fault type classification is needed.

Credits should be given to the work in [57]. Since only positive-sequence quantities are involved in (4.130), the fault location formulation for single-circuit line has been directly utilized for double-circuit line.

2) Fault location with unsynchronized measurements from two buses

Taking the absolute value of (4.129) leads to

$$|d_{kj}| = \left| \frac{Z_{0,pk}^{(1)} \sinh [(1-m)\gamma^{(1)}l] + Z_{0,qk}^{(1)} \sinh (m\gamma^{(1)}l)}{Z_{0,pj}^{(1)} \sinh [(1-m)\gamma^{(1)}l] + Z_{0,qj}^{(1)} \sinh (m\gamma^{(1)}l)} \right| \quad (4.131)$$

The Newton-Raphson approach can be utilized here to iteratively solve for the unknown fault location m .

4.4.2 One-Bus Fault Location Algorithms

This section shows the one-bus fault location algorithms for different types of fault based on voltage measurements from a single bus k ($k = 1, 2, \dots, n$).

1) LG fault

For phase A to ground fault, the boundary condition, $I_f^{(0)} = I_f^{(1)} = I_f^{(2)}$, exists. Eliminating $I_f^{(0)}$ and $I_f^{(2)}$ from (4.122) and (4.123) yields

$$\frac{E_k^{(2)}}{E_k^{(0)}} = \frac{Z_{kr}^{(1)}}{Z_{kr}^{(0)}} \quad (4.132)$$

Replacing the transfer impedance terms in (4.132) by (4.112) and (4.90), a nonlinear equation involving one unknown variable m can be formulated, which can be separated into real and imaginary part to formulate two real equations. To solve it, least squares method can be utilized. An initial value of 0.5 p.u. for m can be adopted.

2) LLG fault

For phase B to C to ground fault, the following condition is satisfied

$$\frac{I_f^{(2)}}{I_f^{(0)}} = \frac{Z_{rr}^{(0)} + 3R_f}{Z_{rr}^{(1)}} \quad (4.133)$$

Using (4.122) and (4.123), (4.133) becomes

$$\frac{E_k^{(2)}}{E_k^{(0)}} = \frac{Z_{kr}^{(1)} (Z_{rr}^{(0)} + 3R_f)}{Z_{kr}^{(0)} Z_{rr}^{(1)}} \quad (4.134)$$

By employing (4.90), (4.100), (4.112) and (4.120), we can formulate a nonlinear equation with two unknowns m and R_f from (4.134), which can be separated into two real equations. Newton-Raphson approach similar to (4.131) can be adopted to solve for the two unknown variables.

3) LL fault

For phase B to C fault, the following boundary conditions hold,

$$I_f^{(1)} = -I_f^{(2)} \quad (4.135)$$

$$I_f^{(1)} = \frac{E_r^{(1)0}}{R_f + 2Z_{rr}^{(1)}} \quad (4.136)$$

Substituting (4.122) and (4.136) into (4.135) results in

$$\frac{E_k^{(2)}}{Z_{kr}^{(1)}} = \frac{E_r^{(1)0}}{R_f + 2Z_{rr}^{(1)}} \quad (4.137)$$

where $E_r^{(1)0}$ denotes the pre-fault positive-sequence voltage at the fault point and can be calculated as

$$E_r^{(1)0} = \frac{2 \left(E_p^{(1)0} z_{qr}^{(1)} + E_q^{(1)0} z_{pr}^{(1)} \right)}{\left(y_{pr}^{(1)} + y_{qr}^{(1)} \right) z_{pr}^{(1)} z_{qr}^{(1)} + 2 \left(z_{pr}^{(1)} + z_{qr}^{(1)} \right)} \quad (4.138)$$

where $E_p^{(1)0}$ and $E_q^{(1)0}$ are the pre-fault positive-sequence voltages at the two terminals of the faulted line and are assumed to be known. Combining (4.103)-(4.106), (4.112), (4.120) and (4.137) will produce a non-linear equation with m and R_f as unknowns, the solution of which is similar to (4.134).

4) LLL fault

For three phase fault, we have

$$I_f^{(1)} = \frac{E_r^{(1)0}}{R_f + Z_{rr}^{(1)}} \quad (4.139)$$

Replacing $I_f^{(1)}$ in (4.121) with (4.139) gives rise to

$$E_k^{(1)} = E_k^{(1)0} - Z_{kr}^{(1)} \frac{E_r^{(1)0}}{R_f + Z_{rr}^{(1)}} \quad (4.140)$$

A non-linear formulation with two unknowns m and R_f can be derived by substituting (4.112), (4.120) and (4.138) into (4.140), which can be solved similar to (4.134). Fault location formulas involving other phases can be deduced similarly.

It should be pointed out that the proposed one-bus method requires the fault type to be known while the two-bus method utilizing positive-sequence voltages does not. In addition, it is assumed that the faulted section can be decided based on relay operations; otherwise, a list of possible faulted sections can be attempted, leading to a list of possible fault locations.

For LLG fault, multiple valid solutions may be obtained. The erroneous solutions can be filtered out utilizing the method proposed in Section 2.3.1.2.

For LL and LLL faults, two valid solutions may arise. Based on short-circuit analysis, both fault conditions corresponding to the two solutions will yield the same voltage phasors as the measured ones. Hence, unless more information is available, there may be more than one likely fault location estimates.

4.5 Optimal Fault Location Estimation Considering Measurement Errors

When synchronized voltage measurements at multiple buses are available, the following optimal fault location estimator with the ability to detect bad measurements is developed.

4.5.1 Proposed Optimal Estimator

Suppose the positive-sequence superimposed voltages caused by the fault at buses k_1, k_2, \dots, k_N , are available, which form the following vector

$$S = [\Delta V_{k_1}, \Delta V_{k_2}, \dots, \Delta V_{k_N}]^T \quad (4.141)$$

where T is the vector transpose operator; N is the total number of measurement set. For any two sets of measurements from buses k_i and k_j ($i, j = 1, \dots, N$), the following equation is yielded based on (4.129)

$$\frac{\Delta V_{k_i}}{\Delta V_{k_j}} = \frac{Z_{0,pk_i}^{(1)} \sinh [(1-m)\gamma^{(1)}l] + Z_{0,qk_i}^{(1)} \sinh (m\gamma^{(1)}l)}{Z_{0,pk_j}^{(1)} \sinh [(1-m)\gamma^{(1)}l] + Z_{0,qk_j}^{(1)} \sinh (m\gamma^{(1)}l)} \quad (4.142)$$

Define the unknown variables as

$$X = [x_1, x_2, \dots, x_{2N}, x_{2N+1}] \quad (4.143)$$

where

x_{2i-1}, x_{2i} $i = 1, \dots, N$ variables to represent the positive-sequence superimposed voltage caused by the fault, i.e. $\Delta V_{k_i} = x_{2i-1}e^{jx_{2i}}$;

x_{2N+1} fault location variable.

The combinations of any two sets of measurements out of N sets include $[k_1k_2, \dots, k_1k_N, k_2k_3, \dots, k_{N-1}k_N]$, the total number of which is $M = C_N^2$. For any possible combination, say k_ik_j , by employing the defined variables, (4.142) can be written as

$$f_{k_ik_j}(X) = \frac{Z_{0,pk_i}^{(1)} \sinh [(1-x_{2N+1})\gamma^{(1)}l] + Z_{0,qk_i}^{(1)} \sinh (x_{2N+1}\gamma^{(1)}l)}{Z_{0,pk_j}^{(1)} \sinh [(1-x_{2N+1})\gamma^{(1)}l] + Z_{0,qk_j}^{(1)} \sinh (x_{2N+1}\gamma^{(1)}l)} \times x_{2j-1}e^{jx_{2j}} - x_{2i-1}e^{jx_{2i}} = 0 \quad (4.144)$$

In total, we can have M equations in the form of (4.144). Let's introduce Y and $F(X)$ as measurement vector and function vector, respectively. Y is formed as [72]

$$Y_i = 0, \quad i = 1, \dots, 2M \quad (4.145)$$

$$Y_{2M+2i-1} = |S_i|, \quad i = 1, \dots, N \quad (4.146)$$

$$Y_{2M+2i} = \angle S_i, \quad i = 1, \dots, N \quad (4.147)$$

where \angle yields the angle in radian of the input argument. $F(X)$ is formulated as follows

$$F(X) = [\text{Re}(f_{k_1 k_2}), \text{Im}(f_{k_1 k_2}), \dots, \text{Re}(f_{k_1 k_N}), \text{Im}(f_{k_1 k_N}), \text{Re}(f_{k_2 k_3}), \text{Im}(f_{k_2 k_3}), \dots, \text{Re}(f_{k_{N-1} k_N}), \text{Im}(f_{k_{N-1} k_N}), x_1, x_2, \dots, x_{2N}]^T \quad (4.148)$$

where $\text{Re}()$ and $\text{Im}()$ yield the real and imaginary part of the input argument, respectively. The measurement vector and function vector are related by

$$Y = F(X) + \mu \quad (4.149)$$

where μ is a vector representing measurement error and dependent on the meter characteristic. The optimal estimate of X is obtained by minimizing the cost function defined as

$$J = [Y - F(X)]^T R^{-1} [Y - F(x)] \quad (4.150)$$

where

$$R = E(\mu\mu^T) = \text{diag}[\sigma_1^2, \dots, \sigma_{2M+2N}^2] \quad (4.151)$$

And σ_i^2 signifies the variance of measurement i ; $E()$ indicates the expected value; $\text{diag}()$ means a diagonal matrix consisting of the values contained in the square bracket. $2M + 2N$ is the total number of measurements. A smaller value of σ_i^2 indicates a more accurate measurement. Equation (4.150) can be solved iteratively [73]. During k^{th} iteration, the unknown vector is updated as

$$H = \left. \frac{\partial F(X)}{\partial X} \right|_{X=X_k} \quad (4.152)$$

$$\Delta X_k = (H^T R^{-1} H)^{-1} \{H^T R^{-1} [Y - F(X_k)]\} \quad (4.153)$$

$$X_{k+1} = X_k + \Delta X_k \quad (4.154)$$

where

k iteration number starting from 0,

X_k, X_{k+1} variable vector before and after k^{th} iteration,

ΔX_k variable update during k^{th} iteration.

To initiate the iteration process, we can choose 0.1 p.u. and $\pi/4$ for the magnitude and angle of positive-sequence superimposed voltage, respectively. In addition, we have used an initial value of 0.5 p.u. for the fault location estimate. When the variable update is smaller than the specified tolerance, the iteration process can be terminated. After X is obtained, we can use (4.148) to compute the estimated values of measurements.

4.5.2 Detection and Identification of Bad Measurements

Drawing on the classical method [73], we can detect the existence of bad measurements as follows

1. Compute the expected value of cost function as

$$E(J) = (2M + 2N) - (2N + 1) = 2M - 1 \quad (4.155)$$

2. Compute the actual value of cost function as

$$J = \sum_{i=1}^{2M+2N} \frac{(Y_i - \bar{Y}_i)^2}{\sigma_i^2} \quad (4.156)$$

where \bar{Y}_i is the estimated measurement value calculated from (4.148).

3. If $J \geq AE(J)$, then it is suspected that bad measurement is present; otherwise, it can be judged that there is no bad data. A is a constant and chosen as 3.0 in our study.
4. In case the bad measurement is present, the largest error based approach can be utilized to identify the bad data. The normalized error is calculated as

$$SE_i = \frac{Y_i - \bar{Y}_i}{\sqrt{\Omega_{ii}}}, \quad i = 1, \dots, 2M + 2N \quad (4.157)$$

where Ω_{ii} is the diagonal element of the matrix

$$\Omega = R - H(H^T R^{-1} H)^{-1} H^T \quad (4.158)$$

The largest value of normalized error indicates the bad measurement. After the bad measurement is identified and removed, the rest measurements can be utilized to obtain a new set of estimates, steps 1-4 can be repeated to further detect and identify the rest bad data.

4.6 Simulation Studies

This section presents the simulation results to evaluate the developed fault location algorithms. EMTP has been utilized to simulate the studied power system and generate transient waveforms for faults of different types, locations and fault resistances [67]. We have applied a 4th order Butterworth low-pass filter with a cut-off frequency of 90 Hz to the generated waveforms to filter out the harmonic components. Discrete Fourier Transform is utilized to extract phasors from the generated waveforms to feed into the developed algorithms to obtain the fault distance. The 3rd cycle of the waveform after the fault inception is captured to extract phasors during fault.

The studied power system is a 27-bus, 345 kV, 60 Hz transmission line system, as shown in Fig. 4.10. The line length is labeled in mile. The section between bus 9

and 10 possesses the double-circuit line structure and the fault occurs on one of the parallel lines, with the cross denoting the fault point. The length of the faulted line is 168.2 miles. The double-circuit line is modeled in EMTP based on the distributed parameter line model.

The estimation accuracy is evaluated by the percentage error as in (2.148). The location of the fault is defined as the distance between the fault point and bus 9.

A. Cases without bad measurements

The developed fault location algorithms are tested under various fault conditions. Table 4.1 shows the fault location results produced by two-bus algorithms. The first three columns represent the actual fault type, fault location and fault resistance, respectively. The rest indicate the errors of fault location estimates utilizing both synchronized and unsynchronized voltage measurements from two buses.

In Table 4.1, positive-sequence voltage measurements are used to carry out two-bus fault location. The fault location results are quite satisfactory. It can be observed that quite close fault location estimates are produced by using synchronized and unsynchronized data. Notice that it is impossible to produce fault location estimate by employing voltage measurements from bus combinations such as 4 and 5, 10 and 11, 11 and 22 etc. on account of the reason explained in Section 4.4.1.

Table 4.2 presents the one-bus fault location results for AG and BCG faults. Columns 4-14 display the percentage errors of fault location estimate employing the voltage measurements from a single bus. It can be seen that the fault location estimates in Table 4.2 are quite accurate.

Table 4.3 conveys the one-bus fault location results for BC and ABC faults. Column 3 to the end list the estimated fault location, fault resistance utilizing voltage measurements from a single bus. m is the estimated fault location (p.u.) and R_f is the estimated fault resistance (p.u.). The actual fault resistance is 1Ω (0.00084 p.u.) and the base value of the impedance is 1190.25Ω .

As observed from Table 4.3, the one-bus algorithms for BC and ABC faults are able to yield quite accurate fault location estimate, however, under certain fault conditions, two valid solutions can be produced. Only one of them is the correct solution and the erroneous one is indicated by * next to the fault location estimate. For example, when the actual fault location of a BC fault is 0.5 p.u., using the voltages from bus 6, two valid solutions (0.5004, 0.00088) p.u. and (0.8324, 0.00295) p.u. are yielded with the first element representing the fault location estimate and the second one representing the fault resistance estimate. Here, the second solution is erroneous, whose estimated fault location is followed by *.

When two valid solutions are yielded, our studies indicate that it is not possible to tell which solution is true by utilizing only the voltage measurements at one bus.

B. Cases with bad measurements

Large errors in voltage measurements can lead to significant inaccuracy in fault location estimate. This case study illustrates how to detect and identify bad mea-

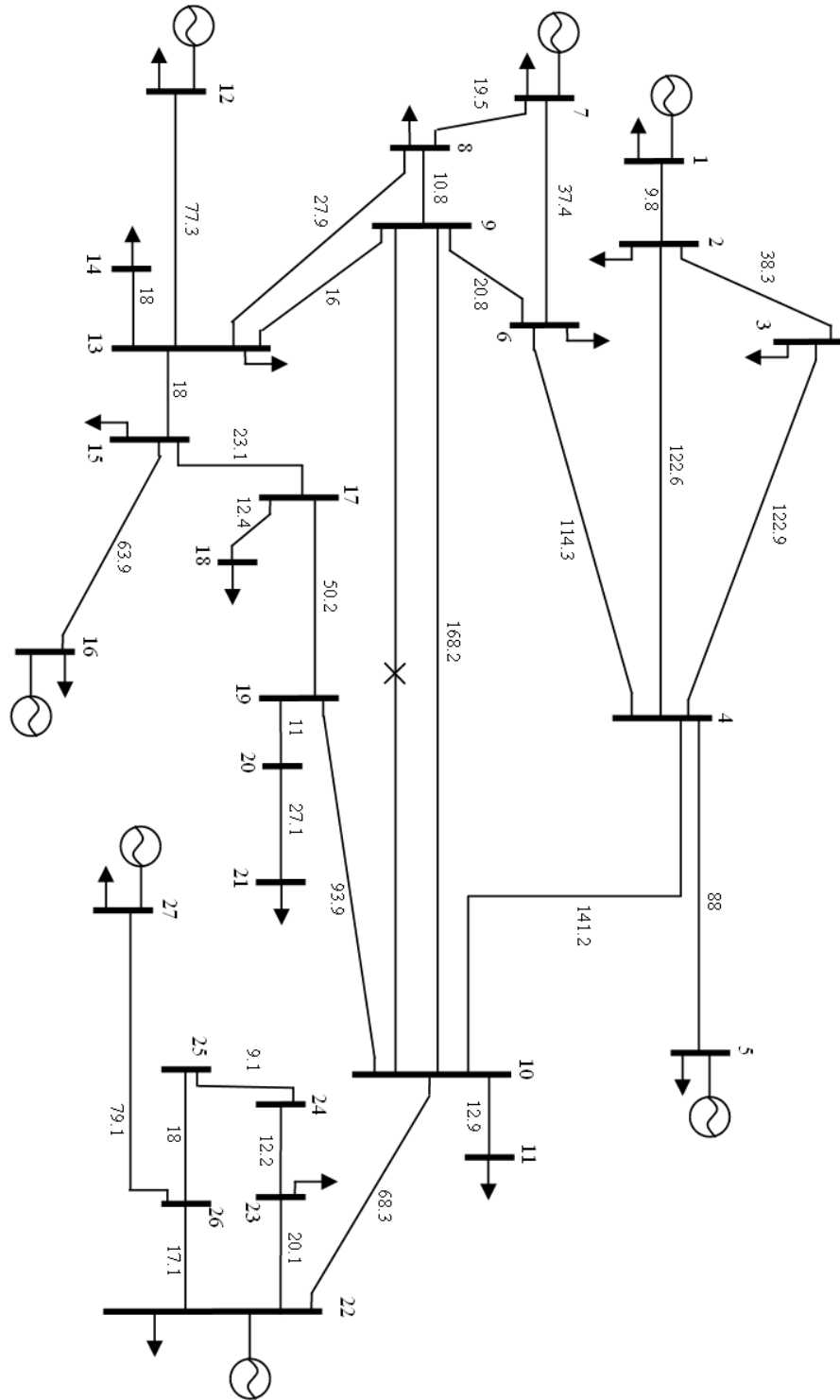


Figure 4.10: Schematic diagram of the studied 27-bus system.

measurements by optimal estimator. A value of 1.0×10^{-6} is chosen as variance for the first $2M$ measurements and 1.0×10^{-4} for the variance of the voltage measurements. In our studied cases, the voltage measurements at buses 4, 6, 8 and 19 are utilized to perform fault location.

Case 1: BCG fault with the actual fault location being 0.3 p.u. and fault resistance being 50Ω . Suppose that there is an error of 50% in the magnitude of superimposed positive-sequence voltage at bus 4.

The optimal estimation result is shown in Table 4.4. There are 20 equations and 9 state variables; therefore the expected value of the cost function is calculated as 11. The actual value of the cost function $J = 34.58 \geq 3 \times 11$, thus the presence of bad measurements is suspected. Following the method outlined in Section 4.5.2, the biggest value of the normalized error vector SE corresponds to the magnitude of superimposed positive-sequence voltage at bus 4. Therefore the data at bus 4 is identified as a bad measurement.

After the bad measurement is removed, a new set of optimal estimates is calculated as shown in Table 4.5. In this scenario, the expected value of the cost function $E(J)$ equals 5 and the actual value of cost function J is 6.0×10^{-4} . Since $E(J)$ is much less than J , all of the data are considered fairly accurate and the estimates are regarded as satisfactory. Comparison with Table 4.4 indicates that the fault location accuracy is considerably improved.

Case 2: ABC fault with the actual fault location being 0.8 p.u. and fault resistance being 1Ω . Suppose that there is a distortion of 20° in the angle of superimposed positive-sequence voltage at bus 6.

The optimal estimation result is shown in Table 4.6. $E(J)$ is equal to 11 and J is obtained as 867.41, which obviously signifies the existence of bad measurement. The biggest value of the normalized error vector SE corresponds to the angle of superimposed positive-sequence voltage at bus 6. Therefore, the data at bus 6 is identified as bad measurement.

The new optimal estimates with the measurement at bus 6 being removed are shown in Table 4.7. In this case, J is equal to 9.0×10^{-4} and $E(J)$ is 5. Since J is much less than $E(J)$, all the measurements are considered fairly accurate and the estimates are regarded as acceptable. It can be seen that the accuracy of estimate of fault location after the bad data being removed is considerably enhanced. Therefore, the optimal estimator is able to detect and identify the bad data and improve the accuracy of fault location estimate.

4.7 Summary

In this chapter, novel one-bus and two-bus fault location algorithms applicable to double-circuit transmission lines are devised. The distinctive feature of the proposed method is that only voltage measurements from one or two buses are needed which may be distant away from the faulted section by making use of the bus impedance matrix technique. The distributed parameter line model is utilized which fully takes the shunt capacitance of long lines into account.

For two-bus fault location algorithms, a unique fault location estimate is produced using both synchronized and unsynchronized voltage measurements and fault type classification is not required. The application range of this type of algorithm is subject to network topology.

As to one-bus fault location algorithms, fault type is a pre-requisite. For LG and LLG faults, a unique fault location estimate can be obtained. As far as LL and LLL faults are concerned, pre-fault measurements at the two terminals of the faulted line are demanded, which can be obtained from state estimation. In certain cases two possible fault location estimates may be produced, both of which will be treated as likely fault location.

An optimal state estimator has also been developed employing synchronized data from multiple buses. It has the ability to detect and identify bad measurements and improve the accuracy of fault location estimation.

Simulation studies have shown the fault location algorithms can yield quite accurate estimates under various fault conditions.

Table 4.1: Two-bus fault location results

Fault type	Fault loca. (p.u.)	Fault res. (Ω)	Est. fault location error using voltages from two buses (%)													
			4&8		6&19		7&20		8&11		12&26		13&20			
			Syn	Unsyn	Syn	Unsyn	Syn	Unsyn	Syn	Unsyn	Syn	Unsyn	Syn	Unsyn	Syn	Unsyn
AG	0.3	1	0.0515	0.0029	0.0067	0.0027	0.0206	0.0216	0.0132	0.0121	0.0322	0.0142	0.0056	0.0016		
		50	0.2574	0.2215	0.0236	0.0237	0.0339	0.0414	0.0251	0.0265	0.1385	0.1228	0.0178	0.0187		
	0.5	1	0.0384	0.0037	0.0083	0.0121	0.0279	0.0368	0.0195	0.0245	0.0342	0.0275	0.0059	0.0100		
		50	0.2297	0.1982	0.0064	0.0132	0.0231	0.0375	0.0095	0.0159	0.0886	0.0833	0.0007	0.0085		
	0.8	1	0.0807	0.0807	0.0015	0.0120	0.0220	0.0384	0.0059	0.0131	0.0141	0.0185	0.0050	0.0172		
		50	0.1492	0.1448	0.0274	0.0140	0.0145	0.0064	0.0231	0.0130	0.0041	0.0107	0.0330	0.0181		
BCG	0.3	1	0.0176	0.0061	0.0121	0.0198	0.0354	0.0468	0.0224	0.0301	0.0625	0.0912	0.0079	0.0152		
		50	0.0204	0.0050	0.0127	0.0213	0.0353	0.0482	0.0208	0.0293	0.0548	0.0858	0.0090	0.0170		
	0.5	1	0.0106	0.0354	0.0309	0.0379	0.0564	0.0671	0.0375	0.0435	0.0892	0.1126	0.0276	0.0344		
		50	0.0020	0.0264	0.0295	0.0367	0.0541	0.0656	0.0356	0.0422	0.0819	0.1070	0.0261	0.0330		
	0.8	1	0.0371	0.0516	0.0454	0.0486	0.0728	0.0791	0.0487	0.0518	0.1092	0.1242	0.0437	0.0469		
		50	0.0291	0.0453	0.0456	0.0496	0.0723	0.0800	0.0502	0.0539	0.1082	0.1250	0.0438	0.0477		
BC	0.3	1	0.0126	0.0145	0.0133	0.0213	0.0307	0.0417	0.0201	0.0281	0.0638	0.0956	0.0109	0.0186		
	0.5	1	0.0062	0.0308	0.0275	0.0337	0.0476	0.0569	0.0330	0.0389	0.0898	0.1154	0.0253	0.0313		
	0.8	1	0.0275	0.0435	0.0384	0.0410	0.0595	0.0647	0.0429	0.0457	0.1108	0.1274	0.0380	0.0407		
ABC	0.3	1	0.0235	0.0141	0.0031	0.0060	0.0121	0.0150	0.0091	0.0125	0.0277	0.0428	0.0014	0.0041		
	0.5	1	0.0101	0.0015	0.0128	0.0145	0.0231	0.0250	0.0173	0.0194	0.0418	0.0538	0.0111	0.0128		
	0.8	1	0.0123	0.0194	0.0172	0.0162	0.0272	0.0266	0.0192	0.0189	0.0474	0.0542	0.0175	0.0168		

Table 4.2: One-bus fault location results for AG and BCG faults

Fault type	Fault loca. (p.u.)	Fault res. (Ω)	Est. fault location error using voltages from a single bus (%)													
			4	5	6	7	8	11	13	14	22	24	27			
AG	0.3	1	0.2463	0.2558	0.0763	0.0791	0.0171	0.0746	0.0106	0.0116	0.0903	0.0949	0.1134			
		50	0.0530	0.1400	0.3893	0.3316	0.2874	0.0242	0.4982	0.4990	0.0462	0.0485	0.0716			
	0.5	1	0.3515	0.3649	0.0959	0.0886	0.0504	0.0969	0.0744	0.0749	0.1322	0.1440	0.1766			
		50	0.0364	0.0532	0.1514	0.1379	0.1178	0.0030	0.1827	0.1830	0.01724	0.0166	0.0477			
	0.8	1	0.3639	0.4990	0.0958	0.0918	0.0668	0.1460	0.0870	0.0868	0.2312	0.2481	0.3292			
		50	0.0112	0.0680	0.0677	0.0616	0.0558	0.0499	0.0779	0.0776	0.0760	0.0761	0.1192			
BCG	0.3	1	0.1715	0.2108	0.0671	0.1025	0.0434	0.1083	0.0495	0.0500	0.1635	0.1564	0.1934			
		50	0.7465	0.0243	0.0226	0.0300	0.0353	0.1321	0.0226	0.0241	0.1650	0.1282	0.2078			
	0.5	1	0.0270	0.1543	0.1287	0.1941	0.0912	0.0695	0.1097	0.1109	0.1418	0.1304	0.2482			
		50	0.1900	0.0424	0.0179	0.0156	0.0055	0.0982	0.0023	0.0040	0.3629	0.3299	0.0934			
	0.8	1	0.1860	0.1461	0.6027	0.5755	0.3517	0.0059	0.8512	0.8622	0.0335	0.0235	0.2216			
		50	0.0063	0.2054	0.3990	0.2912	0.2842	0.1688	0.4373	0.4314	0.4228	0.4041	0.1549			

Table 4.3: One-bus fault location results for BC and ABC faults

Fault type	Fault loca. (p.u)	Result using voltages at a single bus															
		4			6			8			11			13			22
		m	R_f	m	R_f	m	R_f	m	R_f	m	R_f	m	R_f	m	R_f	m	R_f
BC	0.3	0.3001	0.00085	0.3001	0.00087	0.3001	0.00087	0.2957	0.00080	0.3001	0.00087	0.2902	0.00068	0.3001	0.00087	0.2902	0.00068
		0.6843*	0.00252	0.9897*	0.00415			0.3287*	0.00093	0.9772*	0.00421	0.3344*	0.00086				
	0.5	0.4991	0.00085	0.5004	0.00088	0.5003	0.00088	0.5005	0.00082	0.5004	0.00088	0.5012	0.00071	0.5004	0.00088	0.5012	0.00071
ABC	0.3	0.3002	0.00082	0.3000	0.00084	0.3000	0.00084	0.2975	0.00082	0.3000	0.00084	0.2978	0.00078	0.3000	0.00084	0.2978	0.00078
		0.6842*	0.00169	0.9902*	0.00237			0.3266*	0.00089	0.9777*	0.00241	0.3262*	0.00084				
	0.5	0.4973	0.00081	0.5001	0.00083	0.5000	0.00083	0.5003	0.00082	0.5000	0.00083	0.5003	0.00078	0.5000	0.00083	0.5003	0.00078
	0.8	0.8001	0.00084	0.7996	0.00087	0.7996	0.00087	0.8002	0.00083	0.8001	0.00083	0.8002	0.00073	0.8001	0.00083	0.8002	0.00073
	0.8	0.8001	0.00082	0.8001	0.00083	0.8001	0.00083	0.8002	0.00083	0.8001	0.00083	0.8002	0.00079	0.8001	0.00083	0.8002	0.00079

Table 4.4: Optimal estimates with bad magnitude measurement

Quantity	Unit	Actual value	Optimal estimate
$ \Delta V_4 $	p.u.	0.1924	0.1386
$\angle \Delta V_4$	rad.	1.1336	1.1376
$ \Delta V_6 $	p.u.	0.2296	0.2350
$\angle \Delta V_6$	rad.	1.1215	1.1171
$ \Delta V_8 $	p.u.	0.2375	0.2426
$\angle \Delta V_8$	rad.	1.1260	1.1212
$ \Delta V_{19} $	p.u.	0.2233	0.2436
$\angle \Delta V_{19}$	rad.	1.1314	1.1367
m	p.u.	0.3	0.3934

Table 4.5: Optimal estimates with bad magnitude measurement removed

Quantity	Unit	Actual value	Optimal estimate
$ \Delta V_6 $	p.u.	0.2296	0.2297
$\angle \Delta V_6$	rad.	1.1215	1.1214
$ \Delta V_8 $	p.u.	0.2375	0.2376
$\angle \Delta V_8$	rad.	1.1260	1.1259
$ \Delta V_{19} $	p.u.	0.2233	0.2232
$\angle \Delta V_{19}$	rad.	1.1314	1.1315
m	p.u.	0.3	0.2991

Table 4.6: Optimal estimates with bad angle measurement

Quantity	Unit	Actual value	Optimal estimate
$ \Delta V_4 $	p.u.	0.2672	0.2527
$\angle \Delta V_4$	rad.	1.0817	1.1584
$ \Delta V_6 $	p.u.	0.3534	0.3752
$\angle \Delta V_6$	rad.	1.3742	1.1259
$ \Delta V_8 $	p.u.	0.3604	0.3849
$\angle \Delta V_8$	rad.	1.0264	1.1215
$ \Delta V_{19} $	p.u.	0.4902	0.4555
$\angle \Delta V_{19}$	rad.	1.0857	1.1621
m	p.u.	0.8	0.6184

Table 4.7: Optimal estimates with bad angle measurement removed

Quantity	Unit	Actual value	Optimal estimate
$ \Delta V_4 $	p.u.	0.2672	0.2672
$\angle \Delta V_4$	rad.	1.0817	1.0819
$ \Delta V_8 $	p.u.	0.3604	0.3604
$\angle \Delta V_8$	rad.	1.0264	1.0263
$ \Delta V_{19} $	p.u.	0.4902	0.4901
$\angle \Delta V_{19}$	rad.	1.0857	1.0855
m	p.u.	0.8	0.8000

Chapter 5

Fault Location for Series-Compensated Lines

The layout of this chapter is as follows. First of all, the basic features of the proposed fault location method for series-compensated single-circuit are introduced, followed by the nomenclature in Section 5.2. Section 5.3 derives the fault location algorithm by applying two subroutines and introduces the principle to identify the correct fault location estimate. The system configuration, fault location result and application of the fault location identification are presented in Section 5.4. At last, a summary of this chapter is provided in Section 5.5.

5.1 Introduction

Several intelligent fault location algorithms being able to avoid the equivalent V-I model of SC&MOV bank have been developed in the past few years. Reference [74] proposes a synchronous two-end algorithm that includes two steps: the first step ignores the existence of SC&MOV bank and calculates a pre-location of the fault; the second step iteratively computes the voltage on the right side of the compensation device and corrects the location of the fault. Reference [75] derives an analytical formula of the general fault loop, from which both fault location and fault resistance can be solved using iterative method. The synchronization angle is computed in advance using pre-fault measurements or sometimes fault quantities. Both [74] and [75] are independent of the model of series compensator and utilize distributed parameter line model, whereas [75] considers the double-circuit compensated line and a more general unsynchronized case.

Aiming at the series-compensated single-circuit line, a novel fault location method based on the distributed parameter line model is presented in this chapter. It utilizes unsynchronized two-terminal voltage and current phasors as inputs. As in [75], the currents flowing out of the fault point are formulated in terms of unknown fault location. Then boundary conditions of different fault types are exploited to derive the fault location formula [19]. The synchronization angle can be calculated using pre-fault quantities or fault quantities [75]. The fault impedance is assumed to be

pure resistive, the fault type is assumed to be known in advance from relay operations and the system is transposed.

5.2 Nomenclature

- P, Q Two terminals of the series-compensated transmission line;
- R The point where the series compensation device is installed;
- F The fault point;
- i The symmetrical component index, $i = 0, 1, 2$ for zero-, positive- and negative-sequence, respectively;
- m The unknown fault location in p.u.;
- l_1 The distance between buses P and R in km;
- l_2 The distance between buses Q and R in km;
- l The total length of the transmission line between buses P and Q in km and $l = l_1 + l_2$;
- δ The synchronization angle between buses P and Q with P as the reference;
- $V_p^{(i)}, V_q^{(i)}$ i^{th} -sequence voltage phasors at buses P and Q during the fault, respectively;
- $I_p^{(i)}, I_q^{(i)}$ i^{th} -sequence current phasors at buses P and Q during the fault, respectively;
- $I_{sc}^{(i)}$ i^{th} -sequence current flowing through the SC&MOV bank during the fault;
- $V_f^{(i)}$ i^{th} -sequence voltage at the fault point;
- $I_f^{(i)}$ i^{th} -sequence fault current;
- $I_{pf}^{(i)}$ The contribution of fault current from terminal P under i^{th} -sequence network;
- $I_{qf}^{(i)}$ The contribution of fault current from terminal Q under i^{th} -sequence network;
- $Z_c^{(i)}$ i^{th} -sequence characteristic impedance of the transmission line;
- $\gamma^{(i)}$ i^{th} -sequence propagation constant of the transmission line;
- $V_{sc-l}^{(i)}$ i^{th} -sequence voltage at the left side of the series compensation device during the fault;
- $V_{sc-r}^{(i)}$ i^{th} -sequence voltage at the right side of the series compensation device during the fault.

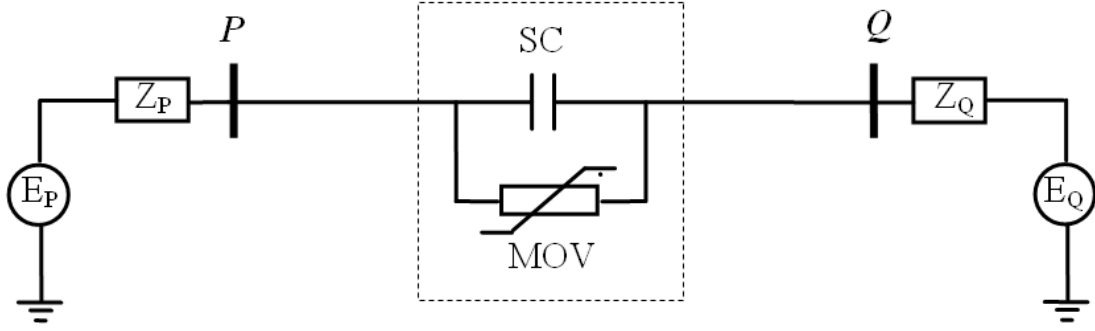


Figure 5.1: A schematic diagram of a series-compensated transmission line.

5.3 Proposed Fault Location Algorithms

A schematic diagram of a series-compensated transmission line is shown in Fig. 5.1. The series capacitor is installed at a fixed place along the transmission line. The MOV, equipped in parallel with SC, will conduct when an overvoltage across the series capacitor is detected. The voltage and current phasors from both ends are available. The series compensation device divides the transmission line into two sections. Since on which side the fault occurs is unknown to us, it is necessary to develop two subroutines addressing possible fault on either side. The subroutine 1 and 2, which assume the fault on the left and right side of the series compensation device are derived in detail. Later, the principle to decide the true fault location estimation is illustrated.

5.3.1 Subroutine 1: Location for Fault on the Left Side of Series Compensator

The schematic diagram of the transmission line with a fault on the left of SC&MOV bank is shown in Fig. 5.2. In the figure, $Z_{pf}^{(i)}$, $Z_{fr}^{(i)}$, $Z_{qr}^{(i)}$, $Y_{pf}^{(i)}$, $Y_{fr}^{(i)}$ and $Y_{qr}^{(i)}$ are the impedances and admittances of the equivalent π circuits of sections PF , FR and QR . Based on Fig. 5.2, the following three equations can be established from sections PF , QR and FR :

$$V_f^{(i)} = V_p^{(i)} \cosh(\gamma^{(i)} ml) - I_p^{(i)} Z_c^{(i)} \sinh(\gamma^{(i)} ml) \quad (5.1)$$

$$I_{pf}^{(i)} = I_p^{(i)} \cosh(\gamma^{(i)} ml) - \frac{V_p^{(i)}}{Z_c^{(i)}} \sinh(\gamma^{(i)} ml) \quad (5.2)$$

$$I_{sc}^{(i)} = I_q^{(i)} e^{j\delta} \cosh(\gamma^{(i)} l_2) - \frac{V_q^{(i)} e^{j\delta}}{Z_c^{(i)}} \sinh(\gamma^{(i)} l_2) \quad (5.3)$$

$$-I_{sc}^{(i)} = \left(I_{pf}^{(i)} - I_f^{(i)} \right) \cosh[\gamma^{(i)} (l_1 - ml)] - \frac{V_f^{(i)}}{Z_c^{(i)}} \sinh[\gamma^{(i)} (l_1 - ml)] \quad (5.4)$$

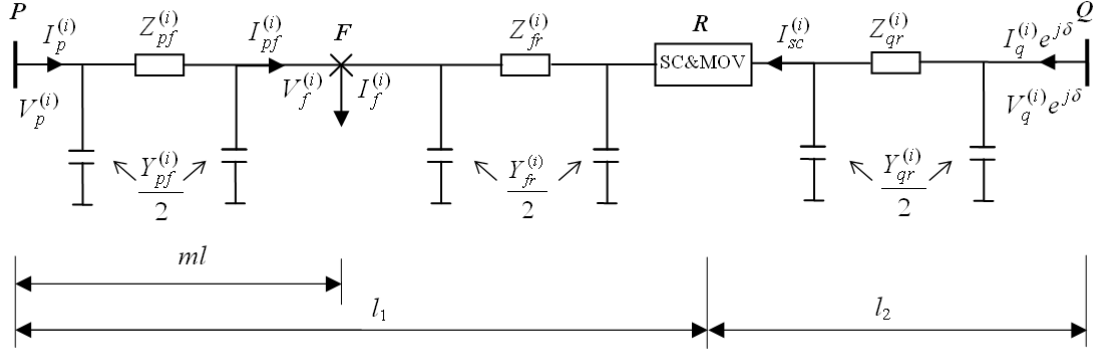


Figure 5.2: The i^{th} -sequence transmission line with fault on the left side of series compensator.

$$i = 0, 1, 2.$$

Substituting (5.1)-(5.3) into (5.4) and utilizing the following identities

$$\begin{aligned} \sinh(x + y) &= \sinh(x) \cosh(y) + \cosh(x) \sinh(y) \\ \cosh(x + y) &= \sinh(x) \sinh(y) + \cosh(x) \cosh(y) \end{aligned} \quad (5.5)$$

can lead to

$$I_f^{(i)} = \frac{I_p^{(i)} \cosh(\gamma^{(i)} l_1) + I_q^{(i)} e^{j\delta} \cosh(\gamma^{(i)} l_2) - \frac{V_p^{(i)}}{Z_c^{(i)}} \sinh(\gamma^{(i)} l_1) - \frac{V_q^{(i)} e^{j\delta}}{Z_c^{(i)}} \sinh(\gamma^{(i)} l_2)}{\cosh[\gamma^{(i)}(l_1 - ml)]} \quad (5.6)$$

Fault location formulas for different fault types can be derived based on (5.1) and (5.6).

(1) *AG fault*

For AG fault, the following boundary conditions are satisfied

$$I_f^{(1)} = I_f^{(2)} \quad (5.7)$$

$$I_f^{(0)} = I_f^{(1)} \quad (5.8)$$

Let $i = 1, 2$ in (5.6) and we will obtain the expressions of $I_f^{(1)}$ and $I_f^{(2)}$. Substituting them into (5.7) and taking advantage of the fact that positive-sequence parameters are the same as negative-sequence ones, it is observed that the unknown fault location is eliminated and we can compute the synchronization angle as follows similar to [75]

$$e^{j\delta} = - \frac{(I_p^{(1)} - I_p^{(2)}) \cosh(\gamma^{(1)} l_1) - \frac{V_p^{(1)} - V_p^{(2)}}{Z_c^{(1)}} \sinh(\gamma^{(1)} l_1)}{(I_q^{(1)} - I_q^{(2)}) \cosh(\gamma^{(1)} l_2) - \frac{V_q^{(1)} - V_q^{(2)}}{Z_c^{(1)}} \sinh(\gamma^{(1)} l_2)} \quad (5.9)$$

With the synchronization angle determined, by making use of (5.8), the formula with only m as the unknown variable can be derived. The iterative approach, such as Newton-Raphson is harnessed to pinpoint the fault location. An alternative approach is also to be discussed. It is known for AG fault, we have

$$V_f^{(0)} + V_f^{(1)} + V_f^{(2)} = 3R_f I_f^{(1)} \quad (5.10)$$

Since R_f is a real number, it indicates that $V_f^{(0)} + V_f^{(1)} + V_f^{(2)}$ and $I_f^{(1)}$ are in phase, which implies an alternative fault location formula as

$$\text{Im} \left\{ \frac{V_f^{(0)} + V_f^{(1)} + V_f^{(2)}}{I_f^{(1)}} \right\} = 0 \quad (5.11)$$

where $V_f^{(0)}$, $V_f^{(1)}$ and $V_f^{(2)}$ can be obtained from (5.1) and $I_f^{(1)}$ can be obtained from (5.6).

The alternative method is favored because of the following two reasons. First, it is a real equation and will provide a real fault location value; while the first method is a complex equation and will produce a complex solution, wherein the real part represents the fault location. Second, a unique solution is obtained from (5.11) regardless of the choice of initial value while the erroneous solution may arise from solving (5.8).

(2) BC fault

For BC fault, the following two equations exist

$$I_f^{(1)} = -I_f^{(2)} \quad (5.12)$$

$$V_f^{(1)} - V_f^{(2)} = R_f I_f^{(1)} \quad (5.13)$$

Similar to AG fault, from (5.12), we can eliminate the unknown fault location variable and obtain the synchronization angle as follows [75]

$$e^{j\delta} = - \frac{(I_p^{(1)} + I_p^{(2)}) \cosh(\gamma^{(1)} l_1) - \frac{V_p^{(1)} + V_p^{(2)}}{Z_c^{(1)}} \sinh(\gamma^{(1)} l_1)}{(I_q^{(1)} + I_q^{(2)}) \cosh(\gamma^{(1)} l_2) - \frac{V_q^{(1)} + V_q^{(2)}}{Z_c^{(1)}} \sinh(\gamma^{(1)} l_2)} \quad (5.14)$$

Upon (5.13), the fault location can be calculated from the following equation

$$\text{Im} \left\{ \frac{V_f^{(1)} - V_f^{(2)}}{I_f^{(1)}} \right\} = 0 \quad (5.15)$$

After m is solved from (5.15), $V_f^{(1)}$ and $V_f^{(2)}$ and $I_f^{(1)}$ can be calculated and therefore R_f can be obtained from (5.13).

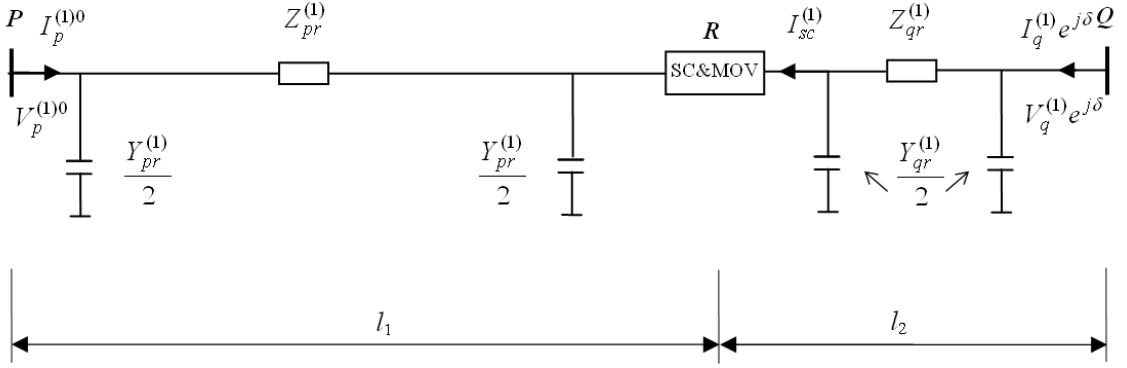


Figure 5.3: Pre-fault positive-sequence series-compensated transmission line.

(3) *BCG fault*

For BCG fault, the following relationships are satisfied at the fault point

$$V_f^{(1)} = V_f^{(2)} \quad (5.16)$$

$$V_f^{(0)} - V_f^{(1)} = 3R_f I_f^{(0)} \quad (5.17)$$

Equation (5.16) has a simple form and is adopted to perform the calculation of the fault distance together with (5.1), which can be expanded as

$$\begin{aligned} V_p^{(1)} \cosh(\gamma^{(1)} ml) - I_p^{(1)} Z_c^{(1)} \sinh(\gamma^{(1)} ml) \\ = V_p^{(2)} \cosh(\gamma^{(1)} ml) - I_p^{(2)} Z_c^{(1)} \sinh(\gamma^{(1)} ml) \end{aligned} \quad (5.18)$$

Also one can see that only voltage and current measurements from terminal P are required, therefore synchronization angle does not need to be known.

(4) *ABC fault*

For ABC fault, the synchronized angle can only be acquired from pre-fault measurements. From Fig. 5.3 we can build two equations

$$-I_{sc}^{(1)0} = I_p^{(1)0} \cosh(\gamma^{(1)} l_1) - \frac{V_p^{(1)0}}{Z_c^{(1)}} \sinh(\gamma^{(1)} l_1) \quad (5.19)$$

$$I_{sc}^{(1)0} = \left[I_q^{(1)0} \cosh(\gamma^{(1)} l_2) - \frac{V_q^{(1)0}}{Z_c^{(1)}} \sinh(\gamma^{(1)} l_2) \right] e^{j\delta} \quad (5.20)$$

Canceling out $I_{sc}^{(1)0}$ from (5.19) and (5.20) results in the synchronization angle of ABC

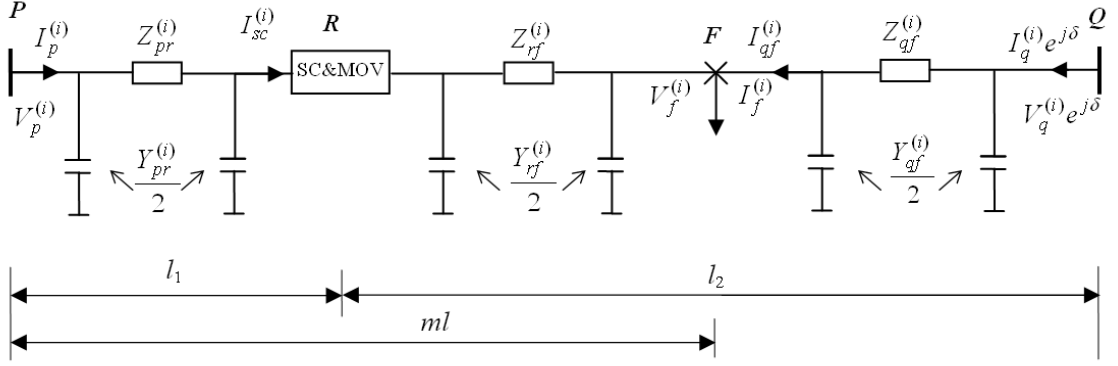


Figure 5.4: The i^{th} -sequence transmission line with fault on the right side of series compensator.

fault similar to [75]

$$e^{j\delta} = -\frac{I_p^{(1)0} \cosh(\gamma^{(1)}l_1) - \frac{V_p^{(1)0}}{Z_c^{(1)}} \sinh(\gamma^{(1)}l_1)}{I_q^{(1)0} \cosh(\gamma^{(1)}l_2) - \frac{V_q^{(1)0}}{Z_c^{(1)}} \sinh(\gamma^{(1)}l_2)} \quad (5.21)$$

$V_p^{(1)0}$ and $I_p^{(1)0}$ represent the pre-fault voltage and current phasors at P . $V_q^{(1)0}$ and $I_q^{(1)0}$ denote the pre-fault voltage and current phasors at Q . Note the acquisition of synchronization angle using (5.21) is also applicable to any other kinds of fault. The condition at the fault point is expressed by the following equation

$$V_f^{(1)} = R_f I_f^{(1)} \quad (5.22)$$

From (5.22), the fault location formula is reached as

$$\text{Im} \left\{ \frac{V_f^{(1)}}{I_f^{(1)}} \right\} = 0 \quad (5.23)$$

Fault location formulas for fault types involving other phases can be similarly deduced.

5.3.2 Subroutine 2: Location for Fault on the Right Side of Series Compensator

The schematic diagram of the transmission line with a fault on the right of SC&MOV bank is shown in Fig. 5.4. In the figure, $Z_{pr}^{(i)}$, $Z_{rf}^{(i)}$, $Z_{qf}^{(i)}$, $Y_{pr}^{(i)}$, $Y_{rf}^{(i)}$ and $Y_{qf}^{(i)}$ are the impedances and admittances of the equivalent π circuits of sections PR , FR and QF . Based on Fig. 5.4, the following three equations can be set up from sections PR , QF and RF :

$$V_f^{(i)} = V_q^{(i)} e^{j\delta} \cosh[\gamma^{(i)}(1-m)l] - I_q^{(i)} e^{j\delta} Z_c^{(i)} \sinh[\gamma^{(i)}(1-m)l] \quad (5.24)$$

$$I_{qf}^{(i)} = I_q^{(i)} e^{j\delta} \cosh [\gamma^{(i)}(1-m)l] - \frac{V_q^{(i)} e^{j\delta}}{Z_c^{(i)}} \sinh [\gamma^{(i)}(1-m)l] \quad (5.25)$$

$$I_{sc}^{(i)} = I_p^{(i)} \cosh (\gamma^{(i)}l_1) - \frac{V_p^{(i)}}{Z_c^{(i)}} \sinh (\gamma^{(i)}l_1) \quad (5.26)$$

$$-I_{sc}^{(i)} = (I_{qf}^{(i)} - I_f^{(i)}) \cosh [\gamma^{(i)}(ml - l_1)] - \frac{V_f^{(i)}}{Z_c^{(i)}} \sinh [\gamma^{(i)}(ml - l_1)] \quad (5.27)$$

Substituting (5.24)-(5.26) into (5.27) and utilizing the identities in (5.5) can lead to

$$I_f^{(i)} = \frac{I_p^{(i)} \cosh (\gamma^{(i)}l_1) + I_q^{(i)} e^{j\delta} \cosh (\gamma^{(i)}l_2) - \frac{V_p^{(i)}}{Z_c^{(i)}} \sinh (\gamma^{(i)}l_1) - \frac{V_q^{(i)} e^{j\delta}}{Z_c^{(i)}} \sinh (\gamma^{(i)}l_2)}{\cosh [\gamma^{(i)}(ml - l_1)]} \quad (5.28)$$

One can easily deduce that for subroutine 2, (5.9), (5.14) and (5.21) are still suitable to compute the synchronization angles for AG, BC and ABC faults, respectively. Fault location formulations (5.11), (5.15), and (5.23) for different types of fault are still applicable for subroutine 2 only the expressions for $V_f^{(i)}$ and $I_f^{(i)}$ are replaced with (5.24) and (5.28). For BCG fault, by substituting (5.24) into (5.16), we have

$$\begin{aligned} V_q^{(1)} e^{j\delta} \cosh [\gamma^{(1)}(1-m)l] - I_q^{(1)} e^{j\delta} Z_c^{(1)} \sinh [\gamma^{(1)}(1-m)l] \\ = V_q^{(2)} e^{j\delta} \cosh [\gamma^{(1)}(1-m)l] - I_q^{(2)} e^{j\delta} Z_c^{(1)} \sinh [\gamma^{(1)}(1-m)l] \end{aligned} \quad (5.29)$$

Canceling out the term $e^{j\delta}$ from both sides of (5.29), we can obtain the fault location formulation for BCG fault as follows

$$\begin{aligned} V_q^{(1)} \cosh [\gamma^{(1)}(1-m)l] - I_q^{(1)} Z_c^{(1)} \sinh [\gamma^{(1)}(1-m)l] \\ = V_q^{(2)} \cosh [\gamma^{(1)}(1-m)l] - I_q^{(2)} Z_c^{(1)} \sinh [\gamma^{(1)}(1-m)l] \end{aligned} \quad (5.30)$$

From (5.30), we can deduce that For BCG fault, the knowledge about synchronization angle is still not required for BCG fault because only voltage and current phasors from terminal Q are employed and the synchronization angle term has been canceled out in the fault location formula.

Another way is to make use of the symmetry of the transmission line and utilize subroutine 1 to consider subroutine 2. We can calculate delta, the synchronization angle, the same way as subroutine 1, and then perform $V_q^{(i)} e^{j\delta} \leftrightarrow V_p^{(i)}$, $I_q^{(i)} e^{j\delta} \leftrightarrow I_p^{(i)}$, $l_1 \leftrightarrow l_2$, and follow subroutine 1 exactly to find the solution. Then the fault location estimate is denoted as m' and the actual fault location can be obtained by carrying out $m = 1 - m'$.

Again, for BCG fault, we do not have to know δ , because the factor $e^{j\delta}$ will be eliminated. So this means we can perform $V_q^{(i)} \leftrightarrow V_p^{(i)}$, $I_q^{(i)} \leftrightarrow I_p^{(i)}$ without caring about the factor $e^{j\delta}$. Then follow the formula of (5.18) and find m' and further $m = 1 - m'$.

5.3.3 Fault Location Identification Method

Various methods to select the valid subroutine have been proposed [53, 55, 74, 75], and they all work properly. Based on these approaches, the fault location identification method suitable to this work is proposed. Suppose the two solutions from both subroutines are denoted as m_1 and m_2 . The fault location estimate can be judged as true only when it satisfies the following three principles:

1. The fault location estimate is within the assumed range.
2. The fault resistance takes on a non-negative value.
3. The equivalent impedances of the series compensation device for all three phases have non-negative real part and negative imaginary part, i.e. $\text{Re}\{Z_{eq-x}\} \geq 0$ and $\text{Im}\{Z_{eq-x}\} < 0$, $x = a, b, c$.

As to principle 1, the assumed range for m_1 is $[0, l_1/l]$ and that for m_2 is $[l_1/l, 1]$. After the fault location is obtained, (5.10), (5.13), (5.17) and (5.22) can be used to calculate the fault resistances for the AG, BC, BCG and ABC faults, respectively. The phase equivalent impedances for subroutine 1 can be formulated as

$$Z_{eq-a} = \frac{(V_{sc.r}^{(0)} - V_{sc.l}^{(0)}) + (V_{sc.r}^{(1)} - V_{sc.l}^{(1)}) + (V_{sc.r}^{(2)} - V_{sc.l}^{(2)})}{I_{sc}^{(0)} + I_{sc}^{(1)} + I_{sc}^{(2)}} \quad (5.31)$$

$$Z_{eq-b} = \frac{(V_{sc.r}^{(0)} - V_{sc.l}^{(0)}) + \alpha^2(V_{sc.r}^{(1)} - V_{sc.l}^{(1)}) + \alpha(V_{sc.r}^{(2)} - V_{sc.l}^{(2)})}{I_{sc}^{(0)} + \alpha^2 I_{sc}^{(1)} + \alpha I_{sc}^{(2)}} \quad (5.32)$$

$$Z_{eq-c} = \frac{(V_{sc.r}^{(0)} - V_{sc.l}^{(0)}) + \alpha(V_{sc.r}^{(1)} - V_{sc.l}^{(1)}) + \alpha^2(V_{sc.r}^{(2)} - V_{sc.l}^{(2)})}{I_{sc}^{(0)} + \alpha I_{sc}^{(1)} + \alpha^2 I_{sc}^{(2)}} \quad (5.33)$$

where $\alpha = e^{j120^\circ}$ and

$$V_{sc.r}^{(i)} = V_q^{(i)} e^{j\delta} \cosh(\gamma^{(i)} l_2) - I_q^{(i)} e^{j\delta} Z_c^{(i)} \sinh(\gamma^{(i)} l_2) \quad (5.34)$$

$$V_{sc.l}^{(i)} = V_f^{(i)} \cosh[\gamma^{(i)}(l_1 - ml)] - (I_{pf}^{(i)} - I_f^{(i)}) Z_c^{(i)} \sinh[\gamma^{(i)}(l_1 - ml)] \quad (5.35)$$

and $V_f^{(i)}$, $I_{pf}^{(i)}$, $I_{sc}^{(i)}$ and $I_f^{(i)}$ can be calculated from (5.1), (5.2), (5.3), and (5.6). Also note that although synchronization angle is not a necessity to calculate the fault distance for BCG fault, it is needed for fault location identification wherein (5.21) can be employed.

The computations of three phase equivalent impedances of the series device for subroutine 2 are

$$Z_{eq-a} = \frac{(V_{sc.l}^{(0)} - V_{sc.r}^{(0)}) + (V_{sc.l}^{(1)} - V_{sc.r}^{(1)}) + (V_{sc.l}^{(2)} - V_{sc.r}^{(2)})}{I_{sc}^{(0)} + I_{sc}^{(1)} + I_{sc}^{(2)}} \quad (5.36)$$

$$Z_{eq-b} = \frac{(V_{sc.l}^{(0)} - V_{sc.r}^{(0)}) + \alpha^2(V_{sc.l}^{(1)} - V_{sc.r}^{(1)}) + \alpha(V_{sc.l}^{(2)} - V_{sc.r}^{(2)})}{I_{sc}^{(0)} + \alpha^2 I_{sc}^{(1)} + \alpha I_{sc}^{(2)}} \quad (5.37)$$

$$Z_{eq-c} = \frac{(V_{sc.l}^{(0)} - V_{sc.r}^{(0)}) + \alpha(V_{sc.l}^{(1)} - V_{sc.r}^{(1)}) + \alpha^2(V_{sc.l}^{(2)} - V_{sc.r}^{(2)})}{I_{sc}^{(0)} + \alpha I_{sc}^{(1)} + \alpha^2 I_{sc}^{(2)}} \quad (5.38)$$

where

$$V_{sc.l}^{(i)} = V_p^{(i)} \cosh(\gamma^{(i)} l_1) - I_p^{(i)} Z_c^{(i)} \sinh(\gamma^{(i)} l_1) \quad (5.39)$$

$$V_{sc.r}^{(i)} = V_f^{(i)} \cosh[\gamma^{(i)}(ml - l_1)] - (I_{qf}^{(i)} - I_f^{(i)}) Z_c^{(i)} \sinh[\gamma^{(i)}(ml - l_1)] \quad (5.40)$$

and $V_f^{(i)}$, $I_{qf}^{(i)}$, $I_{sc}^{(i)}$ and $I_f^{(i)}$ can be calculated from (5.24), (5.25), (5.26), and (5.28), respectively.

The whole process can be illustrated as follows. First of all, two fault location estimates are calculated, if any one of them falls outside the supposed range, it can be filtered out. We can obtain a fault location estimate. If both satisfy principle 1, fault resistances corresponding to each fault location estimate can be calculated, the one assuming a negative value indicates the invalidity of the fault location estimate. If principle 2 is satisfied for both solutions, the corresponding equivalent impedances of the series compensator can be calculated to identify the correct solution.

When applying (5.8) as the fault location formula for AG fault, under different initial values, two different fault location estimates arise for each subroutine and one of them is erroneous. If only one subroutine satisfies both principles 1 and 2, it is still not guaranteed that this solution is correct. Only when the third principle is also satisfied, can it be selected as the correct fault location. Otherwise, we can adjust the initial value to find another estimate. Our observations manifest that there will always be one and only one fault location estimate that satisfies all the three principles.

5.4 Evaluation Study

This section presents the simulation results to evaluate the developed fault location algorithm. Matlab SimPowerSystems [76] is used to simulate the series-compensated single-circuit line and generate voltage and current phasors for faults of different types, locations and resistances. These phasors are fed into the algorithm to produce the fault location estimate. The initial value for the fault location is chosen as 0.5 p.u.. The accuracy of fault location estimate is evaluated by percentage error defined as in equation (2.148).

5.4.1 System Configuration

The sample power system studied is a 500 KV, 1000 MVA, 60 Hz single-circuit transmission line compensated at the degree of 45%. The total length of the line is 350 km, with the series compensation device installed at 200 km (0.5714 p.u.) from terminal P . The synchronization angle is set as 22.5°. Other data are listed in Table 5.1 and 5.2.

The MOV consists of 30 columns of metal-oxide discs connected in parallel inside the same porcelain housing. The characteristic of each column is represented by a

Table 5.1: Voltage source data

Item	Source P	Source Q
Emf (p.u.)	1.0∠20°	1.0∠0°
Positive-sequence impedance(Ω)	17.177+j45.5285	2.5904+j14.7328
Zero-sequence impedance(Ω)	15.31+j45.9245	0.7229+j15.1288

Table 5.2: Transmission line data

Parameter	Positive-sequence	Zero-sequence
R (Ω/km)	0.249168	0.60241
L (mH/km)	1.56277	4.8303
C (nF/km)	19.469	12.06678

combination of three exponential functions [76]

$$\frac{V}{V_{ref}} = k_i \left(\frac{I}{I_{ref}} \right)^{1/\alpha_i} \quad (5.41)$$

where $V_{ref} = 165$ kV, $I_{ref} = 1$ kA, $i = 1, 2, 3$. The parameters of the three segments of (5.41) are

$$\begin{aligned} k_1 &= 0.955, & \alpha_1 &= 50, \\ k_2 &= 1.0, & \alpha_2 &= 25, \\ k_3 &= 0.9915, & \alpha_3 &= 16.5. \end{aligned}$$

The V-I characteristic of MOV is illustrated in Fig. 5.5 [76].

The positive-sequence inductance of the transmission line is 1.56277 mH/km, the total reactance of the line is calculated as

$$X_l = \omega \times L = 2\pi f \times L = 1.56277 \times 10^{-3} \times 350 \times 2\pi 60 = 206.2026 \Omega \quad (5.42)$$

Since the compensation level is 45%, the capacitive reactance of the single-phase series compensator is

$$X_c = 206.2026 \times 45\% = 92.7912 \Omega = \frac{92.7912}{250} = 0.3712 \text{ p.u.} \quad (5.43)$$

where the base impedance is obtained by

$$Z_{base} = \frac{500^2}{1000} = 250 \Omega \quad (5.44)$$

Moreover, the capacitance of single phase series compensator is calculated as

$$C = \frac{1}{\omega X_c} = \frac{1}{2\pi f \times 92.7912} = 2.86 \times 10^{-5} \text{ F} \quad (5.45)$$

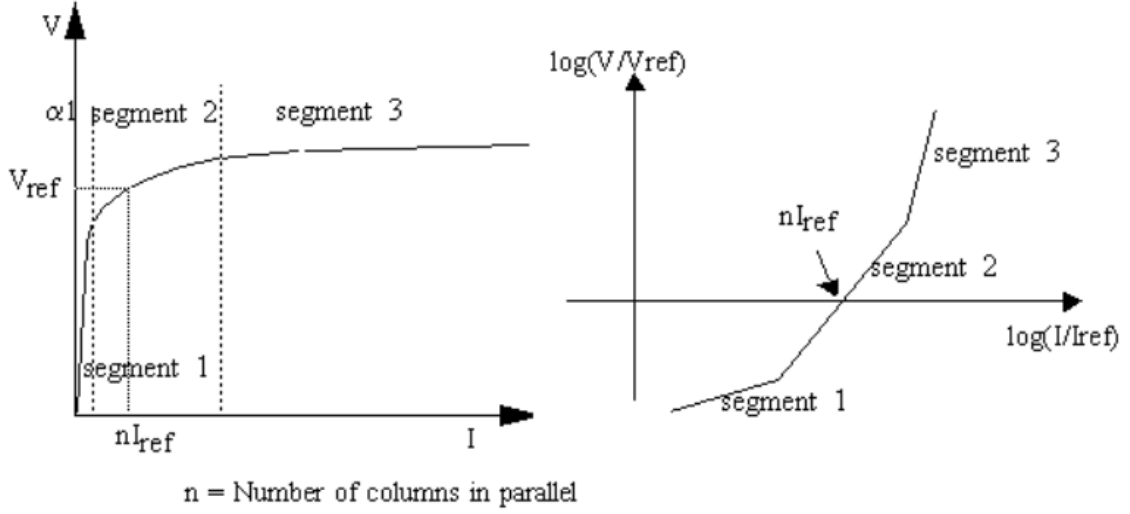


Figure 5.5: V-I characteristic of MOV.

All the three phases of the SC have the same capacitance calculated in (5.45) and there is no mutual coupling among the three phases. As a byproduct of above derivation, the following condition exists

$$|\text{Im} \{Z_{eq-x}\}| \leq X_c, \quad x = a, b, c \quad (5.46)$$

It is proved as follows. The single phase equivalent impedance of SC&MOV is

$$Z_{eq-x} = \frac{1}{\frac{1}{R} + j\omega C} = \frac{\frac{1}{R} - j\omega C}{\left(\frac{1}{R}\right)^2 + (\omega C)^2} = \frac{\frac{1}{R}}{\left(\frac{1}{R}\right)^2 + (\omega C)^2} - \frac{j\omega C}{\left(\frac{1}{R}\right)^2 + (\omega C)^2} \quad (5.47)$$

where R represents the resistance of MOV. Thus it is proved that

$$|\text{Im} \{Z_{eq-x}\}| \leq \frac{1}{\omega C} = X_c$$

Equation (5.46) can also be utilized to filter out the invalid subroutine.

5.4.2 Fault Location Results

The fault location results are summarized in Table 5.3. The first two columns display the actual fault type and fault resistance simulated. The rest columns present the percentage fault location error under various actual fault locations. The results for AG fault are obtained using (5.11), which only yields one solution for each subroutine. From Table 5.3, we can see that the fault location result is highly accurate, with the largest error being 0.023%. Next, we will discuss some cases that further illustrate the fault location identification method.

Table 5.3: Fault location results

Fault type	Fault res. (Ω)	Fault location error (%)		
		100 km	150 km	300 km
AG	1	0.0046	0.016	0.00067
	10	0.0053	0.017	0.00055
	50	0.013	0.023	0.00078
BC	1	0.0040	0.012	0.0012
BCG	1	0.0042	0.014	0.00071
	10	0.0036	0.014	0.00054
	50	0.0052	0.014	0.00055
ABC	1	0.0036	0.010	0.00023

Case 1: AG fault, actual fault location is 300 km (0.8571 p.u.), and actual fault resistance is 10 Ω (0.040 p.u.)

The two fault location estimates from two subroutines are: $m_1 = 0.6217$ p.u., $m_2 = 0.8571$ p.u.

Since m_1 falls outside $[0, 0.5714]$, it is filtered out. We can therefore conclude $m = m_2 = 0.8571$.

Case 2: BC fault, actual fault location is 150 km (0.4286 p.u.) and actual fault resistance is 1 Ω (0.0040 p.u.).

The two fault location estimates from two subroutines are: $m_1 = 0.4287$ p.u., $m_2 = 0.7191$ p.u..

Since they both satisfy principle 1, we will further calculate the two corresponding fault resistances: $R_{f1} = 0.0034$ p.u., $R_{f2} = 0.2245$ p.u.. They are both positive numbers which means we need to compute the three phase equivalent impedances corresponding to both fault location estimates. We have

$$Z_{eq-a1} = 0 - j0.3625, \quad Z_{eq-b1} = 0.1130 - j0.2651, \quad Z_{eq-c1} = 0.1226 - j0.2151,$$

$$Z_{eq-a2} = 0 - j0.3626, \quad Z_{eq-b2} = -0.2878 - j0.2216, \quad Z_{eq-c2} = -0.3779 - j0.2502.$$

Hence, only the solution from subroutine 1 satisfies all three principles, and we can conclude that the true fault location is 0.4287 p.u.

Case 3: BCG fault, actual fault location is 300 km (0.8571 p.u.), and actual fault resistance is 1 Ω (0.0040 p.u.)

The two fault location estimates from two subroutines are: $m_1 = 0.5935$ p.u., $m_2 = 0.8571$ p.u.

Since m_1 falls outside $[0, 0.5714]$, it is recognized as the invalid solution. We can therefore conclude $m = m_2 = 0.8571$.

Case 4: ABC fault, actual fault location is 100 km (0.2857 p.u.) and actual fault resistance is 1 Ω (0.0040 p.u.).

The two fault location estimates from two subroutines are: $m_1 = 0.2858$ p.u., $m_2 = 0.5974$ p.u..

Since both solutions satisfy principle 1, fault resistances corresponding to each fault location need to be calculated: $R_{f1} = 0.0039$ p.u., $R_{f2} = 0.0979$ p.u.. They are both positive numbers which means we need to compute the three phase equivalent impedances corresponding to both fault location estimates. We have

$$\begin{aligned} Z_{eq.a1} &= 0.1180 - j0.2476, & Z_{eq.b1} &= 0.1180 - j0.2476, \\ Z_{eq.c1} &= 0.1180 - j0.2476, \\ Z_{eq.a2} &= -0.2701 - j0.2542, & Z_{eq.b2} &= -0.2701 - j0.2542, \\ Z_{eq.c2} &= -0.2701 - j0.2542. \end{aligned}$$

Only the solution of subroutine 1 meets all the principles and thus $m = m_1 = 0.2858$ p.u..

5.5 Summary

A new method to pinpoint fault location on series-compensated single-circuit line is presented in this chapter. Unsynchronized voltage and current phasors from both ends of the line are utilized. A capacitor bank equipped with a MOV is considered in this work, but the fault location algorithm is still suited when thyristor-controlled series compensator is installed. The algorithms are independent of the source impedance and not influenced by the series capacitor and its MOV.

Two subroutines are developed to pinpoint the possible locations of the fault on both sides of the series compensation device. A fault location identification method can then be applied to reach the true fault distance. The synchronization angle can be acquired independently using either pre-fault measurements for all types of faults or fault measurements for LG and LLL faults, and be treated as known in the fault location derivation. Distributed parameter line model is utilized that fully considers the effect of shunt capacitance. The fault type is assumed to be known.

Evaluation studies using Matlab SimPowerSystems have demonstrated that the proposed fault location algorithm is highly accurate and the fault identification method is valid.

Chapter 6

Conclusions

Short-circuit faults are the most common and severe threat to power transmission lines. With today's power networks often stretching hundreds of miles over complex geographic terrain, precise location of the fault in a timely fashion can speed up restoration and reduce loss of revenues for the utilities. For several decades transmission line fault location has been an important subject of research and many algorithms have been developed.

In this dissertation advanced fault location methods for double-circuit lines and series-compensated single-circuit lines have been proposed, taking advantage of intelligent devices such as DFR, PMU and power quality meter. For double-circuit transmission lines I have developed different fault location algorithms based on the lumped parameter line model. They utilize either sparse voltage phasors, or phase voltage magnitudes, or current phasors, or phase current magnitudes.

Accurate fault location algorithms that employ voltage phasors have also been implemented, taking into account the charging effect of transmission lines in the distributed parameter line model. Simulation studies with EMTP have shown that the proposed algorithms are able to yield quite precise fault location estimates.

The distinctive features of the algorithms for double-circuit lines include:

- Existing algorithms still require measurements from one or two terminals of the faulted section. However, this information may not be available due to the sparse placement of meters. In contrast to these established algorithms this dissertation has proposed and implemented novel fault location algorithms. They utilize sparse measurements which are not necessarily taken at the terminals of the faulty line. We build the bus impedance matrix with an additional fictitious fault bus, and make use of the boundary conditions of different fault types. This allows us to bridge the voltage measurements at any bus during the fault with the sought-after fault location variable.
- Because of the mutual coupling between parallel lines in a zero-sequence network, the addition of a fault bus on a double-circuit line makes the modification of the bus impedance matrix difficult. It is probably therefore never mentioned in textbooks, neither for lumped nor for distributed parameter line models. In

this work the augmented bus impedance matrix is constructed in a novel and efficient way by drawing on fundamental network analysis. The first n by n sub-matrix is identical to the pre-fault bus impedance matrix. Furthermore, both the fault bus driving-point impedance and the transfer impedances associated with the fault bus are analytical functions of the unknown fault location.

- In the lumped parameter line model the elements of the augmented bus impedance matrix take on the same form for both the zero-sequence and positive-sequence networks. This phenomenon implies that the fault location algorithms based on the lumped parameter line model can be universally applied to single-circuit and double-circuit lines.
- Due to the lack of the *equivalent π model*, in all existing literature the nominal π model has been adopted instead to take into account the charging effect of transmission lines. It is a good approximation for short- and medium-length lines, but loses accuracy with increasing line length. In this dissertation, the classical time-domain telegraph equations [64] are put to use in deriving the equivalent π model for a zero-sequence double-circuit line. Two traveling modes rather than one in a single-circuit line, as well as two pairs of characteristic impedance and propagation constant each have been found. With the help of this model accurate fault location algorithms for double-circuit lines have been developed in this dissertation.
- The fault location estimation techniques that employ phase voltage sags or phase current magnitudes require only measurements from relatively simple monitoring devices. In a typical real-life power network a large amount of such power quality meters have been already deployed. Thus, the excessive costs of installing expensive devices such as PMUs can be mitigated.
- Two-bus algorithms utilizing positive-sequence voltage phasors or current phasors as input are suited for all types of faults. They are therefore immune from any errors caused by a potentially wrong fault type classification.
- By means of the state estimation theory, the implemented optimal estimator can detect bad data if redundant measurements are available. With the bad data removed it is able to yield highly accurate fault location estimates.

Sometimes the fault location algorithms for double-circuit lines yield more than one unique fault location estimate, with no means of further constraining the true location. In general, however, if there are enough measurement data, then a unique fault location estimate can be reached. *Fault location observability analysis* as well as meter placement within the network may help determine the optimal measurements required to uniquely pinpoint the true fault location for a given network. Research for single-circuit lines was already reported in [77]. Studies for double-circuit lines must be performed in the future.

Following this dissertation the fault location algorithms that are based on the distributed parameter line model and that use current measurements, will be developed next.

Furthermore, for series-compensated transmission lines a novel fault location technique using two-terminal unsynchronized voltage and current measurements as input has been presented in this dissertation. The distributed parameter line model was applied to fully consider the shunt capacitance of the lines. Simulation studies carried out with Matlab SimPowerSystems have satisfactorily validated the proposed method.

Most existent algorithms rely on the approximation of the V-I characteristic of the capacitor bank and its MOV. This approximation introduces an error. The fault location method proposed for series-compensated single-circuit lines has avoided the calculation of voltages and currents across the SCs & MOVs. This method is therefore independent of the model accuracy. Another salient feature is that no synchronization of two terminal measurements is required, which greatly relieves the network communication burden.

In the future research on accurate fault location for series-compensated double-circuit lines should be undertaken.

Bibliography

- [1] C. S. Chen, C. W. Liu, and J. A. Jiang. A new adaptive PMU based protection scheme for transposed/untransposed parallel transmission lines. *IEEE Trans. on Power Delivery*, 17:395–404, April 2002.
- [2] L. B. Sheng and S. Elangovan. A fault location method for parallel transmission lines. *Electrical Power and Energy Systems*, 21:253–259, 1999.
- [3] Y. Hu, D. Novosel, M. M. Saha, and V. Leitloff. An adaptive scheme for parallel-line distance protection. *IEEE Trans. on Power Delivery*, 17:105–110, January 2002.
- [4] A. A. Girgis, A. A. Sallam, and A. K. El-Din. An adaptive protection scheme for advanced series compensated (ASC) transmission lines. *IEEE Trans. on Power Delivery*, 13:414–420, April 1998.
- [5] F. Ghassemi, J. Goodarzi, and A. T. Johns. Method to improve digital distance relay impedance measurement when used in series compensated lines protected by a metal oxide varistor. *IEE Proc.-Gener. Transm. Distrib.*, 145:403–408, July 1998.
- [6] A. Newbould and I. A. Taylor. Series compensated line protection: system modeling & relay testing. In *Fourth International Conference on Developments in Power Protection*, pages 182–186, 1989.
- [7] H. Meyar Naimi and M. Sanaye-Pasand. A new distance measurement algorithm for series compensated transmission lines. *International Review of Electrical Engineering*, 4, October 2009.
- [8] A. A. Girgis, D. G. Hart, and W. L. Peterson. A new fault location technique for two- and three-terminal lines. *IEEE Trans. on Power Delivery*, 7:98–107, January 1992.
- [9] D. Novosel, D. G. Hart, E. Udren, and J. Garitty. Unsynchronized two-terminal fault location estimation. *IEEE Trans. on Power Delivery*, 11:130–138, January 1996.
- [10] M. Sachdev and R. Agarwal. A technique for estimating transmission line fault locations from digital impedance relay measurements. *IEEE Trans. on Power Delivery*, 3:121–129, January 1988.

- [11] M. Djuric, Z. Radojevic, and V. Terzija. Distance protection and fault location utilizing only phase current phasors. *IEEE Trans. on Power Delivery*, 13:1020–1026, October 1998.
- [12] Z. Galijasevic and A. Abur. Fault location using voltage measurements. *IEEE Trans. on Power Delivery*, 17:441–445, April 2002.
- [13] J. A. Jiang, J. Z. Yang, Y. H. Lin, C. W. Liu, and J. C. Ma. An adaptive PMU based fault detection/location technique for transmission lines-part I: theory and algorithms. *IEEE Trans. on Power Delivery*, 15:486–493, April 2000.
- [14] J. A. Jiang, C. S. Chen, and C. W. Liu. A new protection scheme for fault detection, direction discrimination, classification, and location in transmission lines. *IEEE Trans. on Power Delivery*, 18:34–42, January 2003.
- [15] B. R. Bhalja and R. P. Maheshwari. High-resistance faults on two-terminal parallel transmission line: analysis, simulation studies, and an adaptive distance relaying scheme. *IEEE Trans. on Power Delivery*, 22:801–812, April 2007.
- [16] Y. H. Lin, C. W. Liu, and C. S. Chen. A new PMU-based fault detection/location technique for transmission lines with consideration of arcing fault discrimination-part I: theory and algorithms. *IEEE Trans. on Power Delivery*, 19:1587–1593, October 2004.
- [17] S. M. Brahma. Fault location scheme for a multi-terminal transmission line using synchronized voltage measurements. *IEEE Trans. on Power Delivery*, 20:1325–1331, April 2005.
- [18] Y. Liao. Fault location utilizing unsynchronized voltage measurements during fault. *Electric Power Components & Systems*, 34:1283–1293, December 2006.
- [19] Y. Liao and N. Kang. Fault-location algorithms without utilizing line parameters based on the distributed parameter line model. *IEEE Trans. on Power Delivery*, 24:579–584, April 2009.
- [20] Y. Liao and S. Elangovan. Unsynchronised two-terminal transmission-line fault-location without using line parameters. *IEE Proc.-Gener. Transm. Distrib.*, 153:639–643, November 2006.
- [21] C. W. Liu, K. P. Lien, C. S. Chen, and J. A. Jiang. A universal fault location technique for N-terminal ($N \geq 3$) transmission lines. *IEEE Trans. on Power Delivery*, 23:1366–1373, July 2008.
- [22] J. Izykowski, R. Molag, E. Rosolowski, and M. M. Saha. Accurate location of faults on power transmission lines with use of two-end unsynchronized measurements. *IEEE Trans. on Power Delivery*, 21:627–633, April 2006.

- [23] J. Izykowski, E. Rosolowski, M. M. Saha, M. Fulczyk, and P. Balcerek. A fault-location method for application with current differential relays of three-terminal lines. *IEEE Trans. on Power Delivery*, 22:2099–2107, October 2007.
- [24] M. Kezunovic and B. Perunicic. Synchronized sampling improves fault location. *IEEE Comput. Appl. Power*, 8:30–33, 1995.
- [25] G. G. Richards and O. T. Tan. An accurate fault location estimator for transmission line. *IEEE Trans. on Power Apparatus and Systems*, PAS-101:945–950, April 1982.
- [26] A. M. Ranjbar, A. R. Shirani, and A. F. Fathi. A new approach for fault location problem on power lines. *IEEE Trans. on Power Delivery*, 7:146–151, January 1992.
- [27] M. Kezunovic and B. Perunicic. Automated transmission line fault analysis using synchronized sampling at two ends. *IEEE Trans. on Power Systems*, 11:441–447, February 1996.
- [28] A. Gopalakrishnan, M. Kezunovic, S. M. McKenna, and D. M. Hamai. Fault location using distributed parameter transmission line model. *IEEE Trans. on Power Delivery*, 15:1169–1174, October 2000.
- [29] A. O. Ibe and B. J. Cory. A travelling wave-based fault location for two- and three-terminal networks. *IEEE Trans. on Power Systems*, PWRD-1:283–288, April 1986.
- [30] P. F. Gale, P. A. Crossley, B. Xu, Y. Ge, B. J. Cory, and J. R. G. Barker. Fault location based on travelling waves. In *Fifth International Conference on Developments in Power System Protection*, pages 54–59, 1993.
- [31] Hosung Jung, Young Park, Moonseob Han, Changmu Lee, Hyunjune Park, and Myongchul Shin. Novel technique for fault location estimation on parallel transmission lines using wavelet. *Electrical Power and Energy Systems*, 29:76–82, 2007.
- [32] W. J. Cheong and R. K. Aggarwal. A novel fault location technique based on current signals only for thyristor controlled series compensated transmission lines using wavelet analysis and self organising map neural networks. In *Eighth IEE International Conference on Developments in Power System Protection*, volume 1, pages 224–227, 2004.
- [33] L. Sousa Martins, J. F. Martins, V. Fernao Pires, and C. M. Alegria. A neural space vector fault location for parallel double-circuit distribution lines. *Electrical Power and Energy Systems*, 27:225–231, 2005.
- [34] J. Gracia, A. J. Mazon, and I. Zamora. Best ANN structures for fault location in single- and double-circuit transmission lines. *IEEE Trans. on Power Delivery*, 20:2389–2395, October 2005.

- [35] D. Novosel, B. Bachmann, D. Hart, Y. Hu, and M. M. Saha. Algorithms for locating faults on series compensated lines using neural network and deterministic methods. *IEEE Trans. on Power Delivery*, 11:1728–1736, October 1996.
- [36] A. Hosny and M. Safiuddin. ANN-based protection system for controllable series-compensated transmission lines. In *Power Systems Conference and Exposition 2009*, pages 1–6, 2009.
- [37] R. Salat and S. Osowski. Accurate fault location in the power transmission line using support vector machine approach. *IEEE Trans. on Power Systems*, 19:979–986, May 2004.
- [38] T. Takagi, Y. Yamakoshi, M. Yamaura, R. Kondow, and T. Matsushima. Development of a new type fault locator using the one-terminal voltage and current data. *IEEE Trans. on Power Apparatus and Systems*, PAS-101:2892–2898, August 1982.
- [39] L. Eriksson, M. M. Saha, and G. D. Rockefeller. An accurate fault locator with compensation for apparent reactance in the fault resistance resulting from remote-end infeed. *IEEE Trans. on Power Apparatus and Systems*, PAS-104:424–436, February 1985.
- [40] Tamer Kawady and Jurgen Stenzel. A practical fault location approach for double circuit transmission lines using single end data. *IEEE Trans. on Power Delivery*, 18:1166–1173, October 2003.
- [41] Y. Liao and S. Elangovan. Digital distance replaying algorithm for first-zone protection for parallel transmission lines. *IEE Proc.-Gener. Transm. Distrib.*, 145:531–536, September 1998.
- [42] Q. Zhang, Y. Zhang, W. Song, Y. Yu, and Z. Wang. Fault location of two-parallel transmission line for non-earth fault using one-terminal data. *IEEE Trans. on Power Delivery*, 14:863–867, July 1999.
- [43] Y. Ahn, M. Choi, S. Kang, and S. Lee. An accurate fault location algorithm for double-circuit transmission systems. In *Power Eng. Soc. Summer Meeting*, volume 3, pages 1344–1349, 2000.
- [44] J. Izykowski, E. Rosolowski, and M. M. Saha. Locating faults in parallel transmission lines under availability of complete measurements at one end. *IEE Proc.-Gener. Transm. Distrib.*, 151:268–273, March 2004.
- [45] S. Kang, Y. Ahn, Y. Kang, and S. Nam. A fault location algorithm based on circuit analysis for untransposed parallel transmission lines. *IEEE Trans. on Power Delivery*, 24:1850–1856, October 2009.
- [46] A. J. Mazon, J. F. Minambres, M. A. Zorroza, I. Zamora, and R. Alvarez-Isasi. New method of fault location on double-circuit two-terminal transmission lines. *Electric Power Systems Research*, 35:213–219, 1995.

- [47] A. T. Johns and S. Jamali. Accurate fault location technique for power transmission lines. *IEE Proc.-Gener. Transm. Distrib.*, 137:395–402, November 1990.
- [48] A. L. Dalcastagne, S. N. Filho, H. H. Zurn, and R. Seara. An iterative two-terminal fault-location method based on unsynchronized phasors. *IEEE Trans. on Power Delivery*, 23:2318–2329, October 2008.
- [49] D. J. Lawrence, L. Cabeza, and L. Hochberg. Development of an advanced transmission line fault location system, part II-algorithm development and simulation. *IEEE Trans. on Power Delivery*, 7:1972–1983, October 1992.
- [50] T. Nagasawa, M. Abe, N. Otsuzuki, T. Emura, Y. Jikihara, and M. Takeuchi. Development of a new fault location algorithm for multi-terminal two parallel transmission lines. *IEEE Trans. on Power Delivery*, 7:1516–1532, July 1992.
- [51] T. Funabashi, H. Otoguro, Y. Mizuma, L. Dube, and A. Ametani. Digital fault location for parallel double-circuit multi-terminal transmission lines. *IEEE Trans. on Power Delivery*, 15:531–537, April 2000.
- [52] G. Song, J. Suonan, Q. Xu, P. Chen, and Y. Ge. Parallel transmission lines fault location algorithm based on differential component net. *IEEE Trans. on Power Delivery*, 20:2396–2406, October 2005.
- [53] M. M. Saha, J. Izykowski, E. Rosolowski, and B. Kasztenny. A new accurate fault locating algorithm for series compensated lines. *IEEE Trans. on Power Delivery*, 14:789–797, July 1999.
- [54] J. Sadeh, N. Hadjsaid, A. M. Ranjbar, and R. Feuillet. Accurate fault location algorithm for series compensated transmission lines. *IEEE Trans. on Power Delivery*, 15:1027–1033, July 2000.
- [55] M. Kizilcay and P. La Seta. A new unsynchronized two-terminals fault location method on series compensated lines. In *Proceedings of IEEE Russia Power Tech Conference*, pages 1–7, Russia, 2005.
- [56] M. Al-Dabbagh and S. K. Kapuduwage. Using instantaneous values for estimating fault locations on series compensated transmission lines. *Electric Power Systems Research*, 76:25–32, 2005.
- [57] Y. Liao. Fault location for single-circuit line based on bus-impedance matrix utilizing voltage measurements. *IEEE Trans. on Power Delivery*, 23:609–617, April 2008.
- [58] Y. Liao. Fault location using sparse voltage measurements. In *NAPS 2007*, Las Cruces, New Mexico, USA, September 2007.
- [59] N. Kang and Y. Liao. Fault location for double-circuit lines utilizing sparse voltage measurements. In *Power & Energy Society General Meeting 2009*, Calgary, Canada, July 2009.

- [60] N. Kang and Y. Liao. Advanced fault location technique for parallel power transmission lines. In *Electric Power Systems in Transition*. Nova Science Publishers, 2010.
- [61] N. Kang and Y. Liao. Fault location estimation for transmission lines using voltage sag data. In *Power & Energy Society General Meeting 2010*, Minneapolis, MN, USA, July 2010.
- [62] W. Peterson, E. Makram, and T. Baldwin. A generalized PC based bus impedance matrix building algorithms. In *IEEE Proceedings of Energy and Information Technologies in the Southeast*, pages 432–436, Columbia, SC, USA, April 1989.
- [63] K. Takahashi, J. Fagan, and M. Chen. Formation of a sparse bus impedance matrix and its application to short circuit study. In *Proceedings of the 8th PICA Conference*, pages 63–69, Minneapolis, MN, USA, June 1973.
- [64] John Grainger and William Stevenson. *Power System Analysis*. McGraw-Hill Inc., New York, USA, 1994.
- [65] Y. Liao. New fault location approach using voltage measurements. In *Southeast-Con 2007*, pages 407–412, Richmond, VA, March 2007.
- [66] S. E. Westlin and J. A. Bubenko. Newton-Raphson technique applied to the fault location problem. In *Proceeding of the IEEE Power Summer Meeting*, Portland, OR, USA, July 1976. paper no. A76 334-3.
- [67] *Alternative Transient Program, User Manual and Rule Book*. Leuven EMTP Centre, Leuven, Belgium, 1987.
- [68] N. Kang and Y. Liao. New fault location technique for double-circuit transmission lines based on sparse current measurements. In *NAPS 2009*, Starkville, Mississippi, USA, October 2009.
- [69] N. Kang and Y. Liao. Fault location estimation using current magnitude measurements. In *SoutheastCon 2010*, pages 214–217, Charlotte-Concord, NC, USA, March 2010.
- [70] Y. Liao. Fault location using sparse current measurements. In *NAPS 2007*, Las Cruces, New Mexico, USA, September 2007.
- [71] Y. Liao. Equivalent pi circuit for zero-sequence networks of parallel transmission lines. *Electric Power Components and System*, 37:787–797, July 2009.
- [72] Y. Liao. Optimal estimate of transmission line fault location considering measurement errors. *IEEE Trans. on Power Delivery*, 22:1335–1341, July 2007.
- [73] A. Abur and A. G. Exposito. *Power System State Estimation-Theory and Implementation*. Marcel Dekker, New York, 2004.

- [74] C. S. Yu, C. W. Liu, S. L. Yu, and J. A. Jiang. A new PMU-based fault location algorithm for series compensated lines. *IEEE Trans. on Power Delivery*, 17:33–46, January 2002.
- [75] M. Fulczyk, P. Balcerek, J. Izykowski, E. Rosolowski, and M. M. Saha. Two-end unsynchronized fault location algorithm for double-circuit series compensated lines. In *IEEE PES General Meeting*, pages 1–9, July 2009.
- [76] *MATLAB SimPowerSystems help documentation*. Mathworks Inc., 2009.
- [77] Y. Liao. Fault location observability analysis and optimal meter placement based on voltage measurements. *Electric Power Systems Research*, 79:1062–1068, July 2009.

VITA

Ning Kang

Date and place of birth

19 April 1982, Taiyuan / China

Educational institutions attended and degrees awarded

August 2006 - present

University of Kentucky, Ph.D. in Electric Power Systems Engineering, 2010
(expected)

September 2004 - July 2006

Xi'an Jiaotong University, graduate study in Systems Engineering

September 2000 - July 2004

Xi'an Jiaotong University, B.S. in Information Engineering

Professional positions held

Research Assistant, University of Kentucky, 2009 - present

Teaching Assistant, University of Kentucky, 2006 - 2009

Professional Publications

1. N. Kang and Y. Liao, Fault location estimation for transmission lines using voltage sag data, *PES General Meeting 2010*, Minneapolis, MN, July 2010.
2. N. Kang and Y. Liao, Advanced fault location technique for parallel power transmission lines, *Electric Power Systems in Transition*, Nova Science Publishers, 2010, ISBN: 978-1-61728-313-0.
3. N. Kang and Y. Liao, Fault location estimation using current magnitude measurements, *SoutheastCon 2010*, pp. 214-217, Charlotte-Concord, NC, March 2010.
4. N. Kang and Y. Liao, New fault location technique for series compensated transmission lines, *International Review of Electrical Engineering*, v.4, n.6, pp. 1385-1390, Dec. 2009.
5. N. Kang and Y. Liao, New fault location technique for double-circuit transmission lines based on sparse current measurements, *41st North American Power Symposium*, Starkville, Mississippi, Oct. 2009.

6. N. Kang and Y. Liao, Fault location for double-circuit lines utilizing sparse voltage measurements, *PES General Meeting 2009*, pp. 1-7, Calgary, Canada, July 2009.
7. Y. Liao and N. Kang, Fault location algorithms without utilizing line parameters based on the distributed parameter line model, *IEEE Transactions on Power Delivery*, v.24, n.2, pp. 579-584, April 2009.
8. N. Kang and Y. Liao, Some experiences in estimation of synchronous generator parameters, *41st Southeastern Symposium on System Theory*, pp. 133-138, Tullahoma, Tennessee, March 2009.
9. Y. Liao, T. Nguyen, and N. Kang, Transmission system harmonic benchmarking and statistical analysis with field data, *PES General Meeting 2007*, pp. 1-6, June 2007.
10. N. Kang, J. Zou, C. Li, L. Yang, and H. Wang, Transient parameters and numerical calculation model on VFT in three-phase enclosed GIS, *Proceedings of the Chinese Society for Electrical Engineering*, v.25, n.20, p.112, Oct. 2005.
11. J. Zou, N. Kang, C. Li, and H. Wang, Research on mechanism in formation and depression of Very Fast Transient Overvoltage, *Journal of Xi'an Jiaotong University*, v.39, n.4, p.417, April 2005.
12. N. Kang, Y. Li, L. Yang, Q. Zhang, H. Wang, and J. Zou, Analysis of simplified models for numerical calculation of VFT in GIS, *High Voltage Engineering*, v.30, n.10, p.1, Oct. 2004.